Effectiveness of Headgear for Children with Cerebral Palsy: A Simulation Study

Shaghayegh Kiani Mehr

Supervisor: Dr. Carlos Zerpa

Committee Member:

Dr. Kathryn Sinden and Dr. Paolo Sanzo

In partial fulfillment of the requirements for the degree of Master of Science in Kinesiology

Department of Kinesiology, Lakehead University

Thunder Bay, Ontario, Canada

Summer 2026

Table of Contents

Abstract

Cerebral palsy (CP) is a lifelong neurological disorder that affects movement, posture, and balance in children, making them vulnerable to falls and subsequent head injuries. Falls are one of the most common causes of head trauma in children with CP. One major concern associated with these falls is concussion, a mild traumatic brain injury (mTBI) that can result in cognitive, emotional, and physical complications. Although protective headgear may be prescribed for children with CP, there is limited research evaluating the effectiveness of these helmets in mitigating head injury risk and concussion when interacting with ground surfaces. The current study aimed to address this gap by evaluating the effectiveness of a helmet for children with CP in mitigating concussion risk across different impact locations of the head and ground surfaces. The researcher performed the dynamic tests using a child-sized surrogate headform fitted with a CP LYCRA® headgear. The headform was attached to a mechanical neckform mounted on a vertical monorail drop rig. Impact measures were analyzed using mixed factorial ANOVAs. Significant interaction effects were observed between impact location and ground surface on the concussion risk measures. The influence of impact location varied across biomechanical measures, with the greatest reductions observed at side impacts for linear acceleration and front impacts for rotational acceleration when using the foam surface. The foam surface consistently demonstrated lower injury risk measures across impact locations compared with stiffer surfaces. These findings provide biomechanical evidence to support the development of safer headgear and playground surfaces for children with CP.

Acknowledgement

First, I would like to express my gratitude to my supervisor, Dr. Carlos Zerpa, for his expertise and continuous support, guidance, feedback and encouragement throughout this research journey. I truly appreciate his availability and patience in answering my questions and addressing my concerns throughout the entire process.

I would also like to sincerely thank my committee members, Dr. Kathryn Sinden and Dr. Paolo Sanzo, for their valuable feedback, thoughtful comments, and constructive questions throughout this research process.

I would like to thank my external examiner, Dr. Jinan Fiaidhi, for her thoughtful evaluation of my work and for providing valuable perspectives and feedback throughout the examination process.

I would like to thank Mr. Carl Goodwin, laboratory technologist and technician, for his assistance in troubleshooting technical issues and supporting the successful completion of the experimental setup.

I would also like to thank Ms. Sofia Grosheva for her help with data collection. The many hours we spent together in the laboratory collecting data were an important part of this research experience, and I truly appreciate her time, dedication, and support.

My sincere appreciation goes to the Thunder Bay Orthopaedic Clinic and Mr. Alex Tempelman for designing and developing the custom headgear for children with CP used in this study.

Finally, I would like to express my deepest gratitude to my husband and my family back home for their unconditional support, encouragement, and positive energy throughout this journey.

List of Figures

List of Tables

List of Equations

List of Appendixes

List of Abbreviations

ACPR	Australian Cerebral Palsy Register
AGSI	Angular Gadd Severity Index
ATDs	Anthropomorphic test devices
BOS	Base of support
CDC	Center s for disease control and prevention
COM	Center of mass
COR	Coefficient of restitution
CP	Cerebral Palsy
CPSC	Consumer product safety commission
DAI	Diffuse axonal injury
EPS	Expanded polystyrene
EWF	Engineered wood fiber
FE	Finite element
GMFCS	Gross Motor Function Classification System
HIC	Head Injury Criteria
HYB	Hybrid surface systems
ICCs	Intraclass correlation coefficients
mTBI	Mild traumatic brain injury
NICE	National institute for health and care excellence
NOCSAE	National operating committee on standards for athletic equipment
PES	Anisotropic polyether sulfone
PIP	Poured in place rubber

PLA	Peak linear acceleration
PRA	Peak rotational acceleration
RLA	Reluctant linear acceleration
ROM	Range of motion
SCPE	Surveillance of CP in Europe
SRHIs	Seizure-related head injuries
TBI	Traumatic brain injury
TD	Typically developing
TIL	Tiles
TPU	Thermoplastic
WSUBIM	Wayne State University Brain Injury Model

Chapter 1 – Introduction

Cerebral palsy (CP) relates to a group of permanent neurological disorders that affect children's movement and posture attributed to a non-progressive development of the fetal or infant brain (Obembe et al., 2013). CP was originally identified by William John Little in 1861, and the study of this neurological disorder has evolved in the last 160 years (Rosenbaum et al., 2007). CP is considered a serious brain-related disability in children around the world, leading to high levels of illnesses and death rates (Donald et al., 2014; Michael et al., 2019).

Balance problems are a major challenge for children with CP, making it hard for them to keep steady and maintain balance. Children with CP often have weaker neuromotor perception, poorer stability when standing, slower responses when preparing for movement, and difficulty activating the appropriate muscle groups required for stability and coordinated movement (Abd-Elfattah et al., 2022). Many children with CP demonstrate poor walking ability and difficulties with manipulation tasks. One major contributing factor to these challenges is impaired balance control, as maintaining postural stability is essential for all forms of movement (Woollacott & Shumway-Cook, 2005). Research has consistently shown that children with CP, particularly those with spastic hemiplegia (stiff or tight muscles of one side of body) and spastic diplegia (stiff or tight muscles of the legs), exhibit marked differences in balance responses compared to typically developing (TD) children (Nashner et al., 1983; Shumway-Cook et al., 2003).

Earlier research by Nashner et al. (1983) and Burtner et al. (1998) identified that children with CP have limited neuromuscular responses needed for effective balance recovery, including delayed reaction times and reduced ability to generate coordinated postural adjustments. Nashner et al. (1983) found that children with spastic hemiplegia exhibited disordered timing of muscular responses. These neuromuscular alterations result in slower and more disorganized recovery of balance after perturbations (Woollacott & Shumway-Cook, 2005). These balance issues may result in more frequent falls in children with CP, and these falls can have serious physical consequences, including head injuries and concussions (Bulut, 2006).

A concussion may be caused by a direct blow to the head, face, neck, or an indirect force transmitted to the head, causing the brain to move or rotate within the skull. A concussion leads to a temporary disturbance in brain function due to rapid acceleration–deceleration or rotational forces, which can alter brain cell metabolism and impair normal neural activity (Browne et al., 2011; Dupuis et al., 2005; Kazl & Torres, 2019; Meaney & Smith, 2011; Orr et al., 2024).

Preventing falls that cause head injuries and concussions in CP children requires effective balance. To maintain effective balance, however, anticipatory as well as proactive and reactive control strategies are needed to uphold the body's center of mass (COM) within the base of support (BOS). Children with CP, however, lack these strategies and have been shown to be more unstable during walking compared to their TD peers (Bruijn et al., 2013). This may be the result of common gait impairments such as reduced knee flexion-extension range of motion (ROM) or in-toeing of the feet (Boyer & Patterson, 2018).

A common practice to prevent head injuries and ultimately concussions in children with CP is the use of protective helmets or headgear; yet current evidence supporting their effectiveness remains limited. Studies show that children with CP and epilepsy are at significantly higher risk of seizure-related head injuries, with one study reporting a high risk of concussion compared to children without epilepsy (Deekollu et al., 2005; Nakken & Lossius, 1993; Neufeld et al., 2000). However, even among children wearing helmets, injuries still occur, raising concerns about helmet design and fit (Deekollu et al., 2005). For children with CP or other motor impairments that result in an increased frequency of falls, helmet prescription often relies on clinical judgment rather than standardized criteria or injury data, with few studies providing specific design recommendations and clinical practice guidelines on prescription (Sneed et al., 2008). These findings highlight the urgent need for condition-specific research and improvements in helmet design and testing tailored to understanding and preventing the risk of concussions faced by children with CP.

In addition to headgear designs, the characteristics of fall surfaces and playgrounds for children with CP are a crucial factor influencing the risk and severity of head injuries. Research has shown that compliant surfaces, such as foams or carpets, may reduce ground stiffness and absorb impact energy, making them a passive intervention strategy in fall-prone environments (Bertocci et al., 2004; Lachance et al., 2017). Further research, however, is needed to better understand the combined protective capabilities of headgears and surfaces to mitigate head injuries and concussion risk.

The proposed study aimed to address this gap by examining the combined effect of CP headgear material and ground surface in minimizing the risk of concussion based on measures of linear acceleration, rotational acceleration, Head Injury Criteria (HIC), and Angular Gadd Severity Index (AGSI) during simulated free-fall head collisions.

Dynamic impact testing was performed using a child-sized surrogate headform fitted with a CP LYCRA® headgear and attached to a mechanical neck mounted on a vertical monorail drop rig. The headform was dropped onto four ground surfaces (wood, playground foam, linoleum, and carpet) at three impact locations (front, side, and back) across impact velocities ranging from 2.80 to 4.43 m/s. Each condition was repeated three times, yielding 468 impacts. A mixed factorial design was used, with impact location as the between-subjects factor and ground surface type as the within-subjects factor. Impact measures were analyzed using two-way mixed factorial ANOVAs.

The results of this study demonstrated statistically significant interaction effects between headgear impact location and ground surface for linear acceleration, $F(6, 108) = 39.10$, $p < .05$, $\eta^2 = .685$; rotational acceleration, $F(6, 108) = 10.89$, $p < .05$, $\eta^2 = .377$; HIC, $F(3.36, 60.47) = 15.76$, $p < .05$, $\eta^2 = .467$; and AGSI, $F(6, 108) = 14.324$, $p < .05$, $\eta^2 = .433$. Linear acceleration varied across both impact location and surface type, with front impacts generally producing higher linear acceleration values than side impacts on some surfaces, while playground foam consistently demonstrated lower linear acceleration. HIC values were significantly reduced on the foam surface across impact locations, indicating lower overall head injury severity under more compliant surface conditions, with no consistent advantage of one impact location over another. Rotational acceleration varied across impact locations and surface types, with the greatest reduction observed during front impacts on the foam surface. AGSI values were also reduced on the foam surface across impact locations, suggesting more uniform attenuation of rotational impact severity due to the compliant properties of the surface and headgear materials.

Overall, the findings of this study demonstrate that both head impact location and ground surface compliance play important roles in determining head injury severity, highlighting the importance of environmental conditions in evaluating protective headgear for children with CP. The findings may contribute to future improvements in pediatric headgear evaluation, environmental safety recommendations, and concussion prevention strategies for children with CP.

Chapter 2 - Literature Review

Cerebral Palsy, Falls, and Head Injury

According to the Centers for Disease Control and Prevention (CDC) in 2010, the most recent global estimates of children diagnosed with CP is 1 to 4 in every 1,000 children and 1 in 345 in the United States alone (Audu & Daly, 2017; Boone, 2024). The prevalence of CP in Canada shows variation within different provinces. In Alberta, a study using administrative databases reported a prevalence of 2.57 per 1,000 live births at age 8 years (Robertson et al., 2017). In British Columbia, a similar estimate of prevalence of 2.68 per 1,000 live births is reported (Smith et al., 2008). A recent Quebec study reported a slightly lower rate of 1.8 per 1,000 children, compared to 2.0 per 1,000 children when data from administrative health databases were used (Oskoui et al., 2017). Out of 2,110,177 live births in Ontario, 5,317 children were diagnosed with CP, resulting in an overall prevalence rate of 2.52 per 1,000 live births among children aged 0 to 16 years (Ahmed et al., 2023).

The Surveillance of CP in Europe (SCPE) and the Australian Cerebral Palsy Register (ACPR) report that the lesion in the brain which leads to CP usually occurs before the child is 24 months of age, while the National Institute for Health and Care Excellence (NICE) in the UK identified that CP occurs before the age of 5 years in most children (Patel et al., 2020). As a result, children around 5 years of age are among the most common participants in research studies.

Common causes of CP include complications during pregnancy, such as exposure to radiation, maternal infections, or the inadequate growth of the baby in the womb. Injuries during birth, such as a difficult or traumatic delivery, and serious health problems around the time of birth or in early childhood can also lead to CP (Ahmed & Hamdy, 2018; Nelson & Blair, 2015).

About 40-50% of children with CP are born prematurely, and most of them experience issues, including brain injury, lack of oxygen, infections, or other neonatal complications, that occur at the time of birth (Vincer et al., 2014). Children with CP usually have smaller muscles and slower muscle growth compared to TD children. As children with CP get older, the difference in muscle development compared to TD children becomes more noticeable. This slower growth can lead to changes in the shape and function of the muscles, contributing to muscular deformities (Gillett et al., 2018). Since muscle size plays a role in how strong a person is, having smaller muscles may explain why children with CP often experience muscle weakness and limited ability to perform everyday movements including walking (Gillett et al., 2018).

Studies have shown that children and adults with CP have about 50% less strength in the plantarflexor muscles, and they produce less than half of the ankle power needed for normal walking compared to people without CP (Riad et al., 2007). This impairment often leads to abnormal and inefficient gait patterns due to problems with movement and coordination (Gillett et al., 2018). As a result, frequent tripping and falling are common concerns for those who can walk (Boyer & Patterson, 2018). It is reported that these children experience 35% of daily falls and 30% of weekly or monthly falls (Boyer & Patterson, 2018). It is recognized that most children fall regardless of their health status, however, normal children from 5 years of age show considerably more stability in their gait patterns and fall less than children with CP (Massaad et al., 2004).

Children with CP are at a Higher Risk of Falling

One study with over 1,000 children found that those grouped at the Gross Motor Function Classification System (GMFCS) level II had the highest number of falls (Boyer & Patterson, 2018). The GMFCS is widely used to describe mobility in children and youth with CP and has five levels. Children within Level I, walk independently but may have difficulty with running or jumping. Children categorized within Level II, walk without aids but struggle with long distances or uneven surfaces. Children within Level III, require a walker or crutches, especially outside the home. Children in Level IV have limited self-mobility and primarily use a wheelchair, while children categorized in Level V have very restricted movement even with assistance (Palisano et al., 1997). It is unclear, however, if this pattern continues into adulthood. Since many studies have small and mixed samples, their findings might not apply to all age groups or GMFCS levels. Because falls are a concern across age groups, evidence from other settings can provide insight into effective strategies. For example, a study conducted in 26 Veterans hospitals found that after implementing safety interventions such as staff education and post-fall huddles, fall-related injury rates decreased from 7.4 to 5.6 injuries per 100 census days (McDonald et al., 2019). Although this research focuses on adults, it highlights the potential value of structured fall-prevention approaches that could be adapted for pediatric CP populations.

Thill et al. (2023) revealed that the incidence of falls and their associated physical and psychological consequences were considerably higher in individuals with CP throughout their lifespan, when compared to individuals without disabilities and those with other neurological conditions. However, there is no treatment guidelines for children with CP, these findings support the need for early intervention, fall prevention strategies, and the use of protective devices to minimize the risk of injuries (Till et al, 2023). This perspective aligns closely with the goals of biomechanical and rehabilitation research focused on improving balance and safety in individuals with CP (Thill et al., 2023). As children with spastic types of CP grow older, many experiences progressive changes in gait patterns—including reduced joint excursions, slower walking velocity, and shorter stride length. These gait impairments increase instability, making them more susceptible to falls and head impacts (Bell et al., 2002). Since gait instability is a known contributor to falls and given that children with CP often have reduced muscular strength and impaired motor control to balance, the risk of falls resulting in head trauma becomes a significant concern (Hägglund et al., 2005). The ability of children with CP to balance may be compromised due to their posture and body deformity issues. Hodgkinson et al. (2002) found that 66.2% of children with CP who could not walk, had scoliosis. More than one-third of them had severe curves over 60 degrees. Many also had a tilted pelvis (59.9%), which was more common on the left side (68.4%) than the right (31.6%), which increases the risk of falling and consequently, the risk of head injuries (Hodgkinson et al., 2002). Fall frequency varies across GMFCS levels in children with CP (Boyer & Patterson, 2018). Boyer and Patterson (2018) reported that fall frequency generally increased from GMFCS level I to level III and then decreased with increasing motor impairment up to level IV. They also found differences in GMFCS distribution among children with different gait pathologies, suggesting that fall patterns may vary depending on the severity of motor impairment and gait characteristics.

Head Injuries due to a Fall

Head injuries, especially cranial trauma, are the most frequent type of injury from falls in children (Alemdaroğlu, et al., 2017). Head injuries that occur in children due to falling are one of the main reasons they go to the hospital. Although most head injuries are minor, some can lead to more serious problems such as bleeding or injury inside the skull (Kuppermann et al., 2009). The percentage of childhood head injuries caused by falls ranges from 19% (Parslow, et al., 2005) to 89% with younger children, especially babies under 12 months being at the highest risk of falls (Crowe et al., 2012; Warrington et al., 2001). These findings should be interpreted cautiously, however, as differences in sample size and the inclusion of broad age groups may influence the variability of the reported fall-related injury rates across studies.

Goldsmith and Plunkett (2004) analyzed the biomechanical mechanisms underlying infant and child traumatic brain injury in the context of loading conditions, injury criteria, and fall impacts. Applying the linear impulse-momentum relationship, they estimated forces during head impacts. The researchers found that, a backward fall from 0.91 meters (m; 3 feet; ft) with a surrogate head weight of 22.4 N resulted in an impact velocity of 4.24 meter per second (m/s), 5 millisecond (ms) contact time and a peak force of 4,070 Newtons (N), producing 173 g (unit of gravity) of acceleration. This magnitude exceeds commonly reported linear acceleration levels associated with an increased risk of head injury in pediatric biomechanical studies (Campolettano et al., 2019). The researchers also modeled falls from increased heights. A fall from 5.63 m (18 ft) resulted in a contact time of 10 ms, velocity of 10.37 m/s, and a force of 14,190 N, much higher than shaking-induced forces. This study claimed that shaking alone can mimic injuries from high falls. Estimated impact velocities (4.57–6.10 m/s) and compressive stresses were below the fracture threshold but near the tensile limits of bridging veins, explaining the bleeding. This study also mentioned that even low to moderate falls can produce brain injuries like subdural hematomas without skull fractures. The outcome of this study emphasized the importance of understanding fall mechanics in pediatric trauma cases that lead to brain injuries (Goldsmith & Plunkett, 2004).

Brain injuries occur when the forces stretch or strain the brain tissue beyond what it can handle. This strain can take different forms including compressing, stretching, or shearing the brain tissue (Mckee & Daneshvar, 2015). Since the brain and blood vessels are nearly impossible to compress, most of the damage comes from stretching and shearing forces (Morgan, 2003).

Brain injuries also fall into two main categories including focal (localized) and diffuse (spread out). Focal injuries happen from direct impacts and include things like skull fractures, bleeding between the brain and skull (epidural or subdural hematomas), and bruising of the brain, which is also referred to as coup contusion (Morgan, 2003). Some injuries, like contrecoup contusions, or deeper bleeding in the brain, result from the brain moving inside the skull. More widespread, or diffuse injuries, happen when the head rotates quickly, tearing of brain fibers (diffuse axonal injury), and bleeding in spaces around or inside the brain and causing a concussion (Morgan, 2003).

Head Trauma and Concussion. The term concussion can be confusing for patients, caregivers, and even some healthcare providers, as its definition is not always clear. It comes from the Latin word *concutere*, which means "*to shake violently*," combining *con*, "*together*" and *quatere*, "*shake*". While it was originally just a verb, today the term refers to the effects caused by such a shaking force. In the medical literature, concussion is often used interchangeably with mild traumatic brain injury (mTBI; Bodin et al., 2011). It is more accurate, however, to view concussion as a type of mTBI, typically involving temporary and immediate symptoms after a head impact (Brody, 2015). So, it is helpful to clarify what a Traumatic brain injury (TBI) is. A TBI happens when a sudden external force, either direct or indirect, disrupts the brain's structure or normal function. This disruption can be physical, functional, or both (Kazl & Torres, 2019). One common cause of TBI is an impact, where the head hits a solid object at a high speed. The impact can create both contact and movement forces that damage the brain. If the head does not move much after being hit, most of the damage comes from the direct force of the hit. But if the head is set in motion, like during a fall or crash, the brain can be injured by how fast it speeds up or slows down (Orr et al., 2024). Another cause of brain injury is an impulsive force, such as a whiplash effect, where the head is quickly thrown forward and then backward. Even though the head does not hit anything, the brain moves around inside the skull sustaining injury (Meaney et al., 2014). A third, much rarer type of injury happens when the head is slowly squeezed by a heavy or slowly moving object, which can crush the skull and cause fracture (Morgan, 2003).

When it comes to children hitting their heads, one of the biggest differences between a child's brain and an adult's, is its size. At birth, the brain makes up about 15% of the body's weight, but by adulthood, it drops to only 3%. The brain grows very fast during early childhood and by the age of 2 years, it is already 75% of adult size, and by the age of 6 years, it reaches about 90% (Ward, 1995). The skull of young children is also different. Until around the age of 3 years, the skull bones have not fully fused, and the skull is thinner and more flexible. This flexibility can help protect the brain by dispersing and spreading out the force from a blow, but it also makes the child's brain more vulnerable to injury (Burgos-Flórez & Garzón-Alvarado, 2020). Children's brains have fewer myelin sheath cells (protective fatty cells insulating the nerves), which makes the nerves more susceptible to injury due to shear impact forces caused by the brain moving or twisting inside the skull (Ward, 1995) The brain's ability to recover after an injury is known as *plasticity* (Puderbaugh & Emmady, 2023). Children, however, seem to recover better than adults because their brains are more plastic and can easily develop new connections after a brain injury (Morgan, 2003).

The vulnerability of the brain during critical maturation periods in childhood and adolescence raises significant concerns that early exposure to concussion may have particularly harmful effects on neurodevelopment, potentially leading to negative long-term clinical and cognitive outcomes (Alosco & Stern, 2019). The relationship between age at the time of injury and concussion-related outcomes is, however, complex (Moody et al., 2022).

Concussions may cause general cognitive problems immediately after injury, long-term effects tend to be more specific, particularly affecting functions controlled by the frontal lobes such as attention, working memory, inhibition, and cognitive flexibility (Botvinick et al., 2001). These abilities, often grouped under the term cognitive control, are essential for learning, academic success, and everyday functioning (Diamond, 2013). Deficits in cognitive control may disrupt a child's ability to focus, adapt to change, and manage goal-directed tasks. Given these risks, it is especially important to monitor and assess these functions in children who have experienced concussions, as even mild injuries can alter their developmental trajectory and impact their future cognitive and emotional well-being (Moore et al., 2015).

Martini et al. (2011) highlighted that there is strong evidence that the physiological impact of a concussion leads to widespread, non-specific disruption across multiple brain regions during the days following injury. This disruption affects both neurocognitive function and motor control, including gait and balance. They showed that the negative effects of concussion on brain function can be long-lasting, with deficits persisting for years and potentially impacting an individual's occupational performance, health status, and overall quality of life. These findings indicate that ongoing motor control difficulties, such as changes in gait, may coexist with long-term cognitive impairments, which can be more severe in individuals with CP who experience a concussion.

Concussion Risk in Children with CP. While the general population shows a lifetime concussion risk of about 24.6% in adolescents (Veliz et al., 2021) and 29% in adults (Daugherty, et al., 2020), the rates observed in individuals with CP in similar age groups are equal to or even higher. Esterley et al. (2024) reported that, among 381 participants, ambulatory individuals with CP (N=201 adults; 18-76 years old) or the caregivers of minors (N=180; 5-17 years old), 78 individuals (13% ± 2%) experienced at least one fall-related concussion, and 13 participants (3%) sustained multiple concussions.

Studies have shown that children with CP are at a significantly higher risk of seizure-related head injuries and concussions (Deekollu et al., 2005; Nakken & Lossius, 1993; Neufeld et al., 2000). Seizure-related head injuries (SRHIs) are typically defined as any dysfunction, impaired consciousness, or pain localized in the head region that results from an accidental occurrence during seizures (Friedman et al., 2012). These injuries are a common complication among people with epilepsy and are often accompanied by postictal disturbances (period of altered consciousness), such as delirium or psychosis, which may further complicate treatment and increase the overall burden of care (Rao et al., 2020). Epileptic seizures frequently result in physical trauma, with head injuries among the most serious consequences. Acute effects of SRHIs can include scalp wounds, concussions, skull fractures, epidural or subdural hematomas, and intracranial hemorrhage (Neguyen & Tellez-Zenteno, 2009). In some cases, post-traumatic syndrome may develop, encompassing a wide range of persistent cognitive, emotional, and physical symptoms following a TBI. Moreover, people with epilepsy face varying levels of risk for head injury depending on seizure type, frequency, motor involvement, and medication adherence (Piwowarczyk et al., 2024).

A European prospective cohort study reported that concussions accounted for 10% of all accidents in individuals with epilepsy and were significantly more common than in control groups, with an odds ratio of 2.6 (95% CI: 1.2–5.8; Beghi & Cornaggia, 2002). In another prospective study involving 298 adults with chronic, long-term epilepsy, a total of 27,934 seizures were recorded, and 45.2% of these were associated with falls. These seizure-related falls resulted in 766 head injuries, 45% of which required stitching. Only three of the injuries were considered severe, including one skull fracture and two intracranial hemorrhages (one extradural and one subdural) (Russell-Jones & Shorvon, 1989). When people fall and hit their head, however, it is essential to understand the impact location to assess the severity of the head injury and the necessary protection to reduce the force of the impact.

Common Head Impact Locations During Falling

Yu et al. (2023) utilized human body models to simulate three types of fall scenarios relevant to workplace accidents in the UK. These included trips (falls onto the same level), forward falls, and backward falls (both representing falls to a lower level). Their results revealed that in forward falls, the head most commonly impacted the front (68%), followed by the side (9%), and top (4%), with only 1% of cases avoiding direct head-ground contact. In contrast, backward falls primarily resulted in impacts to the back of the head (38%) and the top (19%), with just 2% involving the side and none involving the front of the head (Yu et al., 2023).

With regards to children, Hughes et al. (2016) conducted a case study with children under 48 months of age who experienced witnessed falls of less than 3 m to determine the most common impact locations. The researchers compared those who sustained skull fractures with those who had only minor head injuries. They found that severe injuries (skull fracture) were significantly associated with impacts to the temporal (sides of the brain, just behind the ears), parietal (back of the head, directly under the skull bone), or occipital regions of the head (Hughes et al., 2016).

Burns et al. (2016) also conducted a study at 10 Canadian pediatric emergency departments involving children aged 0 to 16 years with minor head injuries to determine the most common impact locations. In this study, out of 1,256 children, 1,189 experienced minor head injuries located in the frontal, parietal, temporal, or occipital regions (Burns et al., 2016). Similarly, Burrows et al. (2015) conducted a study involving children under 6 years of age who were admitted to hospitals in the UK following falls. They found that skull fractures were most commonly located in the parietal and temporal regions (41 cases), followed by the occipital region (11 cases), and the frontal region (6 cases). A few skull fractures, however, occurred at the base of the skull (2 cases). To better understand the severity of impact across different regions of the head that cause a concussion and to test appropriate materials for head protection, researchers have used standardized protocols and surrogate headforms (NOCSAE, 2025). They improve experimental reliability by allowing impacts to be tested under standardized and repeatable conditions. However, their validity is limited by differences in anatomical fidelity and the absence of active neuromuscular control. Previous research has shown that headform design and impact configuration can influence measured kinematics and injury response, because differences in headform properties and impact conditions affect how impact energy is transferred and how head kinematics are generated. Consequently, variations in these factors can lead to differences in measured linear acceleration, rotational motion, and injury metrics used to assess protective performance (Cobb et al., 2014; Foreman, 2024; Singh et al., 2024; Yu et al., 2022).

Head Impact Location Based on Standardized Protocols and Simulations

The National Operating Committee on Standards for Athletic Equipment (NOCSAE; 2025) identified several impact locations relative to the size of a human head using a NOCSAE standard surrogate headform. According to the NOCSAE (2025) standard, for a small child surrogate headform, the reference plane used to identify standardized head impact locations is positioned 55 mm (2.16 in) above the basic plane, which represents the primary anatomical reference line of the headform geometry, as shown in Figure 1.

Figure 1

Reference Plane Location for the Small NOCSAE Standard Headform (child).

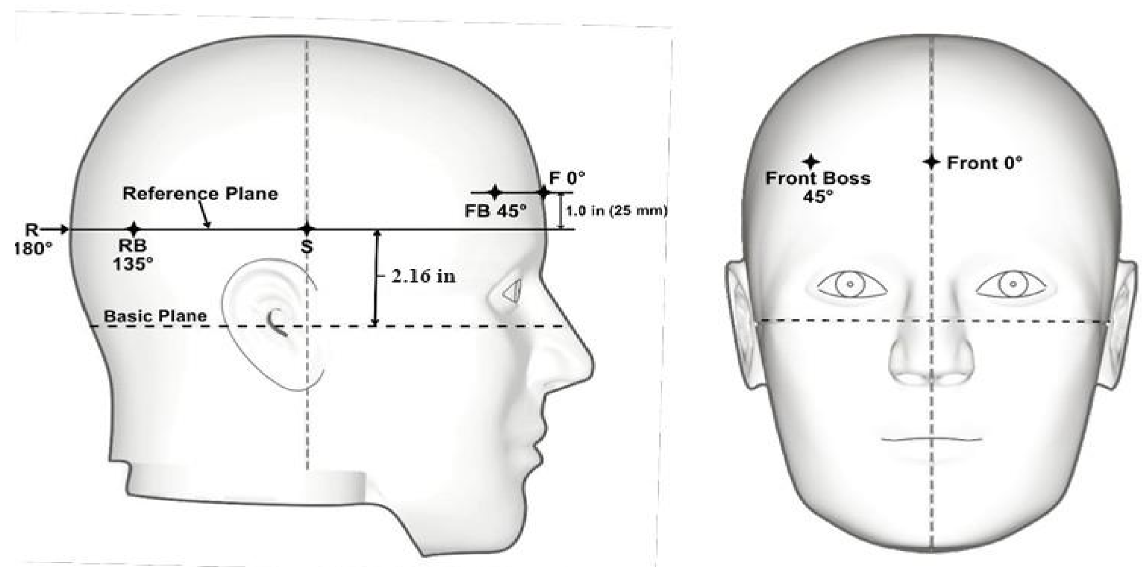

Note. Adapted from NOCSAE Standard Performance Specification (NOCSAE, 2025).

When head protective materials are tested with this headform, the impact area includes the locations on the headform that are above the basic plane, as illustrated in Figure 1, and behind a point that is 57 mm (2.25 in) from where the basic plane intersects the coronal plane, as illustrated in Figure 2. These locations include the front location, which is situated in the median plane approximately 25 mm above the anterior intersection of the median and reference plane. The front boss, which is a point approximately 45° from the median plane measured clockwise and located approximately 25 mm above the reference plane. The side location, which is situated approximately at the intersection of the reference and coronal planes on the right side of the headform. The rear boss region, the curved posterolateral area located between the side and back portions of the headform, is found approximately at the posterior intersection of the median and reference planes. Finally, the rear site, which is located approximately at the intersection of the median and reference planes (NOCSAE, 2017).

Figure 2

Impact Area Boundaries on the Small NOCSAE Standard Headform (child).

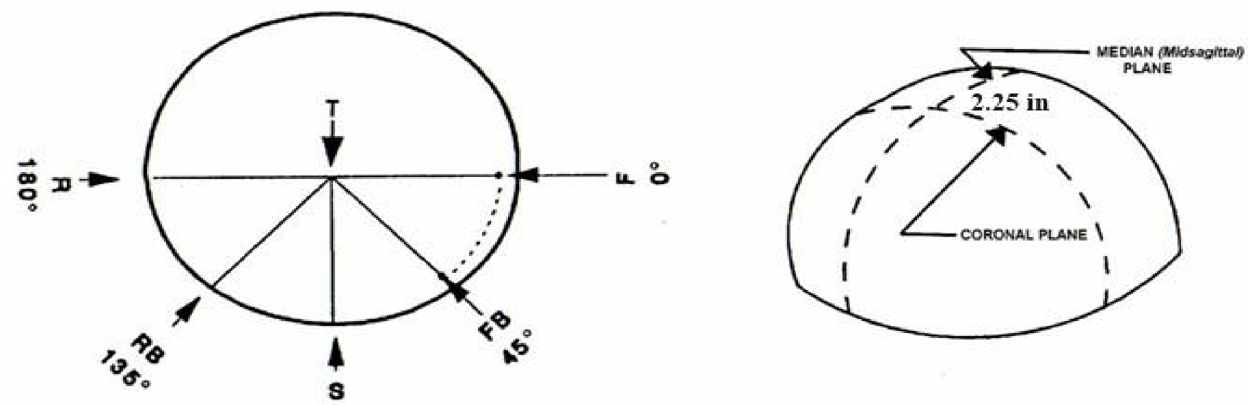

Note. Adapted from NOCSAE Standard Performance Specification (NOCSAE, 2025).

The way the head moves during an impact, especially the direction of the movement, affects how much damage occurs in the brain. Movements that happen in the side-to-side direction (coronal plane), causes the most serious injuries inside the brain (Smith et al., 2000). However, rotational movements in other directions, like front-to-back (sagittal) or horizontal, can also result in injury that results in similar neurological effects (Meaney & Smith, 2011).

Studies have shown that the location and direction of the head impact play a key role in brain injury outcomes. Gennarelli et al. (1982) demonstrated in monkey experiments that rotational motion in the side to side (coronal plane) caused the neurological effects, including frequent axonal damage in the brainstem (Miller et al., 2018). Zhang et al. (2001), using the Wayne State University Brain Injury Model (WSUBIM), found that the brain has lower tolerance to lateral (side) impacts compared to frontal impacts (Zhang et al., 2001). Kleiven (2006), using the finite element model, reported that lateral and axial rotational forces produced the highest brain strains, while translational (straight-line) impacts resulted in significantly lower strains. Post et al. (2012) found that impact direction affected both the magnitude and location of the brain stress and strain, and that even the shape of the impact load curve influenced injury risk. Weaver et al. (2012) observed that frontal and crown (top) impacts caused different strain patterns in the brainstem, and that frontal impacts led to higher strain values (0.088) than crown impacts (0.045). Weaver et al. (2012) confirmed that changing the direction of rotational impacts, even when the force remained the same, led to large variations in brain strain and injury risk (Weaver et al., 2012).

Biomechanical studies investigating head impact protection and injury risk with the use of helmets on ground surfaces often use anthropomorphic test devices (ATDs) to replicate the size, mass, and mechanical behavior of the human body during dynamic impacts (Newman et al., 2005). A study typically involves impacting a helmeted headform using methods such as vertical guided linear drops (Knowles & Dennison, 2017; Rowson & Duma, 2011), horizontal linear impacts with a pneumatic device or pendulum, or oblique impact systems (Newman et al., 2005). The headforms are generally adopted from the automotive industry, such as the Hybrid III, or NOCSAE headform from sports helmet testing NOCSAE standard protocols (Yu & Dennison, 2018).

Impacts at different locations with these head models are measured with arrays of acceleration sensors to capture linear head acceleration, which can be used through post-processing techniques to calculate both linear and rotational kinematics of the head (Yu & Dennison, 2018). These kinematic measures help researchers to quantify the severity of the head impact to the helmet and the ground surface. In some cases, these measures are used to estimate the risk and severity of the head injury. Common kinematic indicators include peak linear acceleration (PLA) and peak rotational acceleration (PRA), as well as measures of risk of head injury such as HIC and AGSI derived from the acceleration kinematic measures (Newman et al., 2005; Rybak, 2021).

Kinematic Measures

Linear Acceleration

The linear acceleration-based injury metric was originally developed from early studies using human cadavers and animal models, where brain injuries were frequently observed in cases involving skull fractures (King et al., 2003). The outcome of these studies led to the assumption that linear acceleration alone could be a reliable predictor of brain injury (Bland et al., 2018). Specifically, linear acceleration has been linked to the development of transient intracranial pressure gradients that lead to focal brain injuries and ultimately a concussion from a direct impact (Bland et al., 2018; King et al., 2003; Unterharnscheidt, 1972).

Gurdjian et al. (1945, 1955, 1961, 1963) believed that a brain injury was mainly caused by deformation of the skull and the pressure changes that occurred when the skull was hit directly. Gennarelli and colleagues (1971, 1972), however, showed that when the head moved straight in a horizontal direction (pure translation), it mostly led to localized brain injuries, such as bruises (contusions) and bleeding (hematomas) in specific areas (King et al., 2003). That is, linear acceleration seemed to cause small blood vessels bursting, possibly due to intracerebral cavitation, leading to a concussion. The resultant linear acceleration (RLA) can be calculated using Equation 1.

$$\text{RLA}= \sqrt{a_x^2 + a_y^2 + a_z^2} \tag{1}$$

where a_x=linear acceleration in the x-direction, a_y=linear acceleration in the y-direction, and a_z=linear acceleration in the z-direction

When associating linear acceleration measures with impact locations on the head of youth football athletes, Miller et al. (2018) found that the magnitude of the linear acceleration varied across six locations with three severity levels (low, moderate, and high). For high-magnitude impacts, the front location exhibited the highest linear acceleration at 67.6 g, followed by the rear (51.7 g), facemask (43.5 g), side (41.0 g), oblique (36.5 g), and front boss (32.1 g). Subsequent research, however, has shown that the biomechanics of mTBI is more complex, with head rotation playing a critical role in injury mechanisms (Gabler et al., 2018).

Rotational Acceleration

Rotational kinematics are more closely associated with the shearing of brain tissue, which can result in diffuse injuries. This shear stress comes from the difference in movement between the brain and the skull (McNamara et al., 2020). Ommaya et al. (1966) argued that rotation alone could not produce the same injuries as direct impacts and it required about twice the rotational speed to cause a concussion through indirect impact, like whiplash. Later, Ommaya and Hirsch (1971) stated that rotation could be responsible for about half of the potential for brain injury, with the other half caused by direct impact (King et al., 2003).

Holbourn (1943) was one of the first to say that rotation, either with or without direct impact, could be a key cause of brain injury. The study findings suggested that the shear and stretching forces caused by rotation could result in both concussion and contrecoup contusions (injuries on the opposite side of impact). Lowenheilm (1975) also emphasized angular acceleration as a cause of gliding contusions, which happens due to too much strain on the brain's blood vessels. The researcher highlighted that the deepest parts of the brain could be injured even when the outer surface was not, and that as the duration of the rotational pulse increased, the area of maximum shear moved deeper inside the brain (King et al., 2003).

A series of studies by Gennarelli et al. (1971–1985) using live primates and mechanical models found that angular acceleration played a bigger role than linear acceleration in causing concussions, diffuse axonal injury (DAI), and subdural hematomas. They concluded that rotational acceleration causes these injuries by generating shear strain, and that nearly every type of brain injury could be caused by rotational motion (King et al., 2003). Since real-world head impacts typically involve both linear and rotational acceleration, combined metrics that account for both types of motion have been shown to be more effective predictors of concussion risk (Bland et al., 2018). The formula for rotational acceleration is shown in Equation 2.

$$\theta= \sqrt{\theta_x^2 + \theta_y^2 + \theta_z^2} \tag{2}$$

where θ_x=angular displacement about the x-direction, θ_y=angular displacement about the y-direction, and θ_z=angular displacement about the z-direction

Risk of Head Injury and Concussion

Indices based on measures of linear and rotational acceleration are frequently used to assess the risk of head injury and concussion. The Head Injury Criteria (HIC) is the most used injury criterion for evaluating head injury risk in motor vehicle safety regulations (Zhang et al., 2001). HIC incorporates both the magnitude and duration of head acceleration during an impact to estimate the likelihood of head injury and is commonly used as an injury metric in biomechanical impact studies (Chang et al., 2001). This index is based on measures of linear acceleration. The formula for HIC is shown in Equation 3.

$$\text{HIC}= \left\{(t_2 - t_1)\left[\frac{1}{t_2-t_1}\int_{t_1}^{t_2} a(t)dt\right]^{2.5}\right\}_{max} \tag{3}$$

where a=linear acceleration, and $t_2 - t_1$=time interval where peak acceleration occurs; $t_2 - t_1 \leq 36$ ms.

The AGSI, on the other hand, uses rotational acceleration in radians/s^2 (Rybak, 2021). The formula for AGSI is shown in Equation 4.

$$\text{AGSI}=\int_0^T \left[\frac{\alpha(t)}{88}\right]^{2.5} dt \tag{4}$$

where *α(t)*=instantaneous resultant angular acceleration of the head form, and *T*=duration of the rotational impact.

These kinematic measures and injury risk indices are used to evaluate the effectiveness of helmets, headgear, and surface materials in reducing head injury risk. Controlled impact research shows that head kinematics can provide useful insight into injury mechanisms and brain loading conditions (Foreman, 2024; Hoshizaki et al., 2022; Zhang et al., 2009), including children with CP, due to their increased exposure to fall-related impacts.

Forms of Head Protection

Headgear Designs

Research on head protection started in the 1960s, investigating how to prevent traumatic brain injuries during head impacts. These studies initially focusing on reducing head and neck injuries associated with high-impact activities, particularly contact sports and aviation environments. Early investigations examined the effectiveness of protective helmets in reducing impact forces and preventing head injuries in high school football players (Alley, 1964) and aircraft-related impacts (Ewing & Irving, 1969; Patrick, 1966; Rayne & Maslen, 1969). These foundational studies contributed to the development of biomechanical approaches for evaluating head protection and understanding the relationship between impact loading and head injury risk. Due to ethical and technical limitations of using human data, as well as a lack of standardized test protocols at the time, researchers also use finite element (FE) models of the human head to simulate impact scenarios and investigate the biomechanical mechanisms underlying stress level in brain tissue (Tse et al., 2016). FE modeling and analysis present a non-invasive method to achieve the dynamic changes of stress/strain within internal tissues during daily activities (Zhang et al., 2025). These studies helped establish a foundation for simulating dynamic responses and developing helmet testing protocols, which were validated with experimental data. Material and liner design have been major focuses in recent years. Researchers have developed and examined how helmet shapes and liner types influence the risk of head injury and concussions (Tse et al., 2016).

Mosleh et al. (2017), for example, proposed an Expanded Polystyrene (EPS) composite foam design, which aimed at lowering head rotational acceleration. When conducting 45° oblique impact tests and comparing the results to a conventional single-layer EPS foam with a density of 80 kg/m^3, the researchers found that the EPS composite foam reduced peak rotational acceleration and velocity by 44% and 19%, respectively. Further analysis using overall HIC confirmed that the EPS composite foams significantly reduced the risk of head injury by 19% and 28% based on linear and rotational acceleration measures, respectively (Mosleh et al., 2017). These findings highlighted the strong potential of EPS composite foams for protective helmet applications.

Vanden Bosche et al. (2017) incorporated anisotropic polyether sulfone (PES) foam into a bicycle helmet liner and conducted oblique impact tests. Their findings revealed that the PES helmet achieved nearly a 40% reduction in both peak rotational and translational accelerations compared to the conventional EPS helmet, indicating that PES foam has strong potential to replace EPS in helmet applications.

Recently, cellulose foams have become a new and promising type of material for helmet design. They are gaining attention because they are biodegradable. Cellulose foams are also being considered as a green alternative to traditional plastic foams, especially for use in packaging and cushioning (Feist et al., 2024). Feist et al. (2024) investigated the sustainability cellulose foams as an impact liner in a helmet. The study has shown that cellulosic fibre network structures have the potential to be used in helmets, offering effective impact energy absorption and a sufficient level of injury protection (Feist et al., 2024).

Despite the advances of helmet design, especially in terms of impact absorption of foams, structure and sensor integration, most of the studies have focused on the sport, military, or general use of helmets. However, when it comes to health, specifically children and children with CP, there is a lack of research on the effectiveness of the material used.

CP Headgears. Protective headgear has long been used as a medical intervention for children with special health care needs to reduce the risk of head injury associated with various neurological and developmental conditions. Despite their widespread clinical use, evidence supporting prescription criteria remains limited, and no consistent standards exist to guide helmet prescription (Sneed & Stencel, 2001). Similarly, Jory et al. (2019) concluded that helmet design for individuals with cerebral palsy and seizures remains in its early stages, and that no international standards currently exist for seizure-specific head protection devices. They further noted that existing helmet designs represent a compromise between maximizing impact protection and ensuring comfort, highlighting the need for continued research and development.

The materials and styles used in existing helmets represented a compromise between providing maximum protection and ensuring comfort. Ongoing research and development are, therefore, essential to advance this field. Current headgear designs for children with CP have moved forward with the use of more advanced materials for impact force absorption. These types of material include the D3O® and Lycra®.

D3O®. These impact-protective materials are specialized foams designed to absorb and distribute the forces generated by direct impacts, such as those resulting from falls or blows. Traditional materials often have limitations including rigidity, inflexibility, and excessive weight, which reduce their applicability in the modern era (Avalle et al., 2001). In contrast, newer materials such as D30® are becoming widely adopted across various fields, including military equipment, sports gear, medical devices, and household products because of their smart transition between softness and stiffness under stress. D3O® is a polyurethane-based foam, developed by Palmer in 2004, which has been recognized as one of the top ten future materials. In its natural state, D3O® remains soft and flexible, but upon impact, it rapidly stiffens to disperse energy before returning to its original form. The precise molecular structure of D3O® remains proprietary, but it is classified as an expanding foam and known as a smart molecule due to its single-material composition with exceptional impact resistance (Tang et al., 2017).

Tang et al. (2017) showed that D3O® has a strong strain rate-dependent stiffness, displaying a distinct softness-to-stiffness transition when subjected to increasing strain rates. D3O® is effective in real-world applications where dynamic impact protection is critical. The combination of its microstructural design and polymer matrix composition underlies its performance as a human body-protective material (Tang et al., 2017)

Shargawi et al. (2023) highlighted that the D3O® materials demonstrated consistent behavior under dynamic impact loading (Shargawi et al., 2023). Kajtaz et al. (2016) investigated smart D3O® for rugby headgear using a repeatable biomechanical test method that replicated common concussion-inducing impact scenarios. Their study showed that traditional foams provided insufficient protection, while D3O® significantly reduced concussion risk. Results indicated up to an approximately 40% reduction in risk based on rotational acceleration compared to bare headforms, outperforming current products. These results demonstrated the potential of D3O® to substantially improve helmet and headgear performance for reducing concussion risk (Kajtaz at al., 2016).

Lycra®. Lycra®, also known by its generic name elastane or spandex, represents a major advancement in the field of synthetic fibers. First developed in Germany in 1937, Lycra® possesses properties that are not found in natural fibers, and it is notable because of its remarkable elasticity (Senthilkumar et al., 2011). Lycra® is the general term used to describe elastomeric fibers that exhibit an extension-at-break greater than 200% and demonstrate rapid and full recovery once the applied tension is released. These fibers behave similarly to rubber, with reversible stretch capabilities reaching 400–800%. Typically, Lycra® fibers are derived from a polyurethane-based spinning solution. In the dry spinning method, hot air is used to evaporate the solvent from the filaments as they are formed (Senthilkumar et al., 2011).

According to Willsallen et al. (2014), Lycra® demonstrated distinct mechanical behavior during mechanical testing. In load-to-failure testing, or stress testing, which is a non-functional performance test that measures how a system performs under increasing real-world loads until it reaches its breaking point (Maâlej et al., 2015), Lycra® showed a significantly lower failure load (95.9 ± 23.4 N) than Ethibond™ (a non-absorbable surgical suture which is made of polyester fibers such as polyethylene terephthalate), which showed a much higher failure load (155.2 ± 24.4 N). Lycra® exhibited, however, a much higher displacement at failure (88.4 ± 6.3 mm for Lycra® versus 13.1 ± 7.1 mm for Ethibond™), indicating its high elasticity (Willsallen et al., 2014). Despite these properties, no studies have examined the use of Lycra® in helmet liners or protective helmet design, highlighting a potential area for future research.

In addition to considering headgear as form a head protection to minimize the risk of concussion, it is also important to consider environmental factors that contribute to injury severity, particularly the characteristics of the surface where a child may fall (Branson et al., 2012; Choi et al., 2014; Fahlstedt et al., 2019; Macarthur et al., 2000). Research on children's falls has further emphasized the role that ground surfaces play in determining the risk and severity of injuries (Bertocci et al., 2004).

Ground Surfaces

Compliant surface is a passive intervention that can reduce the stiffness of the ground, which helps absorb some of the force and minimize fall-related injuries in children (Lachance et al., 2016; Laing & Robinovitch, 2009). Surfaces are potentially beneficial in high-risk places where vulnerable people, older adults, and children are at the risk of falling (Lachance et al., 2017).

Between 2008 and 2012, the National Center on Accessibility at Indiana University-Bloomington carried out a long-term study on playground surfaces for children. The main finding highlighted that every type of the playground surface that includes Poured in Place (PIP) rubber, Tiles (TIL), Engineered Wood Fiber (EWF), and Hybrid Surface Systems (HYB) has its own problems. Regardless of the material used, issues related to safety and accessibility appeared within the first year after installation (Skulski, 2011). Overall, no surface was clearly better than the others and each of them had its own weaknesses, especially in real-world installation and long-term durability (U.S. Access Board, 2025).

In a study from the U.S. Consumer Product Safety Commission (CPSC) in 2005, a variety of flooring materials were evaluated for their properties and assessing their effectiveness in reducing injury risk during falls. Drop tests were conducted from heights ranging between 50 mm (2 in) and 300 mm (12 in). The materials were categorized as mats, pads, carpets, and carpet padding. Mats were typically less than 25 mm in thickness, although several exceeded this and ranged from 28 mm to 46 mm. Some mats included laminated or bonded surface coatings to enhance durability and resistance. Pads were defined as materials thicker than 25 mm and were similar in construction to gymnastics pads. Carpet samples included commercial-grade, residential, and indoor/outdoor types. This study highlighted that mat samples were identified as the most effective option, suggesting the best balance between impact protection, material thickness, and cost-efficiency. In contrast, carpeting with padding did not provide sufficient impact reduction and was not recommended as a suitable protective surfacing material (Sushinsky, 2005).

Bertocci et al. (2004) studied different surfaces during a fall by using an ATD drop. The researchers found that the type of surface made a clear difference in the impact results. When the dummy fell onto a soft playground foam surface, the amount of head acceleration was much lower (114 g) than when it fell on harder surfaces like linoleum, carpet, or wood (245g). This outcome means that the foam surface helped absorb the impact better and was safer for the head. This study also measured the coefficient of restitution (COR) for each four surfaces, which highlights how much energy bounces back after something hits the surface. A COR of 1.0 means that the surface is very bouncy, like a rubber ball bouncing off a hard floor. A COR of 0 means there is no bounce at all, and the object just hits the surface and stays there. Playground foam demonstrated the highest COR value at 0.57, indicating greater energy rebound. Carpet followed with a COR of 0.33, while both linoleum and wood had the lowest COR values at 0.12, reflecting minimal rebound upon impact (Bertocci et al., 2004).

Although previous research has demonstrated that ground surface properties influence head impact severity during falls, the interaction between impact surfaces and protective headgear performance remains unclear for the use of protective headgear for children with CP. In particular, limited research has examined whether commercially available protective headgear designed for children with neurological conditions can effectively reduce head impact severity under different fall scenarios.

Research Problem

Children with CP have poor balance, spastic muscles, suffer from seizures, and demonstrate delayed reactions, causing them to fall (Chakraborty et al., 2020; Emmerik et al., 2016), which increases the risk of head injuries for this population (Kuppermann et al., 2009). Although helmets are often recommended to reduce the risk of injury among individual with special needs (Sneed et al., 2008), current helmet research mostly focuses on sports (Yu & Dennison, 2018), or military use (Huang et al., 2022; Pintar et al., 2013). No studies have tested helmets designed, specifically for individuals with CP, particularly for children with CP when they fall on different types of surfaces that they commonly encounter in their daily life, such as wooden floors, foam, linoleum, or carpets. According to Bertocci et al. (2022), floor surfaces behave differently in mitigating impact forces and accelerations to reduce the risk of head injury during a fall. Furthermore, head impact can occur in different locations of the head such as the front, back, and sides, which are all common points of impact in real-world falls for children with CP (Burns et al., 2016; Dubucs et al., 2024; Yu et al., 2023).

Purpose

The purpose of this study was to evaluate the effectiveness of a commercially available protective headgear in reducing head injury risk during fall-related head impacts commonly experienced by children with cerebral palsy (CP) across different impact locations and ground surface conditions. More specifically, the objective of this study was to assess the performance of a Lycra® headgear designed for children with CP, consisting of an outer Lycra® shell and an inner D3O® liner, in mitigating head injury risk. Headgear effectiveness was quantified using linear acceleration, rotational acceleration, HIC, and AGSI during controlled free-fall drop tests conducted on four surface types. The following research questions guided the study:

Research Questions

1. Does a Lycra® headgear designed for children with CP significantly reduce linear acceleration and Head Injury Criteria (HIC) across different head impact locations (front, back, and side) during simulated free falls on various ground surfaces (linoleum, carpet, wood, and playground foam)?
2. Does a Lycra® headgear designed for children with CP significantly reduce angular acceleration and Angular Gadd Severity Index (AGSI) across different head impact locations (front, back, and side) during simulated free falls on various ground surfaces (linoleum, carpet, wood, and playground foam)?

Hypothesis

The following hypotheses were developed based on previous findings indicating that head geometry and impact location relative to the COM influences impact mechanics, (Cobb et al., 2014; Fung, 2013; Meriam & Kraige, 2007), and that the foam materials possess superior energy absorption capabilities during impact (Bertocci et al., 2004). Based on these concepts, it was hypothesized that:

H_1: The effectiveness of the headgear in reducing linear acceleration and HIC would vary across impact locations and surface types, with the greatest reductions occurring during side impacts on playground foam relative to wood, linoleum, and carpet surfaces.

H_2: The effectiveness of the headgear in reducing rotational acceleration and AGSI would vary across impact locations and surface types, with the greatest reductions occurring during front impacts on playground foam relative to wood, linoleum, and carpet surfaces.

Chapter 3 - Method

Design

This study employed a mixed factorial design with impact location as a between-condition factor and ground surface as a repeated-measures factor. Impact conditions were tested across 13 simulated falling heights representing children with CP (Brunner et al., 2024), operationalized through impact velocities, resulting in 156 unique impact combinations. Each condition was repeated three times to ensure reliability, yielding a total of 468 impacts. Dependent variables included linear head acceleration, rotational head acceleration, and injury risk metrics, including Head Injury Criteria (HIC) and Angular Gadd Severity Index (AGSI).

Instruments

Monorail Drop Rig

A Monorail Drop Rig system as shown in Figure 3, to simulate the falling mechanisms of injury for children with CP and test the protective capability of the CP headgear on different ground surfaces was used. The Monorail Drop Rig was designed to mimic the way a human head would fall in a controlled and guided manner.

The reliability of the Monorail Drop Rig system was assessed in a prior pilot study by Carlson (2016), who conducted 100 identical rear impact trials on a NOCSAE surrogate head form at a velocity of 3.13 m/s. Using the split-half technique, which compared data from even- and odd-numbered impacts, Carlson (2006) reported a strong correlation (r=.922, p<.005, n=100), indicating consistent measurements across repeated trials. Carlson (2006) also provided evidence of concurrent validity. This type of validation technique refers to the extent to which the outcomes of a test correspond with those of an established benchmark test (Cronbach & Meehl, 1955). In the pilot study, Carlson (2006) compared linear acceleration values recorded using the Lakehead University impact drop system to linear acceleration measures obtained from the University of Ottawa Neurotrauma Science Research Lab, which served as the gold standard. This comparison was used to evaluate measurement agreement and support the external validity of the drop system by demonstrating consistency with a previously validated experimental protocol. Intraclass correlation coefficients (ICCs) revealed strong agreement across all impact locations: frontal (ICC=.922, $p<.005$), front boss (ICC=.844, $p<.005$), side (ICC=.934, $p<.005$), rear boss (ICC=.952, $p<.005$), and rear (ICC=.932, $p<.005$), providing robust evidence of concurrent validity (Carlson, 2016).

Figure 3

Monorail Drop Rig.

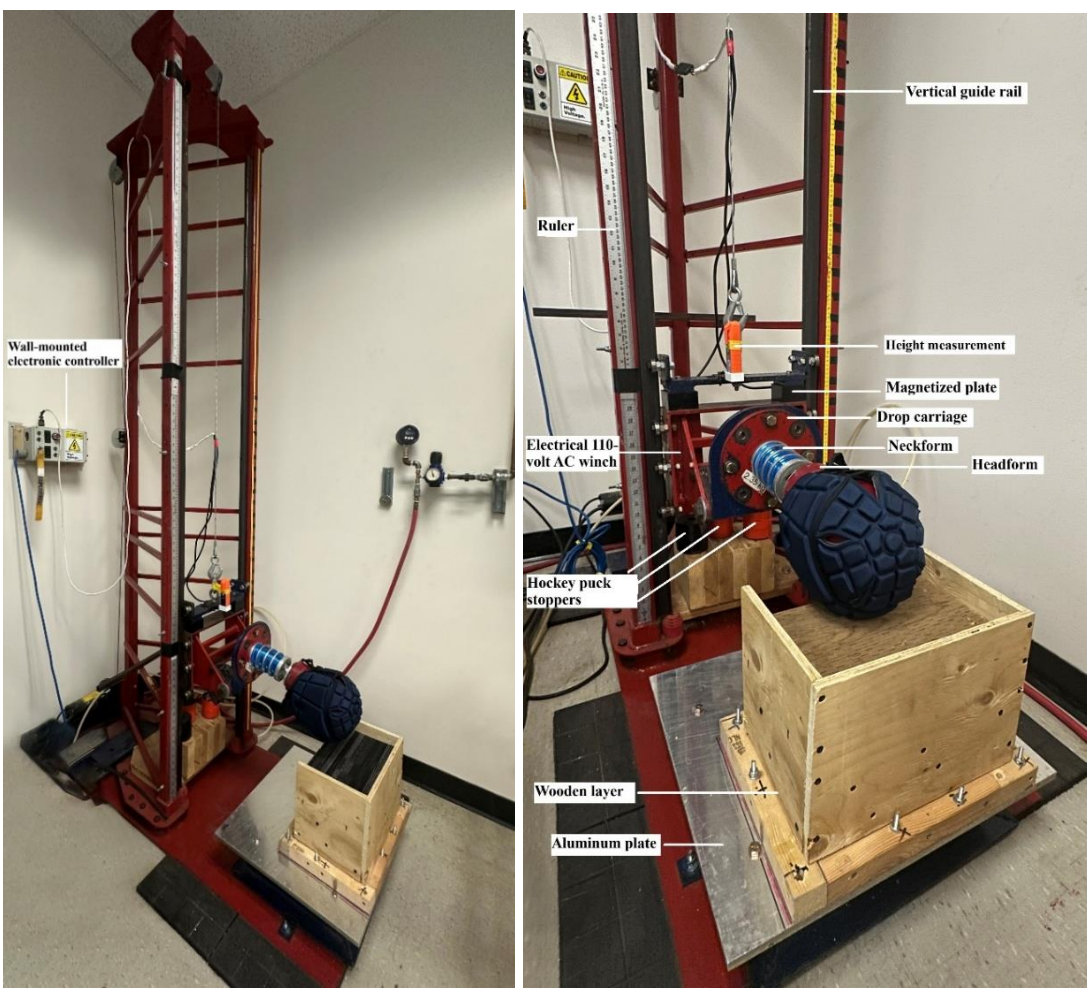

The Monorail Drop Rig system (see Figure 3) consists of several key components designed to control the impact testing. The system featured a vertical guide rail that ensures a consistent drop trajectory. An electrical 110-volt AC winch connected to magnetized plates was used to grab and move the drop carriage, along with a surrogate headform and mechanical neck, to the desired drop height. Once in position, an electronic release switch initiated the movement of the drop carriage in free-falling. The winch was controlled by a wall-mounted electronic controller that had a simple switch to raise or lower the rig, as needed. Pressing the release switch turned off the magnets, allowing the drop carriage and headform to fall freely to the surface below (Gimbel & Hoshizaki, 2008). The impact anvil included a customized aluminum plate (dimensions 51 cm × 46.5 cm with a 1 cm thickness) and a wooden layer (dimensions 32.5 cm × 21.5 cm and a height of 26.5 cm) placed on top of the aluminum plate. This wooden layer was used to position different testing surfaces (as shown in Figure 12), to address the research questions for this study.

HeadForm for Children

A child-sized headform was used to test the CP LYCRA® headgear. This headform has been approved by NOCSAE (2025) and it has a weight of 4.12 kg (9.08 lbs) and head circumference of 53.4 cm (21.02 in). This type of headform accommodates male and female children between the 50^{th} and 75^{th} percentile (World Health Organization, 2024; see Figure 4). This headform is designed to simulate how a child's head reacts during an impact with helmets. The headform is instrumented with high-frequency impact accelerometers to measure the linear impact acceleration units of g (g=9.8 m/s^2). Testing with this headform was conducted using NOCSAE guidelines to assess the effectiveness of the CP headgear at different locations of the head on different ground surfaces while ensuring precision and accuracy during the simulated head collisions. The NOCSAE guidelines ensure safety compliance through rigorous impact testing that evaluates key biomechanical metrics, including PLA to calculate HIC and impact duration, to determine if a helmet meets defined performance thresholds. While the NOCSAE standard includes processes for recertification and requires a visible seal of compliance, this study utilized its core testing methodology to provide a validated and repeatable assessment of the helmet's protective capabilities (NOCSAE, 2025).

Figure 4

Headform for Children

Note. Adapted from Standard Test Method and Equipment Used in Evaluating the Performance Characteristics of Headgear/Equipment (NOCSAE, 2025). https://nocsae.org/standard-test-method-and-equipment-used-in-evaluating-the-performance-characteristics-of-headgear-equipment/

Mechanical Neckform

The neckform that was used in this study consists of four thermoplastic (TPU material) discs positioned between circular aluminum discs. To prevent slippage between the TPU and aluminum discs, each disc material included a protruding cylindrical offset. This design allows both disc materials to be pressed tightly together, while a top aluminum plate and base bracket hold the assembly sturdy (see Figure 5). The TPU discs and aluminum end plates are shaped like a neck to imitate how a real neck moves when a force is applied. The neck form also contains a wire-rope system that can be tightened to adjust the neck stiffness and range of motion to control neck bending and rotation when simulating a child's head collision (Carlson, 2016).

Figure 5

Mechanical Neckform

Linear Accelerometer Sensors and Power Supply

Triaxial linear accelerometers instrumented inside the surrogate headform measured the linear impact acceleration in three directions, including the superior-inferior, anterior-posterior, and left-right directions, noted as x, y, and z (see Figure 6). These analog accelerometer sensors were connected to a PCB model 482A04® power supply and amplifier (see Figure 6). The accelerometer's analog signals were sent from the PCB model 482A04® amplifier unit to an A/D Instruments® PowerLab® 16/30 analog-to-digital converter, which recorded the data at a sampling frequency of 20 kHz. The PowerLab® 16/30 system has 16 analog input channels and can handle input voltages ranging from ±2 mV to ±10 V. Each analog signal from the accelerometers was converted into a digital signal and then recorded using LabChart® data acquisition software (Carlson, 2016).

Figure 6

Linear Acceleration Sensor (Left) and Power Supply (Right)

In this study, the first three analog input channels of the A/D Instruments® PowerLab® unit were used for collecting data from the linear accelerometers. Channel 1 acquired the acceleration in the x-axis, Channel 2 in the y-axis, and Channel 3 in the z-axis. A fourth channel was used to calculate the overall resultant linear acceleration experienced by the headform using Equation 1. A low pass SAE j211 digital filter with a cut-off frequency of 1000 Hz was applied to the resultant acceleration data to eliminate the noise generated due to vibrations induced to the headform during free-falling (Pennock et al., 2021).

Rotational Gyroscope Sensor Integrated in Delsys® System

The rotational gyroscope sensor integrated in the Delsys Trigno™® wireless system (see Figure 7) measures the angular velocity of a moving object in the x, y, and z directions. In the current study, the angular velocity measured by this sensor was used to derive the angular acceleration of the surrogate head form in the x, y, and z directions for each impact. This gyroscope sensor collected the data at a frequency of 148 kHz, which is lower than the frequency of the linear accelerometers. To ensure accuracy, an alignment or synchronization process was conducted by converting the lower frequency data signals of the Delsys Trigno™® wireless system to match the higher frequency data signals of the linear accelerometers. gyroscope sensor was placed on the top location of the surrogate head form and was reinforced with tape to secure during data collection. The resultant angular acceleration was computed using Equation 2.

Figure 7

Delsys Trigno™® Wireless (Right) and Rotational Gyroscope Sensor (Left)

PowerLab® System and Software

The ADInstrument PowerLab® system and Labchart® software (see Figure 8) was used to capture the linear acceleration analog signals from the PCB model amplifier at a frequency of 20 kHz. This PowerLab® system offers reduced interference and connects to the computer via USB (ADInstruments, 2025). More specifically, the ADInstruments PowerLab® data acquisition system is designed for high accuracy and precision in data collection. It functions as a modular platform, enabling configuration and flexibility for data collection. The PowerLab® hardware also allows researchers to interface different systems to collect data simultaneously at high-speed sampling rates to ensure reliable data acquisition.

Figure 8

PowerLab® System and LabChart® Software.

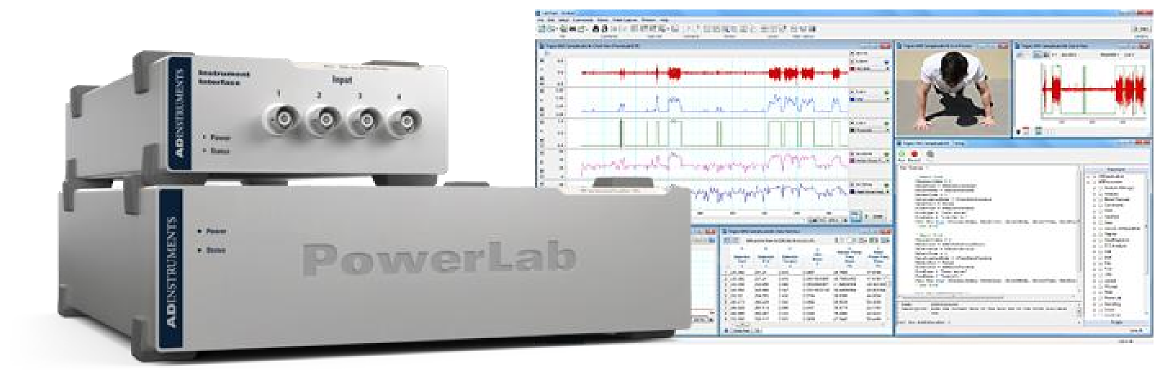

Note. Adapted from PowerLab® for Education, by ADInstruments®, 2025, https://www.adinstruments.com/products/powerlab/education Copyright 2025 by ADInstruments®.

LYCRA® Headgear

This type of headgear (see Figure 9) is available on the global market and commonly used for children with CP. The headgear is made from lightweight, breathable, and medical-grade materials that feel soft and comfortable but are also strong enough to protect the head. This type of material helps prevent the headgear from getting too hot, which is important for children who need to wear it throughout the day. The headgear includes a hook-and-loop chin strap and adjustable laces at the back, which help the helmet fit well on different head shapes and sizes, making it secure and comfortable to wear.

The outside of the headgear is covered with Lycra® fibers (GuardianHelmets, 2020). Lycra® fibers are used in protective equipment due to their stretch and recovery elastic properties. These Lycra® fibers can stretch to approximately 5 to 8 times their original length and return to their initial shape without deformation (Sewport, 2019).

The inside of the helmet is made of an innovative D3O® smart molecule technology material (GuardianHelmets, 2020). As a type of smart molecule technology, D3O® molecular composition remains soft and flexible under normal conditions; however, upon impact, it temporarily locks together, effectively dispersing energy before returning to its original flexible state (Tang et al., 2017).

Figure 9

Guardian Helmet Designed for Children with CP.

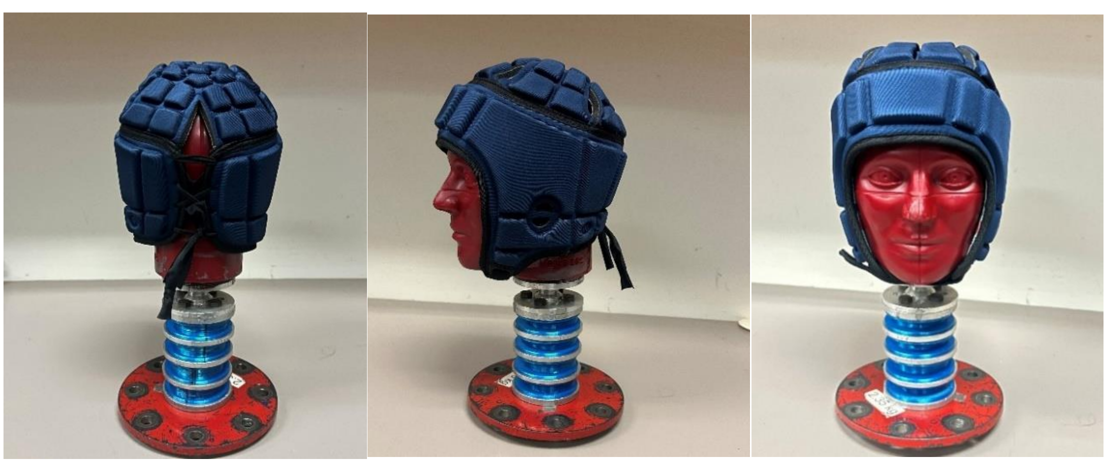

Procedure

Headform and Mechanical Neckform

Before beginning the testing, the mechanical neck form (see Figure 3) was attached to the 4.12 kg (9.08 lb) NOCSAE headform, which has a head circumference of 53.4 cm (21.02 in) to represent a child's head. According to Ouyang et al. (2005), for children from 2 to 12 years old, the mechanical neck was calibrated by applying a torque of 0.72 ± 0.07 Nm (6.37 ± 0.62 lb-in) using a digital torque wrench, which utilizes an electronic strain gauge to measure and display the applied torque in Nm (see Figure 10). This calibrated torque represented the neck strength of a child between 5 to 8 years of age, which is considered the age range with the highest risk of falling (Boyer & Patterson, 2018). After completing the neck calibration, the headform and neckform were attached to the drop carriage, which moved in free-falling along a frictionless rail system of the vertical drop impactor (see Figure 1). A CP LYCRA® headgear designed for children with CP was fitted onto a small-sized headform using the manufacturer's fitting instructions to achieve a secure and appropriate fit.

Figure 10

Calibration of Neckform with a Digital Torque Wrench

Fitting the Headgear to Headform

The process of fitting the headgear on the headform involved placing the thumbs inside the jaw extensions and the index fingers into the ear openings, then rolling the headgear onto the head from front to back (see Figure 11). The headgear should sit low on the forehead, just above the brow line, with the chin strap fastened securely beneath the jaw and securely adjusted (Regis School, 2022). To assess the quality of the headgear fit, the headform was gently rotated to an inverted (top-down) position without fastening the chin strap. If the headgear remains in place without shifting, the fit is considered appropriate. If the headgear moves, it may be too large, or if a visible gap exists between the crown of the headform and the interior surface of the headgear, it may be too small (NOCSAE, 2025). For this study, however, the headgear was designed to fit the child's surrogate headform.

Figure 11

Fitting Instruction of CP LYCRA® Helmet

Ground Surfaces

After the helmet has been properly fitted on the surrogate headform, the researcher selected four different types of surface materials to mimic ground surfaces conditions typically encountered by children with CP. These surface ground conditions include wood, playground foam, linoleum, and carpet. Each ground surface condition was placed on a wooden rectangular frame (dimensions of 32.5 cm × 21.5 cm and height of 26.5 cm) bolted to a metallic plate (dimension of 51 cm × 46.5 cm and 1 cm thickness) at the base of the vertical impactor (see Figure 12). The head form was positioned to strike three impact locations (front, side, and back) respectively for each surface ground condition, as shown in Figure 13.

Figure 12

Ground Surfaces Mounted on the Anvil of the Monorail Drop Rig

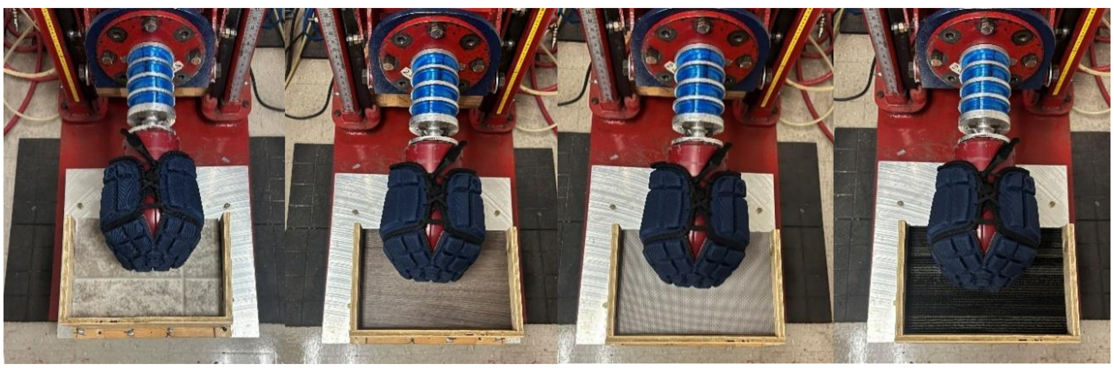

Note. The surfaces from left to right are linoleum, wood, playground foam, and carpet.

Figure 13

Common Impact Locations for Children with CP

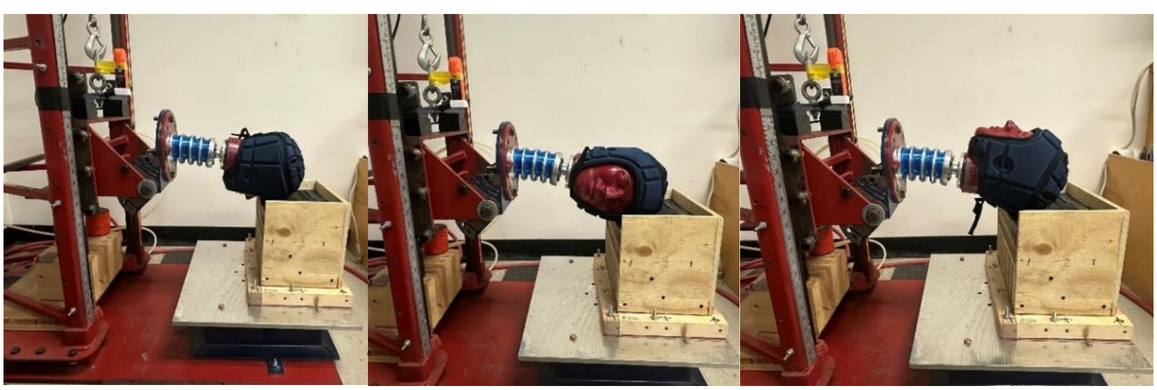

Note. The head locations from left to right are front, side, and back.

These three impact locations were selected because the most frequent head impact locations in children and youth populations occur at the frontal (front of the head/forehead), temporal-parietal (sides and upper sides of the head/temples), and occipital (back of the head) regions during falling. The frontal region, including the forehead, is commonly impacted during falls. In youth sports, it is associated with relatively high linear and rotational accelerations (Cobb et al., 2013; Miller et al., 2018). The temporal-parietal region, which covers the sides and upper back of the head near the temples and parietal bone, is frequently involved in skull fractures and severe head injuries in young children (Burrows et al., 2015; Hughes et al., 2016). The occipital region, located at the back of the head, is also a common impact site during falls in children and older adults and may be exposed to higher accelerations depending on the fall scenario (Dubucs et al., 2023; Kelley et al., 2017; Sedlák et al., 2023).

Identifying Impact Locations on the Headform

The researcher used the NOCSAE standard test methods to identify these three locations on the surrogate head form, as shown in Figure 1. According to Higgins et al. (2007), when referring to the NOCSAE headform, the front location is situated in the median plane approximately 25 mm (1 in) above the anterior intersection of the median and reference plane. The back location is situated approximately at the intersection of the median and reference plane. The side location is situated approximately at the intersection of the reference and coronal planes on the right or left side of the headform.

Neck Flexion Angle at Impact

Neck flexion angle at impact was controlled by adjusting the movement distance between the head when it contacted the ground surface and the drop carriage when it contacted the hockey puck stoppers (see Figure 1). The neck flexion angle was adjusted to approximately 98° to represent the average head–torso angle during ground impact in children between 6 and 10 years of age during a fall (Dibb et al., 2014). This angle represents the relative orientation between the head and torso during the impact event. While the information is based on pediatric computational impact simulations conducted with models representing 6-year and 10-year-old children (Dibb et al., 2014), the focus of this study is on children aged 5–8 years, the age range with the highest risk of falling (Boyer & Patterson, 2018). The findings revealed that the angle of neck flexion relative to head contact and torso position at impact during the fall was approximately 85° (±10°) for a 6-year-old child. Whereas, for a 10-year-old child, the angle of neck flexion reached approximately 110° (±14.6°) (Dibb et al., 2014). The researchers computed the average across these two pediatric age groups, and the angle of neck flexion at impact was found to be 98° (±13°).

This configuration also allowed the researcher to approximate pediatric head–neck orientation during falls across the front, side, and back impact locations. For the front impact location, two hockey puck stoppers were used to allow greater forward motion of the headform–neck system during impact. For the side and back impact locations, one hockey puck stopper was used to produce comparatively more restricted head–neck motion during impact. This approach was supported by previous fall simulation research demonstrating that head impact orientation and impact angle vary according to fall direction and fall mechanics during pediatric falls (Yu et al., 2023).

Age-Specific Modeling

The head impact was modelled based on the dropping heights experienced by younger children with CP between 5 and 8 years of age, including both males and females who fall more often than older children with CP. Furthermore, research shows that the highest risk of falling occurs between the ages of 5 and 8 years, a period when they are still developing critical balance and motor skills (Boyer & Patterson, 2018). Therefore, this study focused on this high-risk age group to test the effectiveness of protective headgear.

Simulated Drop Heights. According to the CDC stature-for-age growth charts, the typical height of TD children between 5 and 8 years varies across percentiles. At the 25th percentile, boys range from approximately 105.5 cm (age 5 years) to 123.0 cm (age 8 years), while girls range from about 104.0 cm to 121.5 cm. At the 50th percentile (median), boys range from about 110.0 cm (age 5 years) to 128.0 cm (age 8 years), and girls from 109.0 cm to 127.0 cm. At the 75th percentile, boys range between 112.5 cm (age 5 years) and 130.5 cm (age 8 years), and girls between 111.0 cm and 129.0 cm. These values suggest that, within this age group, TD children's height spans from about 104 cm to 130 cm, depending on age, sex, and percentile ranking (CDC, 2023).

Research by Kong et al. (1999) suggests that children with CP tend to have delayed physical development and shorter stature compared to TD peers. Brunner et al. (2024) emphasized the importance of growth assessment in children with CP, reporting age- and sex-specific height data, for ages 4–5 years, mean heights were 100.0 cm (SD=10.1) for males and 109.4 cm (SD=11.5) for females; for ages 6–7 years, 112.4 cm (SD=11.8) for males and 111.2 cm (SD=12.9) for females; and for ages 8–9 years, 126.0 cm (SD=5.2) for males and 117.4 cm (SD=12.7) for females (Brunner et al., 2024).

This study examined falls that occur while children with CP are standing, walking, or seated, either on a chair or on the ground, while also considering that the front, side, and back locations of the head are positioned lower than overall body height. Accordingly, a height range from 40 to 100 cm was used to represent the fall heights of children aged 5 to 8 years with CP.

Impact Velocities. The head impact velocities for the CP children simulated falling heights were determined using Equation 5 for free-falling kinematics.

$$V^2 = 2gh \qquad (5)$$

where *V*=final velocity (in m/s), *g*=acceleration due to gravity (≈ 9.81 m/s^2 on Earth), and *h*=height from which the CP child falls (m).

Based on pilot data, 13 observations were required to achieve 80% power at an alpha level of 0.05 for detecting a large effect ($\eta p^2 = 0.25$), with height values ranging from 40 to 100 cm evaluated in 5-cm increments. The 13 corresponding impact velocities are shown in Table 1. The headgear impact tests were conducted at these velocities across three different impact locations and four ground surfaces.

Table 1

Height and Corresponding Impact Velocity

	Height (m)	Impact Velocity (m/s)
1	0.40	2.80
2	0.45	2.97
3	0.50	3.13
4	0.55	3.28
5	0.60	3.43
6	0.65	3.57
7	0.70	3.70
8	0.75	3.83
9	0.80	3.96
10	0.85	4.08
11	0.90	4.20
12	0.95	4.31
13	1.00	4.43

Conducting Dynamic Drop Tests

Once the head form, mechanical neck, headgear impact surfaces, and sensor have been properly set up, the carriage was elevated along the vertical guide rail to the designated drop height using the electronic winch system. The exact height was verified using an electronic height measurement device to ensure precision and consistency across all trials. When the carriage reached the target height, the magnets held it firmly in place until the release command was initiated.

At the start of each trial, the release switch was activated, disengaging the magnetic hold and allowing the drop carriage to descend freely under the influence of gravity. The carriage, along with the headform, neck assembly, and headgear, travelled smoothly along the guide rail to maintain a controlled vertical trajectory. The moment of impact occurred when the headform and headgear contact the designated surface, replicating the dynamic conditions of a child's fall from the corresponding height.

Following the impact, the system was brought to rest, and data from the embedded sensors were recorded for analysis. The headform, neck assembly, and headgear were then carefully reset, and the next drop height or surface condition was prepared. This sequence was repeated systematically across all pre-determined drop heights and surface configurations to ensure a comprehensive evaluation of the protective performance of the headgear. The headgear was readjusted for each drop test, and the calibration of the mechanical neck was rechecked when changing the impact locations of the headform.

Analysis

A two-way mixed factorial ANOVAs were administered to examine the interaction effects between headgear impact location (front, back, and side) and under-mat surface (linoleum, carpet, wood, and playground foam) on each dependent variable, linear acceleration, Head Injury Criteria (HIC), rotational acceleration and Angular Gadd Severity Index (AGSI), respectively. Mauchly's Test was administered to examine if the assumption of Sphericity was met for equal variance. If it was not met, then the Greenhouse-Geisser technique was applied to examine if the interaction was significant.

If a significant interaction between headgear location and ground surface was identified, simple-effects analyses were conducted to examine the effect of headgear location within each ground surface, as well as the effect of ground surface within each headgear location for each dependent variable to further explain the interaction. Post-hoc pairwise comparisons were performed using the least significant difference (LSD) procedure.

Chapter 4 – Results

Dynamic Testing

Research Question One

Does a CP Lycra® headgear designed for children with CP significantly reduce linear acceleration and HIC across different head impact locations (front, back, and side) during simulated free falls on various ground surfaces (playground foam, wood, linoleum, and carpet)?

The researcher hypothesized that the effectiveness of the headgear in reducing linear acceleration and HIC would vary across impact locations and surface types, with the greatest reductions occurring during side impacts on playground foam relative to wood, linoleum, and carpet surfaces (Bertocci et al., 2004; Cobb et al., 2014; Fung, 2013; Meriam & Kraige, 2007). Before addressing this hypothesis inferentially, the mean across the three trials was computed for measures of linear acceleration and HIC. These means trials were then used to calculate the means, standard deviations (SD) and standard errors (SE) for each combination of ground surface and impact location, which are reported in Table 1 Appendix A. These descriptive statistics were subsequently used to compute mean differences and SE for pairwise comparisons in the inferential analyses.

The researcher addressed this hypothesis inferentially by conducting 3 (impact location: front, back, and side) × 4 (ground surface: linoleum, carpet, wood, and playground foam) two-way mixed factorial ANOVAs with repeated measures on ground surface to examine the interaction effect between these factors, on measures of linear acceleration and HIC, respectively.

Linear Acceleration. The assumption of sphericity for measures of linear acceleration was assessed across ground surface types. Mauchly's Test of Sphericity indicated that the assumption of equal variance was not violated, $\chi^2(5)=8.23,\ p>.05$. When conducting the inferential analysis, the mixed factorial ANOVA indicated a statistically significant interaction effect between impact locations and ground surface on measures of linear acceleration, $F\ (6, 108) = 39.10$, $p < .05$, $\eta^2 = .685$ (large effect), as shown in Figure 14. This outcome suggests that the influence of impact location on linear acceleration varies substantially across ground surfaces.

Figure 14

Interaction Between Impact Locations and Ground Surfaces on Linear Acceleration

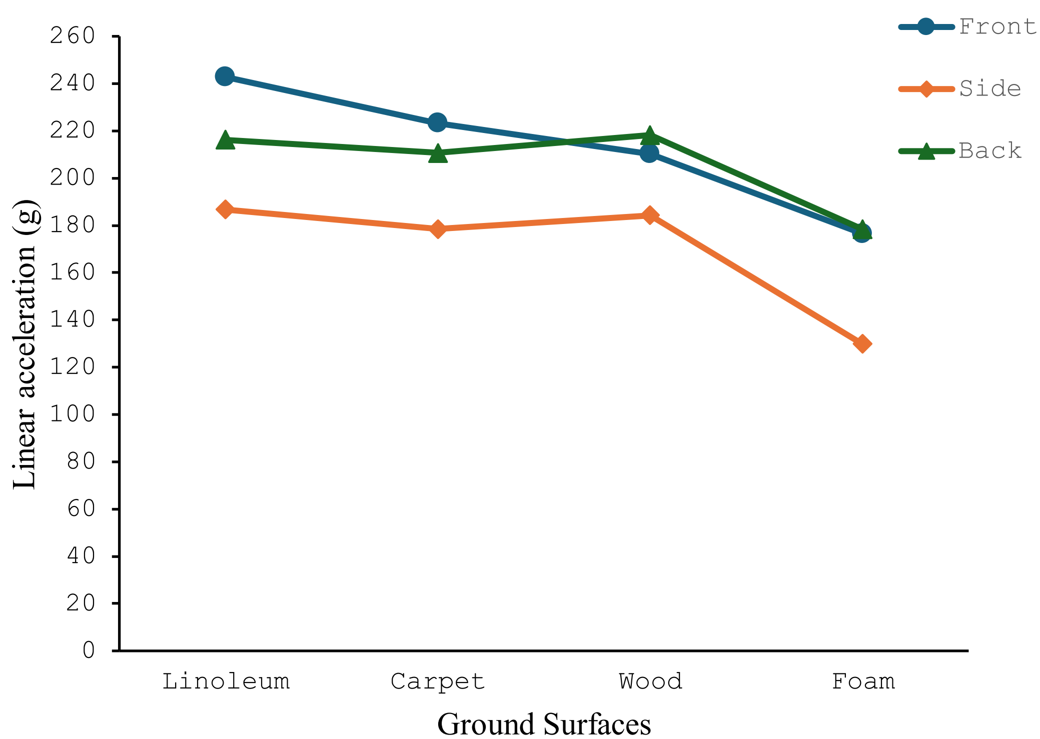

To help explain this interaction, a simple effect analysis was conducted using one-way ANOVAs for independent measures at each ground surface separately to examine if differences between headgear impact locations were statistically significant on linear acceleration (see Figure 15). For the linoleum ground surface, the one-way ANOVA results indicated statistically significant differences between impact locations, $F\ (2, 36) = 3.88$, $p < .05$, $\eta^2 = .18$ (large effect).

This outcome suggests that 18% of the variance in linear acceleration on the linoleum surface is explained by headgear impact location. LSD pairwise comparisons were conducted to identify the differences between impact locations for the linoleum ground surface on measures of linear acceleration. The results indicated statistically significant differences between front and side impact locations ($M_{(diff)}$=56.07g, SE=20.15 g, 95% CI:[15.208, 96.934], p<.05) as shown in Figure 15.

Figure 15

Simple Effect of Linoleum on Linear Acceleration

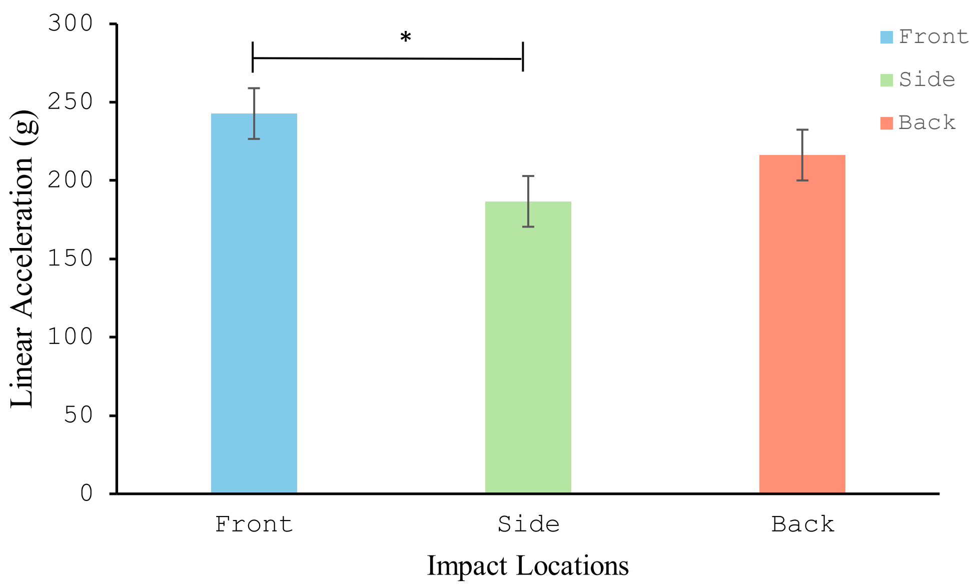

*Note: * indicates significant differences between groups at p<0.05*

For the carpet ground surface, the one-way ANOVA results indicated statistically significant differences between impact locations, F (2, 36)=3.32, p<.05, η^2=.16 (large effect). This outcome suggests that 16% of the variance in linear acceleration on the carpet surface is explained by headgear impact location. LSD pairwise comparisons were conducted to identify the difference between impact locations for the carpet ground surface on measures of linear acceleration. The results indicated statistically significant differences between the front and side impact locations ($M_{(diff)}$=44.85g, SE=17.96 g, 95% CI:[-81.290, -8.422], p<.05) as shown in Figure 16.

Figure 16

Simple Effect of Carpet on Linear Acceleration

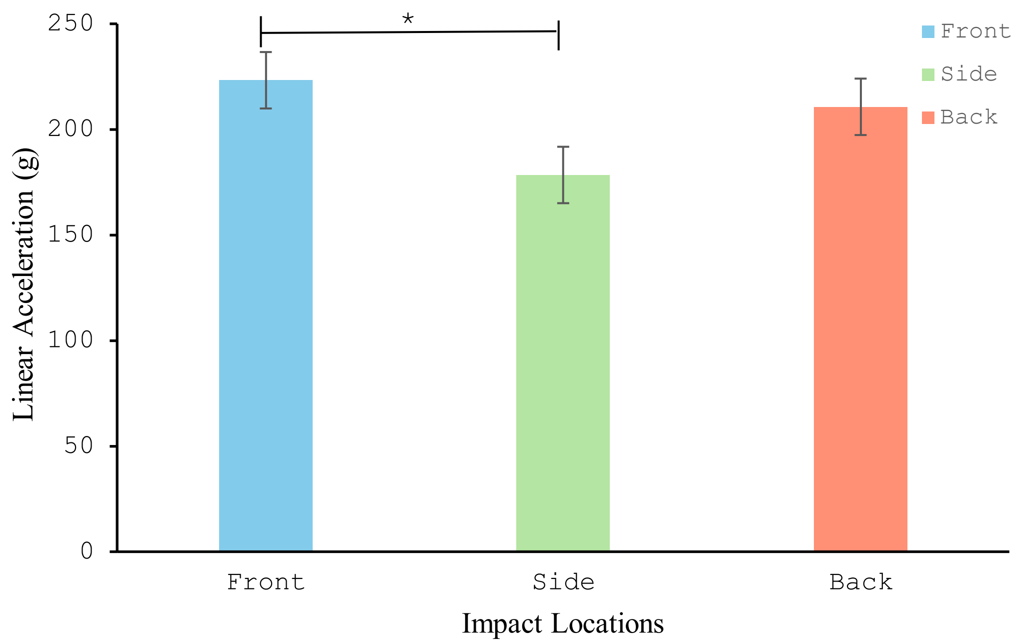

*Note: * indicates significant differences between groups at p<0.05*

For the wood surface, there were no statistically significant differences between impact locations on linear acceleration $F(2,36)=1.89,\ p>0.05, \eta^2=.09$ (small effect). For the foam surface, the one-way ANOVA results indicated statistically significant differences between the impact locations, $F(2, 36)=4.92$, $p<.05$, $\eta^2=.21$ (large effect). This outcome suggests that 21% of the variance in linear acceleration on the foam surface is explained by headgear impact location. LSD pairwise comparisons indicated that there were statistically significant differences between front and side impact locations ($M_{(diff)}$=46.71g, SE=17.56 g, 95% CI:[11.100, 82.334], p<.05) and between side and back impact locations ($M_{(diff)}$=-48.59g, SE=17.56 g, 95% CI:[-84.210, -12.976], p<.05) as shown in Figure 17.

Figure 17

Simple Effect of Foam on Linear Acceleration

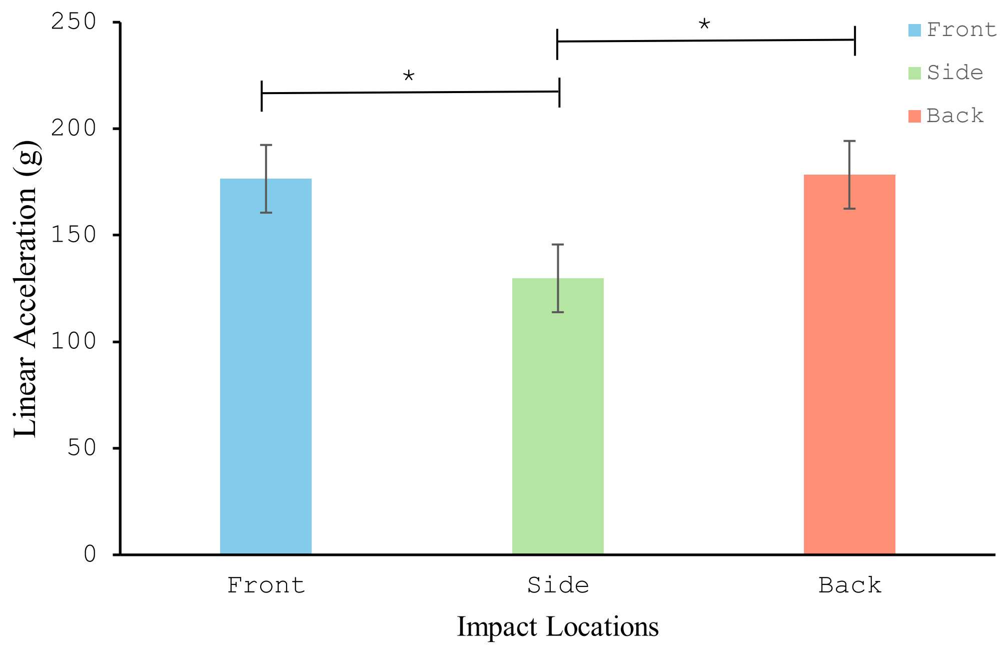

*Note: * indicates significant differences between groups at p<0.05*

Head Injury Criteria (HIC). The assumption of sphericity for measures of HIC was examined across ground surfaces type. Mauchly's Test of Sphericity indicated that the assumption was violated, $\chi^2(5)=41.36, p<.001$. Therefore, the Greenhouse Geisser correction was applied to the degrees of freedom for the within-subjects effects (ε=.617). The mixed factorial ANOVA indicated a statistically significant interaction effect between the impact locations and ground surface on HIC, $F(3.36, 60.47)= 15.76$, $p<.001$, $\eta^2=.467$ (large effect) as shown in Figure 18. This outcome suggests that the influence of impact location on HIC varies substantially across ground surfaces.

Figure 18

Interaction Between Impact Locations and Ground Surfaces on HIC

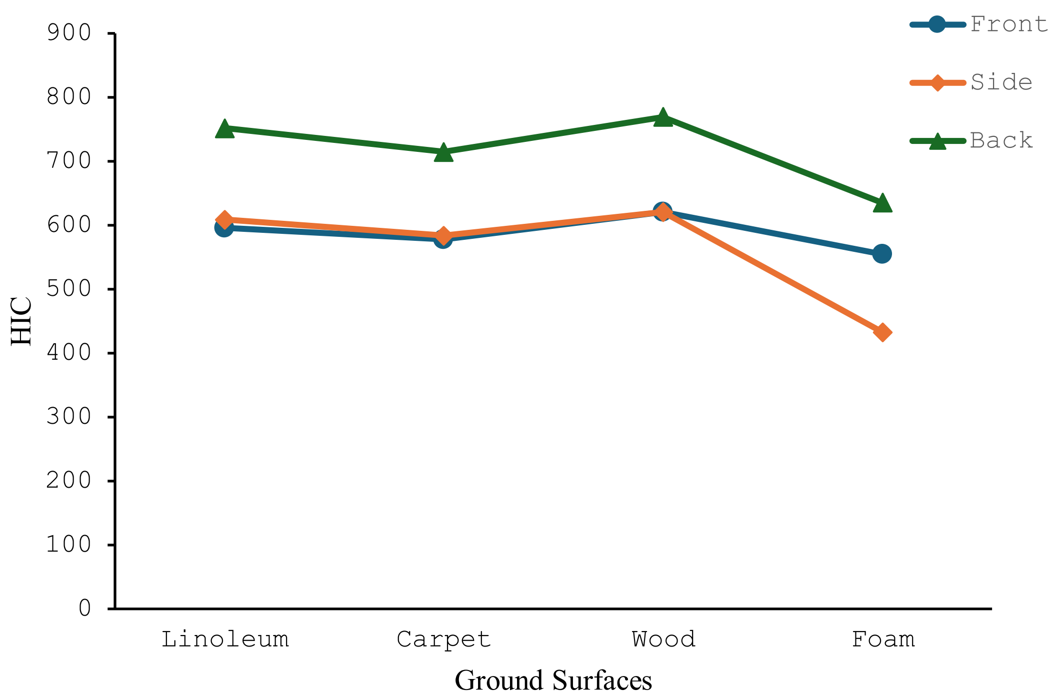

To help explain this interaction, a simple effect analysis was conducted on the between factor using one-way ANOVAs for independent measures to examine the differences between headgear impact locations at each ground surface. The one-way ANOVA results indicated no statistically significant differences between impact locations for the linoleum ground surface, $F\ (2, 36) = 1.819, p > .05, \eta^2 = .092$ (small effect); carpet surface, $F\ (2, 36) = 1.538, p > .05, \eta^2 = .079$ (small effect); wood surface, $F\ (2, 36) = 1.771, p > .05, \eta^2 = .090$ (small effect) and foam ground surface, $F(2, 36) = 2.031, p > .05, \eta^2 = .101$ (medium effect).

To further clarify this statistically significant interaction effect, the researcher conducted an additional simple effect analysis on the within factor using one-way ANOVAs for repeated measures to examine the differences in ground surfaces at each impact location. For the front location, the Mauchly's Test of Sphericity indicated that the assumption of sphericity was violated, $\chi^2(5)=31.60$, $p<.001$; therefore, the Greenhouse–Geisser correction ($\varepsilon=.429$) was applied. The one-way ANOVA results indicated statistically significant differences in ground surfaces at the front impact location, $F(1.22, 14.66)=5.41$, $p<.05$, $\eta^2=.311$ (large effect). This outcome suggests that 31.1% of the variance in HIC is explained by the effect of ground surface at the front location. LSD pairwise comparisons indicated that statistically significant differences were observed between linoleum and carpet ($M_{(diff)}=18.073$, SE=5.81, 95% CI:[5.410, 30.736], $p<.05$), between linoleum and wood ($M_{(diff)}=-24.81$, SE=6.55, 95% CI:[-39.08, -10.54], $p<.05$), between carpet and wood ($M_{(diff)}=-42.89$, SE=7.69, 95% CI:[-59.634, -26.141], $p<.05$) and between wood and foam ($M_{(diff)}=66.076$, SE=21.942, 95% CI:[18.268, 113.884], $p<.05$) surfaces as shown in Figure 19.

Figure 19

Simple Effect of Ground Surfaces across Front Impact Location on HIC

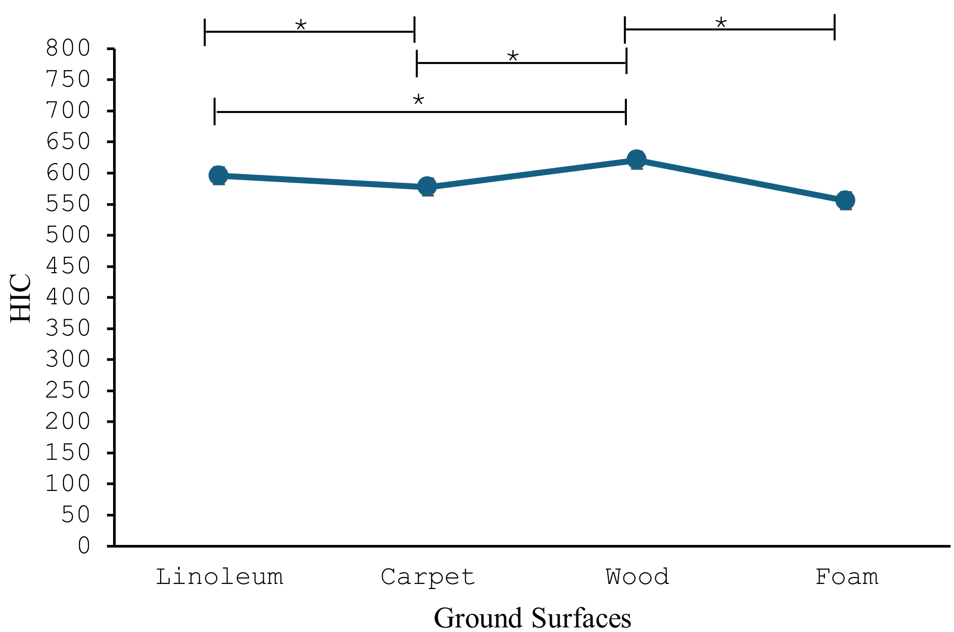

*Note: * indicates significant differences between ground surfaces on HIC for the front location*

For the side impact location, Mauchly's Test of Sphericity indicated that the assumption of sphericity was not violated, $\chi^2(5)=2.37, p>.05,$ suggesting that the variance was homogeneous. The one-way repeated measures ANOVA results indicated statistically significant differences in ground surfaces, $F(3, 36)=191.17$, $p<.05$, $\eta^2=.941$ (large effect), indicating that ground surface accounted for 94.1% of the variance in HIC at the side location. LSD pairwise comparisons indicated that statistically significant differences were observed between linoleum and carpet ($M_{(diff)}=25.164$, SE=9.317, 95% CI:[4.864, 45.465], $p<.05$), between linoleum and foam ($M_{(diff)}=176.02$, SE=8.85, 95% CI:[156.752, 195.293], $p<.05$), between carpet and wood ($M_{(diff)}=-36.97$, SE=9.24, 95% CI:[-57.101, -16.843], $p<.05$), between carpet and foam ($M_{(diff)}=150.86$, SE=7.33, 95% CI:[134.882, 166.835], $p<.05$), between wood and foam ($M_{(diff)}=187.83$, SE=10.20, 95% CI:[165.603, 210.058], $p<.05$) surfaces as shown in Figure 20.

Figure 20

Simple Effect of Ground Surfaces across Side Impact Location on HIC

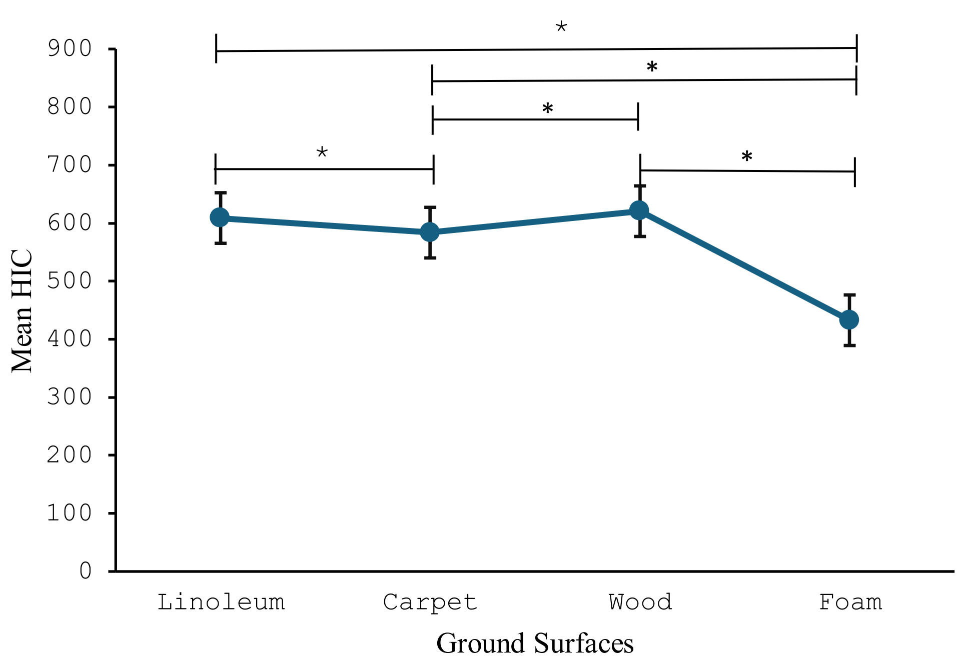

*Note: * indicates significant differences between ground surfaces on HIC for the side location*

For the back impact location, Mauchly's Test of Sphericity indicated that the assumption of sphericity was not violated, $\chi^2(5)=2.7, p>.05,$ suggesting that the variance was homogeneous. The one-way repeated measures ANOVA results indicated statistically significant differences in ground surfaces, $F(3, 36)=231.660$, $p<.001$, $\eta^2=.951$ (large effect), indicating that ground surface accounted for 95.1% of the variance in HIC at the back location. LSD pairwise comparisons indicated that statistically significant differences were observed between linoleum and carpet ($M_{(diff)}=37.02$, SE=4.36, 95% CI:[27.52, 46.508], $p<.05$), between linoleum and wood ($M_{(diff)}=-17.55$, SE=4.92, 95% CI:[−28.268, −6.837], $p<.05$), and between linoleum and foam $M_{(diff)}=116.56$, SE=6.09, 95% CI:[103.297, 129.817], $p<.05$) surfaces. Statistically significant differences were also observed between carpet and wood ($M_{(diff)}=-54.57$, SE=5.86, 95% CI:[−67.340, −41.801], $p<.05$) and between carpet and foam ($M_{(diff)}=79.54$, SE=6.21, 95% CI:[66.000, 93.077], $p<.05$) surfaces. Finally, statistically significant differences were observed between the wood and foam ($M_{(diff)}=134.11$, SE=5.53, 95% CI:[122.069, 146.149], $p<.05$) surfaces as shown in Figure 21.

Figure 21

Simple Effect of Ground Surfaces across Back Impact Location on HIC

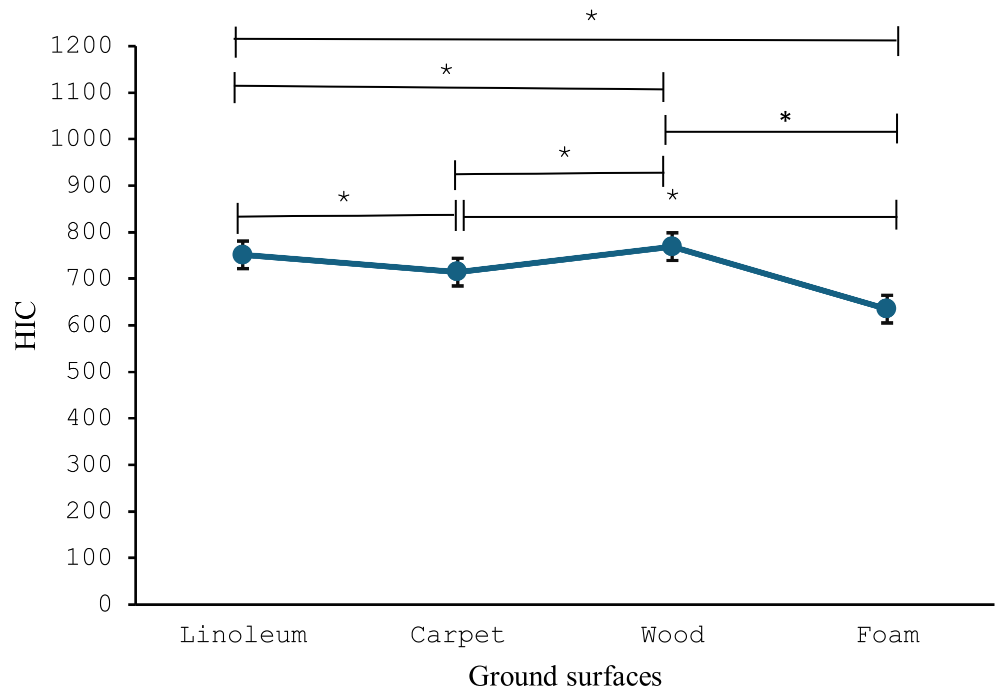

Note: * *indicates significant differences between ground surfaces on HIC for the back location*

Research Question Two

Does a CP Lycra® headgear designed for children with CP significantly reduce rotational acceleration and AGSI across different head impact locations (front, back, and side) during simulated free falls on various ground surfaces (playground foam, wood, linoleum, and carpet)?

It was hypothesized that the effectiveness of the headgear in reducing rotational acceleration and AGSI would vary across impact locations and surface types, with the greatest reductions occurring during front impacts on playground foam relative to wood, linoleum, and carpet surfaces (Bertocci et al., 2004; Cobb et al., 2014; Fung, 2013; Meriam & Kraige, 2007). Before addressing these hypotheses inferentially, the mean across the three trials was computed for measures of rotational acceleration and AGSI. These mean trials were then used to calculate the means, SD, and SE for each combination of ground surface and impact location, which are reported in Table 2 Appendix B. These descriptive statistics were subsequently used to compute mean differences and standard errors for pairwise comparisons in the inferential analyses.

A 3 × 4 two-way mixed factorial ANOVA with repeated measures on ground surface was administered to examine the interaction between impact location (front, back, and side) and ground surface (linoleum, carpet, wood, and playground foam) on rotational acceleration and AGSI.

Rotational Acceleration. The assumption of sphericity for measures of rotational acceleration was assessed across ground surface types. Mauchly's Test of Sphericity indicated that the assumption was not violated $\chi^2(5)=9.01$, $p>.05$. When conducting the inferential analysis, the mixed factorial ANOVA indicated a statistically significant interaction effect between impact locations and ground surface on measures of rotational acceleration, $F(6, 108)=10.89$, $p<.05$, $\eta^2=.377$ (large effect). This outcome indicates that the relationship between impact location and rotational acceleration is dependent on ground surface type.

Figure 22

Interaction Between Impact Locations and Ground Surfaces on Rotational Acceleration

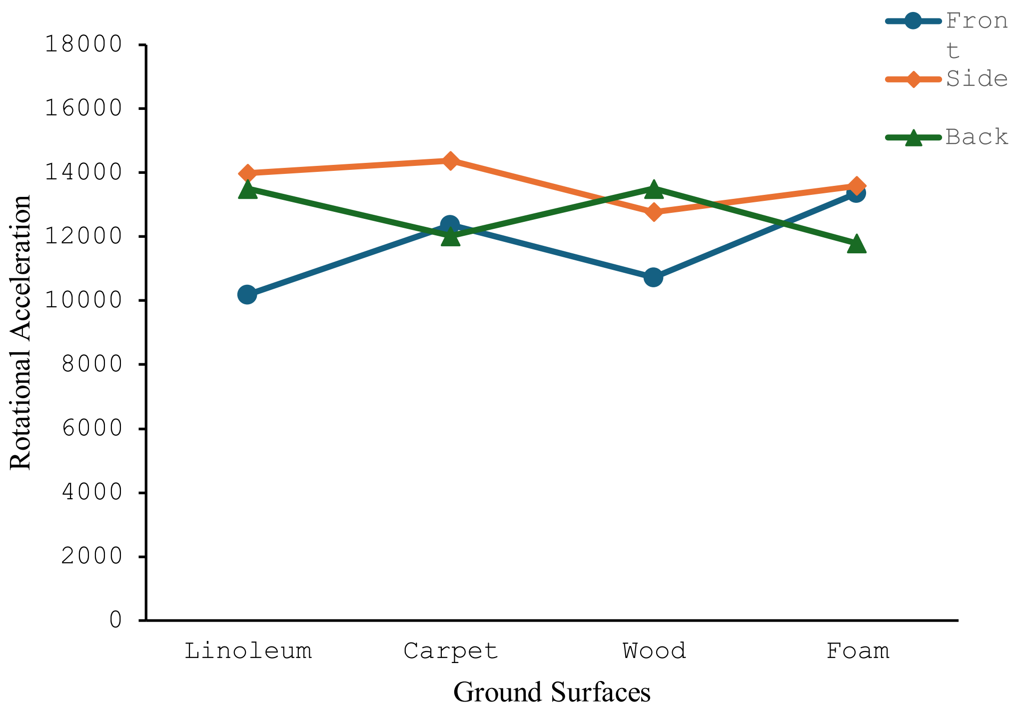

To help explain this interaction, a simple effect analysis was conducted using one-way ANOVAs for independent measures at each ground surface separately to examine if differences between headgear impact locations were statistically significant on rotational acceleration (see Figure 22). When considering the impact of linoleum ground surface on rotational acceleration, the one-way ANOVA results identified statistically significant differences between impact locations, $F(2, 36) = 9.310$, $p < .05$, $\eta^2 = .341$. This outcome suggests that 34.1% of the variance in rotational acceleration on the linoleum surface is explained by headgear impact location. LSD pairwise comparisons were conducted to identify the differences between impact locations for the linoleum ground surface on measures of rotational acceleration. The results indicated statistically significant differences between front and side impact locations ($M_{(diff)} = -3799.93$ rad/s², SE=958.97 rad/s², 95% CI:[-5744.81, -1855.06], $p < .05$) and between front and back impact locations ($M_{(diff)}$=-3318.68 rad/s², SE=958.97 rad/s², 95% CI:[-5263.56, -1373.81], p<.05) as shown in Figure 23.

Figure 23

Simple Effect of Linoleum on Rotational Acceleration

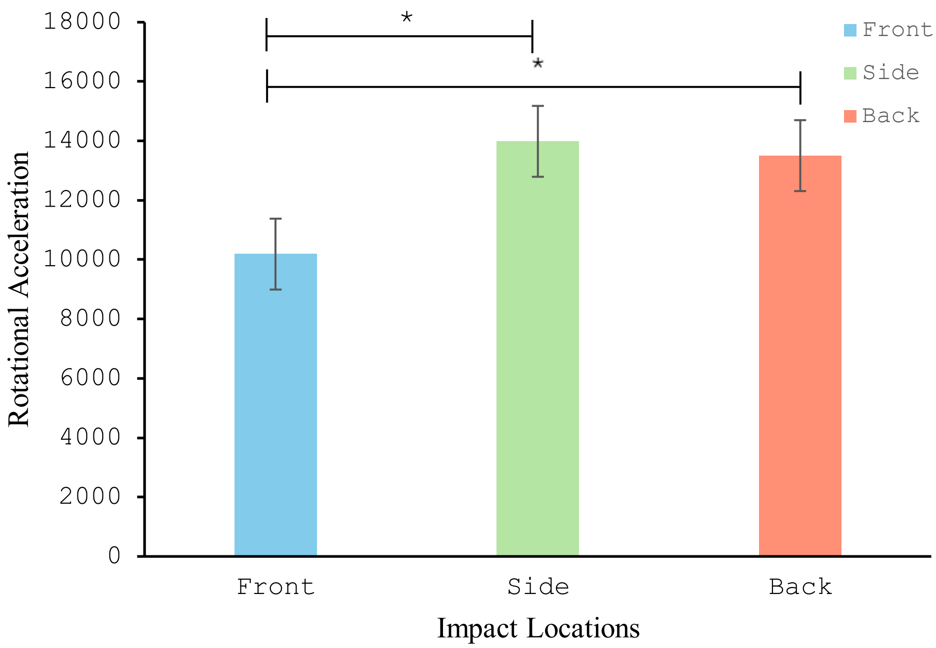

*Note: * indicates significant differences between groups at p<0.05*

For the carpet ground surface, the one-way ANOVA results indicated statistically significant differences between impact locations, $F(2, 36)$ =5.087, p<.05, η^2=.220. This outcome suggests that 22% of the variance in rotational acceleration on the carpet surface is explained by headgear impact location. LSD pairwise comparisons were conducted to identify the differences between impact locations for the carpet ground surface on measures of rotational acceleration. The results indicated significant differences between the front and side impact locations ($M_{(diff)}$=-2019.96 rad/s², SE=798.65 rad/s², 95% CI:[-3639.68, -400.23], p<.05) and between the side and back impact locations ($M_{(diff)}$=2354.06 rad/s², SE=798.65 rad/s², 95% CI:[734.33, 3973.79], p<.05) as shown in Figure 24.

Figure 24

Simple Effect of Carpet on Rotational Acceleration

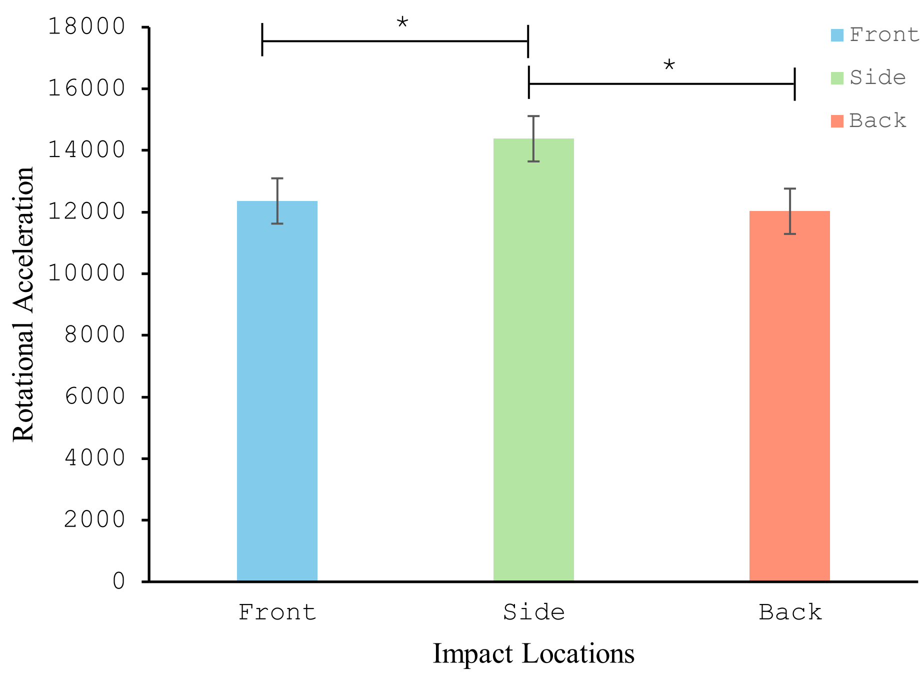

*Note: * indicates significant differences between groups at p<0.05*

For the wood ground surface, the one-way ANOVA results indicated statistically significant differences between impact locations, $F(2, 36) = 10.671$, $p<.05$, $\eta^2=.372$. This outcome suggests that 37.2% of the variance in rotational acceleration on the wood surface is explained by headgear impact location. LSD pairwise comparisons were conducted to identify the differences between impact locations for the wood ground surface on measures of rotational acceleration. The results indicated statistically significant differences between the front and side impact locations ($M_{(diff)}$=-2047.40 rad/s², SE=623.10 rad/s², 95% CI:[-3311.09, -783.70], $p<.05$)

and between front and back impact locations ($M_{(diff)}$=-2776.07 rad/s², SE=623.10 rad/s², 95% CI:[-4039.77, -1512.38], p<.05) as shown in Figure 25.

Figure 25

Simple Effect of Wood on Rotational Acceleration

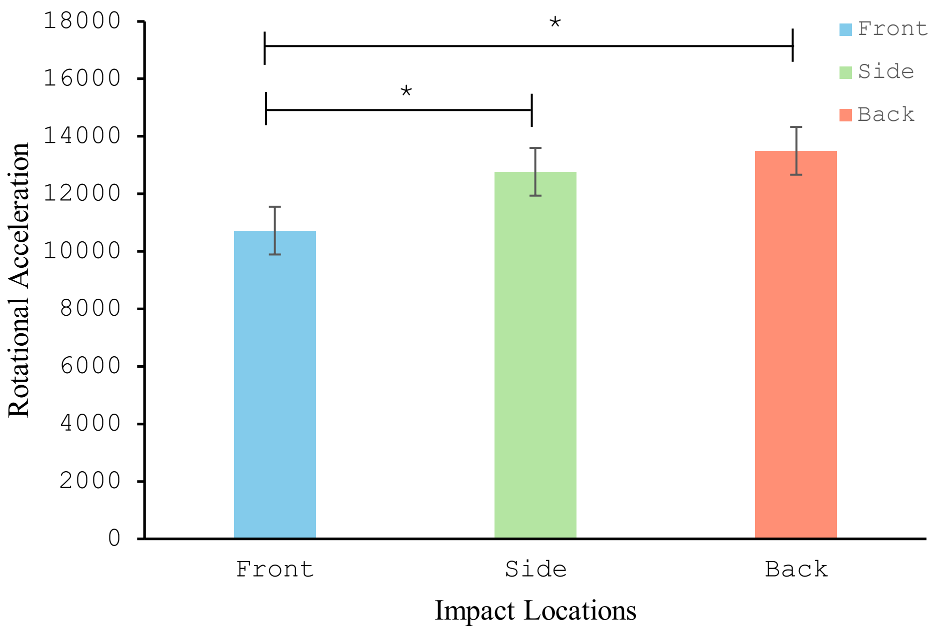

*Note: * indicates significant differences between groups at p<0.05*

For the foam ground surface, the one-way ANOVA results indicated statistically significant differences between impact locations, $F(2, 36)=6.226$, $p<.05$, $\eta^2=.257$. This outcome suggests that 25.7% of the variance in rotational acceleration on the foam surface is explained by headgear impact location. LSD pairwise comparisons were conducted to identify the differences between impact locations for the foam ground surface on measures of rotational acceleration. The results indicated statistically significant differences between the front and back impact locations ($M_{(diff)}$=1569.37 rad/s², SE=554.94 rad/s², 95% CI:[443.89, 2694.85], p<.05) and between the side and back impact locations ($M_{(diff)}$=1798.94 rad/s², SE=554.94 rad/s², 95% CI:[673.47, 2924.42], p<.05) as shown in Figure 26.

Figure 26

Simple Effect of Foam on Rotational Acceleration

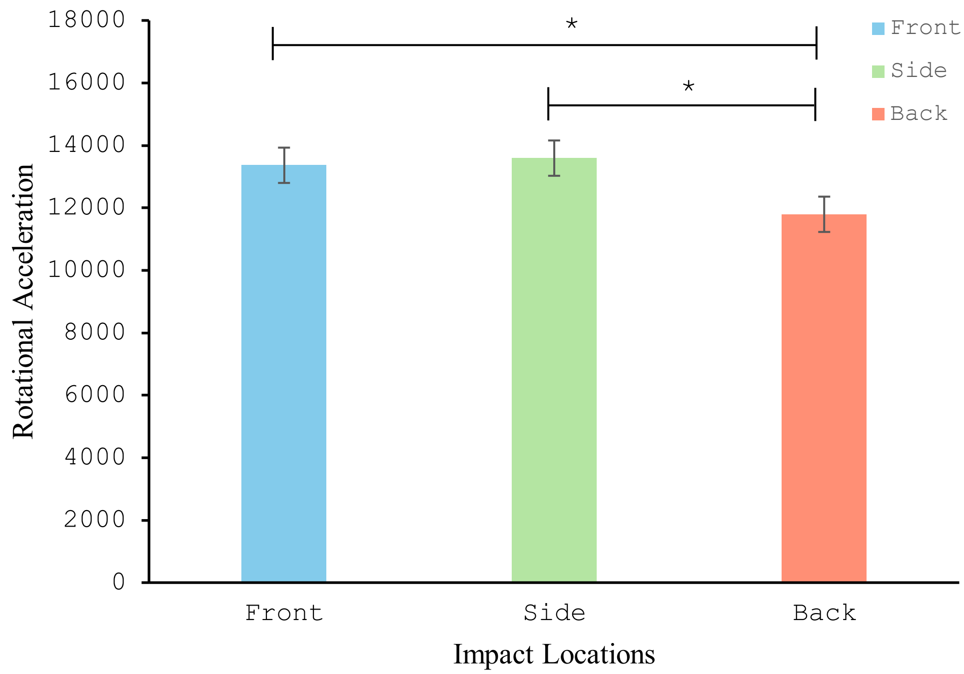

*Note: * indicates significant differences between groups at p<0.05*

Angular Gadd Severity Index (AGSI). The assumption of sphericity for measures of AGSI was assessed across ground surface types. Mauchly's Test of Sphericity indicated that the assumption of sphericity was not violated, $\chi^2(5)=10.508$, $p>.05$, suggesting that the variance was homogeneous. When conducting the inferential analysis, the mixed factorial ANOVA indicated a statistically significant interaction effect between impact locations and ground surface on measures of AGSI, $F(6, 108)=14.324$, $p<.05$, $\eta^2=.433$ (large effect). This outcome indicates that the relationship between impact location and AGSI is dependent on ground surface type as shown in Figure 27.

Figure 27

Interaction Between Impact Locations and Ground Surfaces on AGSI

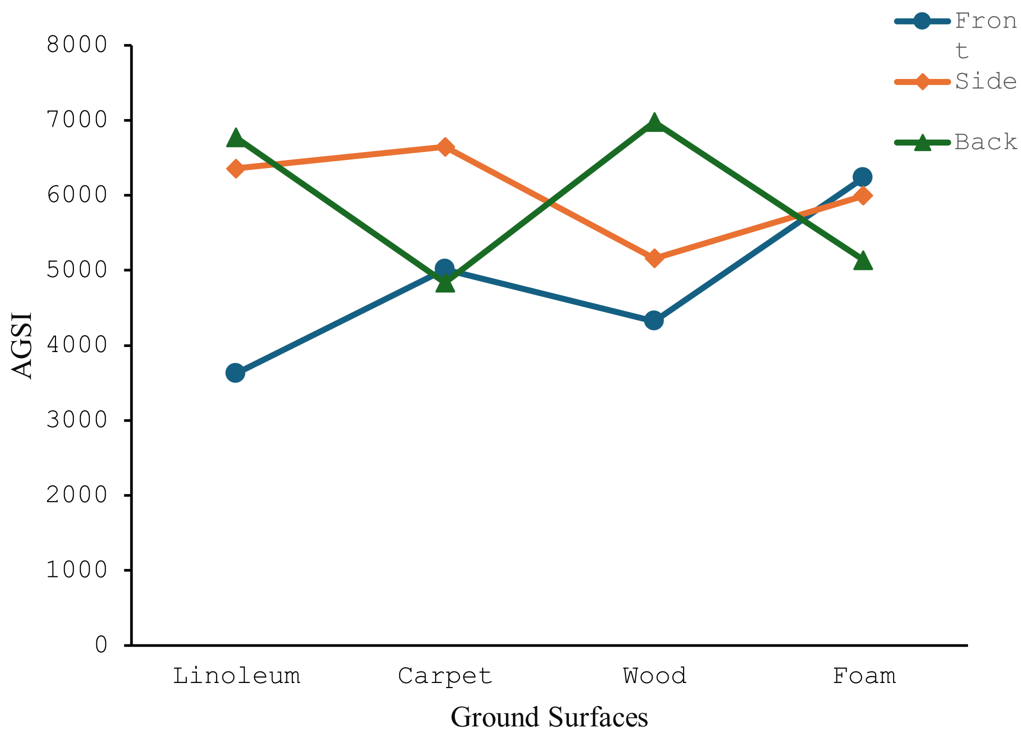

To help explain this interaction, a simple effect analysis was conducted using one-way ANOVAs for independent measures at each ground surface separately to examine if differences between headgear impact locations were statistically significant on AGSI (see Figure 28). For the linoleum ground surface, the one-way ANOVA results indicated statistically significant differences between impact locations, $F(2, 36) = 10.266$, $p < .05$, $\eta^2 = .363$. This outcome suggests that 36.3% of the variance in AGSI on the linoleum surface is explained by headgear impact location. LSD pairwise comparisons were conducted to identify the differences between impact locations for the linoleum ground surface on measures of AGSI. The results indicated statistically significant differences between the front and side impact locations ($M_{(diff)} = -2730.873$, SE=754.667, 95% CI:[-4261.410, -1200.337], $p < .05$) and between front and back impact locations ($M_{(diff)}$=-3147.740, SE=754.667, 95% CI:[-4678.277, -1617.2041], p<.05) as shown in Figure 28.

Figure 28

Simple Effect of Linoleum on AGSI

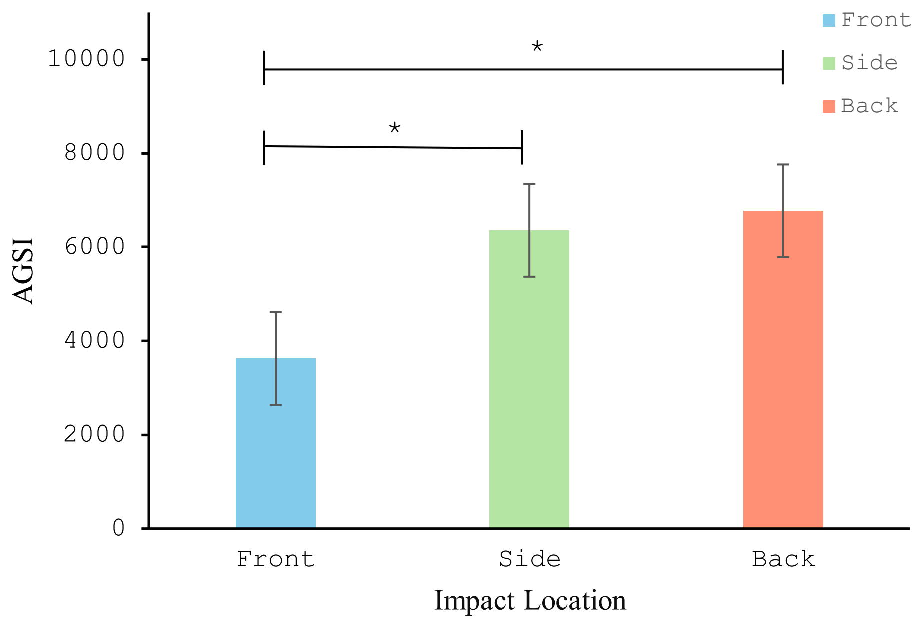

*Note: * indicates significant differences between groups at p<0.05*

For the carpet ground surface, the one-way ANOVA results indicated statistically significant differences between impact locations, $F(2, 36)$ =4.655, p<.05, η^2=.205. This outcome suggests that 20.5% of the variance in AGSI on the carpet surface is explained by headgear impact location. LSD pairwise comparisons were conducted to identify the differences between impact locations for the carpet ground surface on measures of AGSI. The results indicated statistically significant differences between the front and side impact locations ($M_{(diff)}$=-1634.768, SE=654.677, 95% CI:[-2962.514, -307.022], p<.05) and between the side and back impact locations ($M_{(diff)}$=1811.463, SE=654.677, 95% CI:[483.717, 3139.209], p<.05) as shown in Figure 29.

Figure 29

Simple Effect of Carpet on AGSI

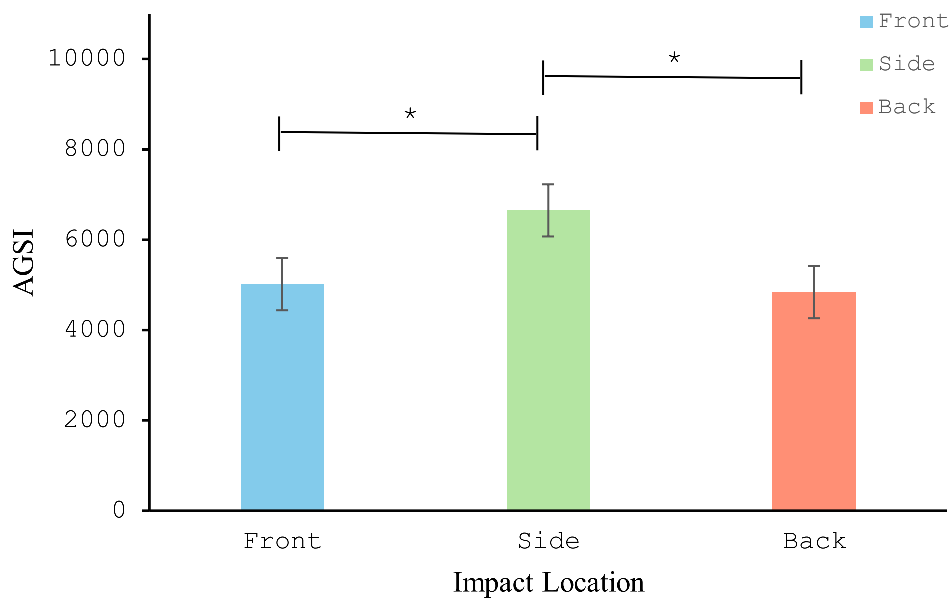

*Note: * indicates significant differences between groups at p<0.05*

For the wood ground surface, the one-way ANOVA results indicated statistically significant differences between the impact locations, $F(2, 36)$ =13.261, $p<.05$, η^2=.424. This outcome suggests that 42.4% of the variance in AGSI on the wood surface is explained by headgear impact location. LSD pairwise comparisons were conducted to identify the differences between impact locations for the wood ground surface on measures of AGSI. The results indicated statistically significant differences between the front and back impact locations ($M_{(diff)}$=-2654.339, SE=527.007, 95% CI:[-3723.159, -1585.519], p<.05) and between side and back impact locations ($M_{(diff)}$=-1817.737, SE=527.007, 95% CI:[-2886.557, -748.916], p<.05) as shown in Figure 30.

Figure 30

Simple Effect of Wood on AGSI

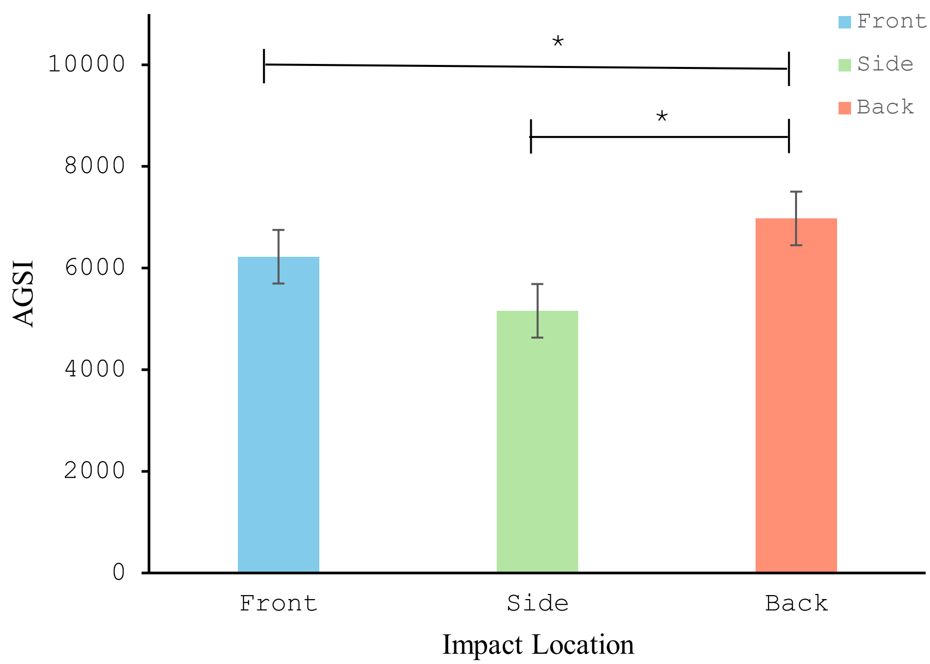

*Note: * indicates significant differences between groups at p<0.05*

For the foam ground surface, the one-way ANOVA results indicated no statistically significant differences between impact locations, $F(2, 36) = 2.566$, $p > .05$, $\eta^2 = .125$ (medium effect).

Chapter 5 - Discussion

CP is a lifelong neurological condition that affects movement, posture, and balance due to early brain injury or abnormal brain development (Obembe et al., 2013). As a result of these motor impairments, children with CP often experience difficulties with stability and coordination, which significantly increases their risk of falls in daily activities (Abd-Elfattah et al., 2022; Woollacott & Shumway-Cook, 2005). Falls in this population are a major safety concern, particularly because they frequently involve head contact with the ground or surrounding objects, causing concussions (Bulut, 2006). A concussion in CP children can occur even in low-height falls and may cause short- and long-term cognitive, emotional, and physical impairments (Boyer & Patterson, 2018; Bruijn et al., 2013), further aggravating their quality of life, independence, and participation in daily activities.

One approach to mitigate head injuries and concussions in this population is the use of protective headgear. Children with CP, particularly those with coexisting seizure disorders, are at an increased risk of seizure-related head injuries, including concussions, skull fractures, and intracranial hemorrhage resulting from falls during seizures (Deekollu et al., 2005; Nakken & Lossius, 1993; Neufeld et al., 2000; Nguyen & Téllez-Zenteno, 2009). Consequently, protective headgear has long been used as a medical intervention for children with special health care needs to reduce the risk of head injury associated with neurological and developmental conditions. However, despite its clinical use, evidence supporting headgear prescription remains limited, and no standardized prescription criteria currently exist (Sneed & Stencel, 2001). Similarly, Jory et al. (2019) concluded that helmet design for individuals with CP and seizures remains in its early stages, and that no international standards currently exist for seizure-specific protective headgear. They further noted that existing helmet designs represent a compromise between maximizing impact protection and ensuring comfort, highlighting the need for continued research and development. Despite these ongoing efforts, little is known about the effectiveness of commercially available headgear designed for children with CP and its ability to attenuate biomechanical indicators of head injury—particularly under different fall conditions (Deekollu et al., 2005; Sneed et al., 2008). Moreover, children with CP encounter a variety of ground surfaces in daily life and function and play, yet limited research has examined how ground surface properties influence headgear performance in mitigating head impact and concussions.

The present study aimed to address this gap by evaluating the effectiveness of a Lycra® headgear designed for children with CP in mitigating head impact severity under conditions that closely reflect real-world scenarios, specifically by simulating a worst-case falling condition in which the head makes first contact with the ground, followed by the torso. This approach allowed the researcher to examine the maximum protective capacity of the headgear to mitigate key biomechanical indicators of head injury and concussion across different ground surfaces. Experimental studies using instrumented pediatric test dummies have demonstrated that impact surface type significantly influences head injury risk, even in short distance (Bertocci et al., 2004). In the current study, the performance of the headgear was assessed across ground surfaces commonly encountered by children with CP in their daily environments, which included linoleum, carpet, wood, and playground foam (Bertocci et al., 2004).

Dynamic Testing

The experimental design of the current study incorporated a free-fall simulation approach as dynamic testing, in which impacts were delivered to three distinct head locations identified as the most frequent points of impact in the children with CP, including the front, side, and back (Boyer & Patterson, 2018). Dynamic testing plays a critical role in understanding injury mechanisms during falls, as it enables evaluation of impact scenarios under controlled conditions (Post et al., 2012; Rowson et al., 2011). Through this integrated approach, the current study aimed to show the extent to which both impact location and ground surface interact to influence the protective performance of the Lycra® headgear in reducing linear acceleration, rotational acceleration, HIC, and AGSI. Previous research has demonstrated that combining linear and rotational head kinematics improves the correlation with concussion risk compared to linear measures alone, highlighting the importance of multi-variable approaches in head injury assessment (Greenwald et al., 2008).

Linear Acceleration

Children with CP experience head injuries and concussions during a fall due to the magnitude of the linear acceleration when the head contacts the ground. As stated in the literature, direct head impacts predominantly produce linear acceleration loading, which is strongly associated with focal brain injury mechanisms (King et al., 2003). The only head injury mitigation strategies are the headgear and the material properties of the ground surface to absorb the impact. Theoretically, headgear and ground surface materials with greater energy-dissipating capabilities can decrease linear acceleration during a head collision (Singh et al., 2024).

The results of the current study showed a statistically significant interaction effect between impact location and ground surface on linear acceleration, with a large effect size. This outcome indicates that the effect of impact location on linear acceleration changes depending on the type of ground surface, and it explains 68.5% of the variance in linear acceleration by the association of these two factors. This outcome supports previous research on headgear and helmet technologies, which demonstrated that linear acceleration varies across impact locations, depending on impact structure and protective design (DiGiacomo et al., 2021). To further interpret this interaction, simple effect analyses revealed the differences in impact location for each ground surface.

For the linoleum and carpet surfaces, differences were noted between the front and side impact locations. Specifically, headgear impact location accounted for 18% of the variance in linear acceleration on the linoleum surface and 16% of the variance on the carpet surface. The slightly greater variance experiences on the linoleum surface seems to reflect reduced energy absorption compared to the carpet, consequently amplifying the effect of impact location on linear acceleration. In addition, the front location produced higher linear impact acceleration than the side location for the linoleum and carpet surfaces, as shown in Figures 15 and 16. One explanation for this outcome is that front impacts align more with the COM of the head, resulting in higher linear acceleration. Side impacts, on the other hand, do not align with the COM of the head, creating more rotational motion rather than pure linear acceleration. As stated by Zaman et al. (2025), impact location significantly influences head injury responses, although the direction of these effects may vary depending on experimental conditions (Zaman et al., 2025).

For the wood surface, no meaningful differences between impact locations were observed, with impact location accounting for only 9% of the variance in linear acceleration. This smaller proportion of explained variance suggests that the wood surface may have produced more consistent impact responses across locations. One possible explanation is that the mechanical properties of the wood surface, such as its stiffness and energy absorption characteristics, reduced the influence of impact location on linear acceleration (Arriaga et al., 2023).

For the foam surface, differences were observed between the front and side as well as between side and back impact locations on measures of linear acceleration. The front produced higher linear acceleration than the side. Similarly, the back produced higher linear acceleration than the side. This outcome indicates that 21% of the variance in linear acceleration is explained by headgear impact location on the foam surface, suggesting that the foam may allow more localized deformation, which alters the contact area and the way impact energy is absorbed and redistributed within the material, making the front, side, and back impact locations behave differently (Islam et al., 2020; Mills, 2006; Rahimidehgolan & Altenhof, 2023).

Ideally, children with CP expect similar headgear protective performance across all impact locations. The observed differences in the current study may be attributed to two possible factors. First, the mechanical properties and structural characteristics of the headgear liner and ground surface seem to influence energy absorption and mitigation of linear acceleration differently across some of the impact locations. Second, the geometry of the NOCSAE® headform, which provides a biofidelic representation of the human head, may also contribute to the observed differences in impact response (Cobb et al., 2014). The front region of the head, for example, is more curved, which can lead to a more concentrated point of contact and higher localized acceleration depending on the ground surface, whereas the side region is relatively flatter, allowing the impact acceleration to be distributed over a larger area and potentially resulting in lower linear acceleration. This interpretation is supported by previous research demonstrating that headform geometry varies across anatomical regions and influences contact interaction and helmet fit (Cobb et al., 2014).

Furthermore, the linear acceleration measures for the foam were lower than the linear acceleration measures for the linoleum, carpet and wood across locations. Previous research has shown that foam materials reduce impact accelerations by deforming and absorbing energy during impact (Bertocci et al., 2004). The way foam behaves depends on how the impact occurs, including the direction and loading conditions. For example, a study have shown that EPS-based foams can reduce linear acceleration during oblique impacts (Mosleh et al., 2017). The findings of the present study are consistent with previous research demonstrating that foam materials absorb impact energy and minimize acceleration through deformation and that their mechanical response is dependent on impact conditions (Li et al., 2019; Ramirez et al., 2018; Yang et al., 2021; Youssef et al., 2020). Overall, these results show that linear acceleration is not only affected by the headgear impact location but also by the type of surface. The interaction between surface stiffness and impact location indicates that real-life fall conditions must be taken into account when testing headgear and providing recommendations for the use of head protective technology and playground surfaces for children with CP.

Head Injury Criteria (HIC)

This measure has been widely used in safety standards to evaluate helmets and headgear protection systems using surrogate headforms (Marjoux et al., 2008). As previously stated in the literature, HIC is computed by integrating the linear acceleration of the head during a dynamic collision based on the duration of the impact (Loyd et al., 2015). While HIC does not completely capture the complexity of the injury mechanism, the measure reveals that the magnitude of the acceleration over a long period of time is harmful to the brain, leading to concussions and skull fractures (Dymek et al., 2021). The severity of HIC, however, can be minimized by the material properties of the protection system and impact surface during a head collision (Cobb et al., 2021; Wu et al., 2022).

The results of the present study showed a statistically significant interaction effect between the impact location and ground surface on HIC for the Lycra® headgear, with a large effect size, accounting for 46.7% of the variance in HIC. Further analysis revealed that there were no statistically significant differences between impact locations within each surface. That is, the proportion of variance explained by impact location within each surface was low for linoleum (9.2%), carpet (7.9%), and wood (9.0%), and only moderate for the foam surface (10.1%). This outcome suggests that the headgear behaved the same across impact locations on HIC measures. One reason maybe because HIC integrates the acceleration over a time window as shown in Equation 3, so it is less sensitive to brief, high peaks in acceleration and more to the area under the curve. Consequently, in a soft pediatric headgear such as the Lycra®, impacts at different locations may end up with similar duration and overall energy, even if the peak differs in linear acceleration. As stated by Chang et al. (2001), while linear acceleration reflects only the peak value at a specific moment, HIC incorporates both the magnitude and duration of acceleration over a critical time interval (Chang et al., 2001). As a result, variations in peak linear acceleration between different impact locations do not necessarily lead to differences in HIC values across those locations (Dymek et al., 2021)

The interaction effect between the headgear and ground surface on HIC, however, revealed an effect of ground surface on headgear location. That is, the proportion of variance explained by ground surface at each impact location was 31.1% for the front, 94.1% for the side and 95.1% for the back, suggesting that the ground surface material properties influenced the side and back locations more than the front location. Some of these differences, as previously stated in peak linear acceleration measures, can be explained by variations in head geometry and contact mechanics. The front region of the head is more curved, which can lead to a more concentrated point of contact and higher localized loading, producing lower variability in HIC values across ground surfaces, whereas the side and back regions are flatter or less curved, which may allow for a more distributed contact area and more variability across ground surfaces on HIC values (Cobb et al., 2014)

Across-ground surface comparisons for each location, the results show that the foam surface significantly mitigated HIC more than the other surfaces. These differences can be explained by the mechanical properties of the ground surfaces, particularly their stiffness and ability to dissipate impact energy (Li et al., 2024; Lin et al., 2008). Foam as a compliant surface is known to deform during impact, which can increase the duration of loading and allow more energy to be absorbed within the material (Romero et al., 2008). This behavior is consistent with the characteristics of cellular materials of foam, where energy is absorbed through deformation mechanisms such as cell wall bending and buckling, resulting in lower transmitted forces during impact and consequently lower risk of injury (Gibson & Ashby, 1999). In contrast, it can be suggested that stiffer surfaces, such as wood and linoleum, undergo minimal deformation and tend to transmit forces more directly to the head over a shorter time period and consequently result in a higher risk of head injury (Bertocci et al., 2022; Johnson, 2004).

Rotational Acceleration

Traditionally, helmet and head protection standards have focused on linear acceleration to evaluate impact performance. However, growing evidence from biomechanics research on head impacts has highlighted the importance of rotational head motion in the development of brain injuries (Yu et al., 2022). As Kleiven (2013) mentioned, rotational kinematics should also be an indicator of TBI risk in addition to linear acceleration. Furthermore, rotational acceleration has been strongly associated with diffuse brain injuries, such as a concussion (Carlsen et al., 2021; Zhang et al., 2009). Evaluating and mitigating rotational head motion is essential when assessing head injury risk and the effectiveness of protective strategies (Tierney, 2021), especially in children with CP. In addition, previous studies on head protective technologies stated that headgear and helmet materials with enhanced energy-absorbing capacity may reduce rotational acceleration during a head collision (Bottlang et al., 2019; Hoshizaki et al., 2022; Mosleh et al., 2018).

The analysis in this study showed a statistically significant interaction effect between impact location and ground surface on rotational acceleration, with a large effect size. This outcome indicates that the effect of headgear impact location on rotational acceleration changes depending on the type of ground surface, explaining 37.7% of the variance in rotational acceleration. This finding is supported by previous research demonstrating that rotational acceleration varies significantly across impact locations and directions (Kis et al., 2013; Hoshizaki et al., 2022; McIntosh & Lai, 2013; Zaman et al., 2025). To further interpret this interaction, simple effect analyses were conducted to examine the differences in impact location for each ground surface.

For the linoleum surface, differences were observed between impact locations on measures of rotational acceleration. Specifically, headgear imp act location accounted for 34.1% of the variance in rotational acceleration on the linoleum surface, indicating a substantial effect of impact location under this condition. This relatively high proportion of explained variance may be influenced by the stiffness and non-compliant nature of the surface, which limits energy absorption and can change the impact response of the head. That is, most of the energy transferred to the head's rotational motion depends more on the impact location of the headgear, contact geometry of the head, and friction rather than the surface. (Thompson-Bagshaw et al., 2022; Zhang et al.,2009). As shown in the results of this study, the front location produced lower rotational acceleration compared to both the side and back locations. This outcome is opposite to the results obtained from linear acceleration, in which the front location produced more linear acceleration than the other locations. The reason may be due to the contact geometry of the head. As stated in the literature, when a force is applied through or close to the COM, it produces mainly linear motion, whereas forces applied away from the COM create a moment that results in rotational motion (Fung, 2013; Meriam & Kraige, 2007), meaning that the front impact location, which is more aligned with the COM of the head due to the geometry of the head, tends to produce more linear motion, while side and back impacts, which are further from the COM, generate greater rotational motion.

For the carpet surface, differences were observed between impact locations on measures of rotational acceleration. Specifically, headgear impact location accounted for 22% of the variance in rotational acceleration on the carpet surface, indicating a moderate effect size of location under this condition. This proportion of variance suggests that the compliant nature of the carpet surface may allow more deformation during impact and more friction, which can influence the impact energy transmitted and distributed to the head rotational motion (Thompson-Bagshaw et al., 2022; Zhang et al.,2009). In addition, the side impact location produced higher rotational acceleration compared to both the front and back locations, which supports the previous rationale and literature finding that when an impact force is applied away from the COM of the head, as in the side location, it creates a moment and more rotational motion of the head (Fung, 2013; Meriam & Kraige, 2007).

For the wood surface, differences were observed between impact locations in measures of rotational acceleration. Specifically, headgear impact location accounted for 37.2% of the variance in rotational acceleration on the wood surface, indicating a relatively large effect size of location under this condition. Similar to the linoleum surface, the proportion of explained variance suggests that the mechanical properties of the wood surface, such as stiffness, compliance, and frictional forces, may have resulted in more energy transmission to the head rotational motion during impact, thereby amplifying the influence of headgear impact location on rotational response and less on ground surface (Thompson-Bagshaw et al., 2022; Zhang et al., 2009). Since the front headgear impact location was closer to the COM of the head, it created a lower moment and consequently lower rotational acceleration compared to both side and back locations (Fung, 2013; Meriam & Kraige, 2007).

For the foam surface, differences were observed between impact locations in measures of rotational acceleration. Specifically, headgear impact location accounted for 25.7% of the variance in rotational acceleration on the foam surface, indicating a moderate effect size of location under this condition. This proportion of explained variance suggests that the compliant nature of the foam surface may have influenced how impact energy was absorbed and redistributed, thereby affecting rotational head response across impact locations. Zhang et al. (2009) suggested that contact surface conditions, including material stiffness and surface curvatures, can change the impact response of the head. In addition, the side impact location produced higher rotational acceleration compared to both front and back locations, while front and back impacts showed relatively similar lower values. It supports previous literature indicating that when an impact force is applied away from the head's COM, as in side impacts, a moment is generated that leads to increased rotational motion of the head (Fung, 2013; Meriam & Kraige, 2007).

In summary, for the linoleum and wood surfaces, headgear impact location accounted for a relatively larger proportion of the variance in rotational acceleration (34.1% and 37.2%, respectively), indicating a stronger influence of impact location. In contrast, the carpet and foam surfaces showed more moderate effects (22% and 25.7%, respectively), suggesting that the influence of impact location was present but less pronounced. These differences may be explained by the mechanical properties of the ground surfaces. Zhang et al. (2009) demonstrated that contact surface conditions, including material stiffness and surface curvatures, can change the impact response of the head. Stiffer surfaces, such as wood and linoleum, are less capable of absorbing impact energy, which may result in more direct transmission of forces to the head and amplify the effect of impact location on rotational acceleration (Yoganandan et al., 2009; Zhang et al., 2009). In contrast, more compliant surfaces, such as carpet and foam, are able to deform during impact, which can dissipate energy and reduce the sensitivity of rotational acceleration to variations in impact location (Thompson-Bagshaw et al., 2022; Zhang et al., 2009).

In addition, side impact location had the highest rotational acceleration in all surfaces except wood, which is supported by some studies that explained side impacts can cause very high rotational motion of the head, which can lead to serious brain injury even without breaking the skull (Yoganandan et al., 2009; Zhang et al., 2009). Experimental and computational studies further support the outcome of the current study by indicating that rotational acceleration is a key contributor to brain strain and injury severity in side impacts (Gennarelli and Thibault, 1982; Margulies and Thibault, 1992). Also, Cobb et al. (2014) compared regional curvature differences between the Hybrid III and NOCSAE headforms, showing that the front region exhibits more curvature for both headforms, whereas the back and side regions are significantly flatter. These geometric differences influence contact mechanics during impact, with flatter regions potentially increasing contact area and reducing localized tangential forces and sliding, which may contribute to lower rotational acceleration (Cobb et al., 2014). In essence, the results of the current study suggest that ground surface compliance and impact location may influence rotational head acceleration in children with CP, indicating that surface properties and more specifically carpet and foam surfaces, as well as side impact locations, may play important roles in mitigating or increasing rotational acceleration during impact when using a Lycra® headgear.

Angular Gadd Severity Index (AGSI)

Rotational head motion has been strongly associated with mild traumatic brain injuries, including concussion and diffuse axonal injury, due to the shear deformation produced within brain tissue during angular motion (King et al., 2003). AGSI provides an avenue to assess the risk of head injury by considering the magnitude and duration of rotational acceleration during head impacts (Rybak, 2021). The original GSI was introduced by Gadd in 1966 to relate injury severity based on the magnitude and duration of the linear acceleration during an impact (Nokes et al., 1995). This measure was later modified by Rybak (2021) to measure AGSI based on rotational accelerations.

The use of AGSI in the present study is supported by previous work suggesting that novel head impact severity measures are needed to improve the prediction of concussion risk by capturing relevant biomechanical variables and their relationships with injury outcomes (Greenwald et al., 2008). Although uncertainty exists in defining absolute brain injury risk thresholds, rotational injury metrics and brain strain measures remain useful for relative comparisons of head impact severity across different impact conditions (Bottlang et al., 2019). Therefore, AGSI may provide valuable insight into variations in rotational head injury severity across impact locations and ground surfaces.

The analysis in the current study demonstrated a statistically significant interaction effect between impact location and ground surface on measures of AGSI, with a large effect size. This outcome indicates that the effect of impact location on AGSI changes depending on the type of ground surface, explaining 43.3% of the variance in AGSI through the association of these two factors. Since AGSI incorporates both the magnitude and duration of rotational acceleration during impact, these findings suggest that impact location and surface compliance together influence the severity of rotational head injury risk. Furthermore, this finding supports the importance of considering impact location when interpreting rotational injury metrics such as AGSI. As stated by Greenwald et al. (2008), head impact severity metrics vary with impact location. To further interpret this interaction effect and explain this outcome, simple effect analyses were conducted to examine the differences in impact location for each ground surface.

For the linoleum, carpet and wood surfaces, headgear impact location accounted for 36.3%, 20.5% and 42.4% of the variance in AGSI, respectively, indicating that the impact location significantly influenced AGSI on these surfaces. The front impact location produced significantly lower AGSI values compared to both the side and back impact locations for the linoleum surface. The side impact location produced significantly higher AGSI values compared to both the front and back impact locations for the carpet surface. The back impact location produced significantly higher AGSI values compared to both the front and side impact locations for the wood surface. Previous studies have shown that impact location influences rotational head injury severity and brain tissue strain, with lateral and posterior impact directions often producing greater rotational responses than frontal impacts (Kleiven, 2006). It is also possible that in the current study, higher rotational accelerations were generated at the side and back locations over a short period of time due to the stiffness properties of the ground surfaces. Since these locations are further away from the COM of the head, they generate higher rotation (Fung, 2013; Meriam & Kraige, 2007) and consequently higher AGSI values were produced compared to the front location in the current study.

For the foam surface, on the other hand, no significant differences were observed between impact locations on measures of AGSI. One possible explanation for this outcome may be related to the compliant mechanical properties of both the foam surface and the inner and outer liners of the Lycra® headgear. The combination of these soft materials during impact may have increased energy absorption and distributed the rotational impact accelerations over a longer period of time, thereby reducing the differences in AGSI between impact locations. This outcome is consistent with previous findings suggesting that foam materials absorb and dissipate impact energy through deformation over time, leading to a more uniform and time-extended loading response that can reduce location-dependent differences (Gibson & Ashby, 1997; Maiti et al., 1984; Ouellet et al., 2006). Furthermore, this behaviour is consistent with the time-dependent deformation characteristics of foam materials, which dissipate mechanical energy through elastic–plastic deformation during compression (Petel et al., 2012). In particular, foam materials exhibit a plateau region during compression in which substantial energy absorption occurs at relatively constant stress, followed by a densification phase where stiffness increases rapidly (Gibson & Ashby, 1997; Maiti et al., 1984). Based on the outcome of this study, it seems that the rotational impact across locations did not cause the foam surface and Lycra® liner material to reach the densification phase and plateau region, which led to non-significant differences in AGSI values between locations

In summary, the outcome of this study suggests that the location of the impact and ground surfaces are key factors influencing AGSI when using a Lycra® headgear and this outcome is supported by previous research (Greenwald et al., 2008; King et al., 2003; Kleiven, 2006;). In particular, the back and side impact locations seem to be more associated with higher AGSI for the linoleum, carpet, and wood surfaces. The foam surface, as the most compliant surface, behaved differently in this study, with all impact locations showing similar AGSI values. The results of the current study suggest that a foam ground surface seems to provide the best results to minimize the risk of head injury due to rotational impacts for CP children wearing a Lycra® headgear.

Strengths

This study has several strengths that contribute to the existing body of literature and practical implementations to mitigate head injury risk. It provides an avenue to dynamically assess the effectiveness of the material properties of a Lycra® headgear composed of D3O® smart molecule technology material and Lycra® fibers structures when compressed by a dynamic impact force, and it includes rotational acceleration and AGSI measures in addition to traditional measures of linear acceleration and HIC, to allow for a broader evaluation of head injury risk. This study also, includes different real-world ground surfaces commonly encountered by children with CP in homes, schools, rehabilitation centers, and playgrounds, which seem to play a role in protecting children with CP against concussions. It also assesses different impact locations on the head to provide a more representative understanding of fall-related injury mechanisms in CP children, evaluating a commercially available Lycra® headgear designed for children with CP. Finally, this study, implements a methodology to provide an avenue to assess the protective capabilities of CP commercial headgears for children's head injury protection.

Limitations

This study had some limitations that should be considered in future research. First, the study used dynamic impact testing only, while static material testing was not performed. Incorporating both static and dynamic testing may have provided a more comprehensive understanding of the mechanical properties of the headgear and ground surfaces, including material stiffness, deformation behaviour, compression characteristics, and energy absorption properties.

Second, only one commercially available Lycra® headgear was evaluated in the present study. Although this headgear is commonly used by children with CP, other commercially available protective headgear may differ in shell structure, liner design, material composition, thickness, and fit. These design differences may influence impact mitigation and alter biomechanical responses during falls.

The present study did not evaluate whether the mechanical properties or protective performance of the headgear changed following repeated impacts. Repeated impacts may alter the stiffness, deformation characteristics, and energy absorption capacity of protective materials, potentially reducing their ability to attenuate impact forces over time.

This study simulated a worst-case fall scenario in which the head made first contact with the ground before the torso. This approach was intentionally selected to evaluate the maximum loading condition on the headgear; however, it may not fully represent the range of real-world falls experienced by children with CP. In actual fall events, body posture, fall direction, protective reactions, and the sequence of body contact may vary substantially and may alter head impact severity.

Although accelerometers and gyroscope sensors were used to capture head kinematics, measurements may have been affected by transient vibrations and slight relative motion between the sensor, headform, and headgear during impact. These effects can introduce signal noise and may influence the precision of linear and rotational acceleration values recorded during the trials. Filtering techniques and high-frequency sampling rate, however, were implemented to mitigate or eliminate signal noise in the MatLab scripts.

Lastly, variability in CP severity (GMFCS I–V) may influence balance, mobility, and fall mechanics, affecting head impact characteristics. As a result, findings are most applicable to ambulatory children with CP and should be generalized with caution to more severe cases.

Future Research

Future research should build on the present findings by addressing several of the limitations identified in this study. First, future studies should integrate dynamic impact testing with static testing and mechanical characterization of headgear components. Static characteristics of the internal padding and Lycra lining, including material flexibility, compression behaviour, stretch, frictional properties, and structural support, are important considerations in the overall protective performance of CP headgear. However, the present study focused specifically on the dynamic impact response during simulated falls, and static material testing was not included in the experimental design. Time constraints and limited access to specialized equipment for static material characterization prevented the inclusion of these assessments. This limitation has been acknowledged in the thesis, and future research should incorporate static material testing alongside dynamic impact evaluation. (Cooke, 2024; Gandhi et al., 2014; Shankar et al., 2020). Also, future studies should investigate the role of padding and lining materials in providing neck support by improving neck stability and limiting abnormal head and neck movement during falls. Evaluating these biomechanical and neck-stabilizing functions may provide a more comprehensive understanding of the protective performance of headgear for children with CP (Cooke, 2024). Future studies should evaluate multiple types of commercially available headgear designed for children with CP. Comparing multiple commercially available products may provide a broader understanding of how design features such as material composition, liner thickness, and structural characteristics affect head injury mitigation under different fall conditions in children with CP (Santhosh et al., 2021). Furthermore, future research should investigate the durability of protective headgear under repeated impact conditions to determine whether repeated loading alters the mechanical properties of protective materials, such as their stiffness, deformation characteristics, and energy absorption capacity. Examining whether protective performance is maintained after repeated impacts would provide valuable information regarding the long-term effectiveness and service life of protective headgear (Jones & Smith, 2026; Sărăndan et al., 2022). Further research also should investigate a wider range of fall scenarios beyond the worst-case condition simulated in this study. Real-world falls may occur with different body positions, directions, and impact sequences. Examining these variations may improve understanding of how fall mechanics influence head injury risk and the protective performance of headgear in practical settings (Esterley et al., 2025). Future study may also consider refining the sensor mounting system to minimize any potential movement of the accelerometer and gyroscope relative to the headform during impact testing. Improving sensor fixation may reduce measurement noise and enhance the accuracy of recorded linear and rotational head kinematics during high-impact events. Future research should consider the heterogeneity of CP severity by examining head impact responses across different functional levels (e.g., GMFCS I–V). This would allow for a more detailed understanding of how variability in balance control, mobility, and fall mechanics influences head injury risk and headgear performance, thereby improving the generalizability of findings across the CP population (Boyer & Patterson, 2018). Finally, future research should consider integrating XR-based neurorehabilitation with biomechanical simulation to better understand the mechanisms of falls in children with CP. The kinematic measures used in the present study, including linear and rotational acceleration, could be incorporated into XR-based simulations to evaluate head impact responses associated with functional activities such as standing, walking, and sitting transitions. This approach may provide a better understanding of how movement patterns and fall mechanisms influence head injury risk and how protective headgear may reduce concussion risk under different fall scenarios. Previous research has demonstrated the potential of XR-based neurorehabilitation for improving motor function in children with CP (Macchitella et al., 2024). Combining XR-based rehabilitation with biomechanical assessment may support a more comprehensive approach to both fall prevention and injury mitigation.

Chapter 6 - Conclusion

The present study evaluated the protective performance of a Lycra® headgear in reducing concussion risk in children with CP by simulating a worst-case falling scenario in which the head makes first contact with the ground, followed by the torso. The study examined the interaction effect of headgear impact location and ground surface on measures of linear acceleration, rotational acceleration, HIC, and AGSI during simulated dynamic free-fall head collisions across common ground surfaces encountered in children's playgrounds.

The researchers hypothesized that the effectiveness of the headgear in reducing linear acceleration and HIC would vary across impact locations and surface types, with the greatest reductions occurring during side impacts on playground foam relative to wood, linoleum, and carpet surfaces. The results supported this hypothesis for linear acceleration, indicating that impact location and ground surface affected linear acceleration and that playground foam produced the greatest reduction at the side impact location. However, the hypothesis was only partially supported for HIC. Although impact location and ground surface affected HIC, playground foam reduced HIC similarly across impact locations rather than producing the greatest reduction specifically at the side location.

The researchers also hypothesized that the effectiveness of the headgear in reducing rotational acceleration and AGSI would vary across impact locations and surface types, with the greatest reductions occurring during front impacts on playground foam relative to wood, linoleum, and carpet surfaces. The results supported this hypothesis for rotational acceleration, indicating that impact location and ground surface affected rotational acceleration and that playground foam produced the greatest reduction at the front impact location. However, the hypothesis was only partially supported for AGSI. Although impact location and ground surface affected AGSI, playground foam reduced AGSI similarly across impact locations rather than producing the greatest reduction specifically at the front location. In terms of ground surfaces, stiffer surfaces, such as linoleum and wood, showed higher rotational accelerations and AGSI values across locations as compared to the foam.

From the theoretical perspective, this outcome supports the concept that the severity of the linear acceleration impact and HIC can be minimized by the material properties of the protection system and impact object during a head collision (Cobb et al., 2021; Wu et al., 2022). Although rotational acceleration and AGSI measures are not commonly used in commercial helmet or headgear testing protocols according to NOCSAE standards, the outcome of this study also supports the research work of Yoganndan et al. (2009) and Zhang et al. (2009) that side impacts can cause very high rotational motion of the head, which can lead to serious brain injury strongly associated with diffuse brain injuries, such as a concussion (Carlsen et al., 2021; Zhang et al., 2009) even without breaking the skull. From the practical perspective, these findings suggest that compliant properties of ground surfaces, along with the material properties of the Lycra® headgear, seem to play an important role in reducing concussion risk during a fall simulation of a child with CP wearing the headgear.

Finally, the simulations in the current study were based on worst-case impact scenarios, with the resulting linear and rotational accelerations exceeding the reported concussion threshold values of 62.4 ± 29.7 g and 2609 ± 1591 rad/s^2, respectively (Campolettano et al., 2019). Nonetheless, the findings contribute to the understanding of fall-related concussion mechanisms in children with CP and provide biomechanical evidence to assess and support the development of safer surface designs and head protection strategies in clinical, school, and home environments.

References

Abd-Elfattah, H. M., Galal, D. O. S. M., Aly, M. I. E., Aly, S. M., & Elnegamy, T. E. (2022). Effect of pilates exercises on standing, walking, and balance in children with diplegic cerebral palsy. *Annals of Rehabilitation Medicine*, *46*(1), 45–52. https://doi.org/10.5535/arm.21148

AD Instruments. (2025). *LabChart Overview Data Acquisition and Analysis Software*. https://m-cdn.adinstruments.com/brochures/ADInstruments_LabChart_Brochure.pdf

Ahmed, A., Rosella, L. C., Oskoui, M., Watson, T., & Yang, S. (2023). Prevalence and temporal trends of cerebral palsy in children born from 2002 to 2017 in Ontario, Canada: Population-based cohort study. *Developmental Medicine and Child Neurology*, *65*(2), 243–253. https://doi.org/10.1111/dmcn.15324

Ahmed, W., & Hamdy, M. (2018). Optimal management of umbilical cord prolapse. *International Journal of Women's Health*, *Volume 10*(10), 459–465. https://doi.org/10.2147/ijwh.s130879

Alemdaroğlu-Gürbüz, İ., İpek, C., Bulut, N., Karaduman, A., & Yılmaz, Ö. (2022). The Impact of "Fear of Falling" on Physical Performance, Balance, and Ambulation in Duchenne Muscular Dystrophy. *Neuropediatrics*, *53*(5). https://doi.org/10.1055/s-0042-1750722

Alley, R. H., Jr. (1964). Head and neck injuries in high school football. *JAMA, 188*, 418–422.

Alosco, M. L., & Stern, R. A. (2019). Youth exposure to repetitive head impacts from tackle football and long-term neurologic outcomes: A review of the literature, knowledge gaps and future directions, and societal and clinical implications. *Seminars in Pediatric Neurology*, *30*, 107–116. https://doi.org/10.1016/j.spen.2019.03.016

Arriaga, F., Wang, X., Íñiguez-González, G., Llana, D. F., Esteban, M., & Niemz, P. (2023). Mechanical properties of wood: A review. *Forests*, *14*(6), 1202–1202. https://doi.org/10.3390/f14061202

ASTM. (2021). *Test Methods for Flexible Cellular Materials Made from Olefin Polymers*. https://doi.org/10.1520/d3575-20

Audu, O., & Daly, C. (2017). Standing activity intervention and motor function in a young child with cerebral palsy: A case report. *Physiotherapy Theory and Practice*, *33*(2), 162–172. https://doi.org/10.1080/09593985.2016.1265621

Avalle, M., Belingardi, G., & Montanini, R. (2001). Characterization of polymeric structural foams under compressive impact loading by means of energy-absorption diagram. *International Journal of Impact Engineering*, *25*(5), 455–472. https://doi.org/10.1016/s0734-743x(00)00060-9

Beghi, Ettore & Cornaggia, C. (2002). Morbidity and accidents in patients with epilepsy: results of a European cohort study. *Epilepsia*, *43*(9), 1076–1083. https://doi.org/10.1046/j.1528-1157.2002.18701.x

Bell, K. J., Ounpuu, S., DeLuca, P. A., & Romness, M. J. (2002). Natural progression of gait in children with cerebral palsy. *Journal of pediatric orthopedics*, *22*(5), 677–682.

Bertocci, G., Mary Clyde Pierce, Deemer, E., Aguel, F., Janosky, J. E., & Vogeley, E. (2004). Using test dummy experiments to investigate pediatric injury risk in simulated short-distance falls. *Archives of Pediatrics & Adolescent Medicine*, *157*(5), 480–480. https://doi.org/10.1001/archpedi.157.5.480

Bertocci, G., Smalley, C., Brown, N., Dsouza, R., Hilt, B., Thompson, A., Bertocci, K., McKinsey, K., Cory, D., & Pierce, M. C. (2022). Head biomechanics of video recorded falls involving children in a childcare setting. *Scientific Reports*, *12*(1). https://doi.org/10.1038/s41598-022-12489-7

Bland, M. L., McNally, C., & Rowson, S. (2018). Differences in impact performance of bicycle helmets during oblique impacts. *Journal of Biomechanical Engineering*, *140*(9), 091005. https://doi.org/10.1115/1.4040019

Bloodworth-Race, S., Critchley, R., Hazael, R., Peare, A., & Temple, T. (2021). Testing the blast response of foam inserts for helmets. *Heliyon*, *7*(5), e06990. https://doi.org/10.1016/j.heliyon.2021.e06990

Bodin, D., Yeates, K. O., & Klamar, K. (2011). Definition and classification of concussion. *Pediatric and Adolescent Concussion*, 9–19. https://doi.org/10.1007/978-0-387-89545-1_2

Boone E. (2024). Caring for children with cerebral palsy: A commentary on cerebral palsy in children: a clinical practice review. *Current problems in pediatric and adolescent health care*, *54*(11), 101701. https://doi.org/10.1016/j.cppeds.2024.101701

Bottlang, M., Rouhier, A., Tsai, S., Gregoire, J., & Madey, S. M. (2019). Impact performance comparison of advanced bicycle helmets with dedicated rotation-damping systems. *Annals of Biomedical Engineering*, *48*(1), 68–78. https://doi.org/10.1007/s10439-019-02328-8

Botvinick, M. M., Braver, T. S., Barch, D. M., Carter, C. S., & Cohen, J. D. (2001). Conflict monitoring and cognitive control. *Psychological Review*, *108*(3), 624–652. https://doi.org/10.1037//0033-295x.108.3.624

Boyer, E. R., & Patterson, A. (2018). Gait pathology subtypes are not associated with self-reported fall frequency in children with cerebral palsy. *Gait & Posture*, *63*, 189–194. https://doi.org/10.1016/j.gaitpost.2018.05.004

Branson, L. J., Latter, J., Currie, G. R., Nettel-Aguirre, A., Embree, T., & Hagel, B. E. (2012). The effect of surface and season on playground injury rates. *Paediatrics & Child Health*, *17*(9), 485–489. https://doi.org/10.1093/pch/17.9.485

Brody, D. L. (2015). *Concussion care manual: a practical guide*. Oxford University Press. https://doi.org/10.1093/med/9780199383863.001.0001

Browne, K. D., Chen, X.-H., Meaney, D. F., & Smith, D. H. (2011). Mild traumatic brain injury and diffuse axonal injury in swine. *Journal of Neurotrauma*, *28*(9), 1747–1755. https://doi.org/10.1089/neu.2011.1913

Bruijn, S. M., Millard, M., van Gestel, L., Meyns, P., Jonkers, I., & Desloovere, K. (2013). Gait stability in children with cerebral palsy. *Research in Developmental Disabilities*, *34*(5), 1689–1699. https://doi.org/10.1016/j.ridd.2013.02.011

Brunner, M. R., Cieri, M. E., Lucero, R. A., Condinanzi, A. L., Gil, C., & Cuestas, E. (2024). Software and equations using segmental measures to estimate height in children and adolescents with cerebral palsy considering the level of gross motor function. *Clinical Nutrition ESPEN*, *62*, 234–240. https://doi.org/10.1016/j.clnesp.2024.05.014

Bulut, M., Koksal, O., Korkmaz, A., Turan, M., & Ozguc, H. (2006). Childhood falls: characteristics, outcome, and comparison of the Injury Severity Score and New Injury Severity Score. *Emergency Medicine Journal*, *23*(7), 540–545. https://doi.org/10.1136/emj.2005.029439

Burgos-Flórez, F. J., & Garzón-Alvarado, D. A. (2020). Stress and strain propagation on infant skull from impact loads during falls: a finite element analysis. *International Biomechanics*, *7*(1), 19–34. https://doi.org/10.1080/23335432.2020.1719196

Burns, E. C. M., Grool, A. M., Klassen, T. P., Correll, R., Jarvis, A., Joubert, G., Bailey, B., Chauvin-Kimoff, L., Pusic, M., McConnell, D., Nijssen-Jordan, C., Silver, N., Taylor, B., & Osmond, M. H. (2016). Scalp hematoma characteristics associated with intracranial injury in pediatric minor head injury. *Academic Emergency Medicine*, *23*(5), 576–583. https://doi.org/10.1111/acem.12957

Burrows, P., Trefan, L., Houston, R., Hughes, J., Pearson, G., Edwards, R. J., Hyde, P., Maconochie, I., Parslow, R. C., & Kemp, A. M. (2015). Head injury from falls in children younger than 6 years of age. *Archives of Disease in Childhood*, *100*(11), 1032–1037. https://doi.org/10.1136/archdischild-2014-307119

Burtner, P. A., Qualls, C., & Woollacott, M. H. (1998). Muscle activation characteristics of stance balance control in children with spastic cerebral palsy. *Gait & Posture*, *8*(3), 163–174. https://doi.org/10.1016/s0966-6362(98)00032-0

Campolettano, E. T., Gellner, R. A., Smith, E. P., Bellamkonda, S., Tierney, C. T., Crisco, J. J., Jones, D. A., Kelley, M. E., Urban, J. E., Stitzel, J. D., Genemaras, A., Beckwith, J. G., Greenwald, R. M., Maerlender, A. C., Brolinson, P. G., Duma, S. M., & Rowson, S. (2019). Development of a concussionr function for a youth population using head linear and rotational acceleration. *Annals of Biomedical Engineering*, *48*(1), 92–103. https://doi.org/10.1007/s10439-019-02382-2

Carlsen, R. W., Fawzi, A. L., Wan, Y., Kesari, H., & Franck, C. (2021). A quantitative relationship between rotational head kinematics and brain tissue strain from a 2-D parametric finite element analysis. *Brain Multiphysics*, *2*, 100024. https://doi.org/10.1016/j.brain.2021.100024

Carlson, S. (2016). *The influence of neck stiffness, impact location, and angle on peak linear acceleration, shear force, and energy loading measures of hockey helmet impacts* (Publication No. 10169573) [Master Thesis, Lakehead University]. http://knowledgecommons.lakeheadu.ca/handle/2453/779

CDC. (2023). *Growth Charts - Percentile Data Files with LMS Values*. www.cdc.gov. U.S. Centers for Disease Control and Prevention. https://www.cdc.gov/growthcharts/cdc-data-files.htm

Chakraborty, S., Nandy, A., & Kesar, T. M. (2020). Gait deficits and dynamic stability in children and adolescents with cerebral palsy: A systematic review and meta-analysis. *Clinical Biomechanics*, *71*, 11–23. https://doi.org/10.1016/j.clinbiomech.2019.09.005

Chang, L.T., Chang, C.H., & Chang, G.L. (2001). Fit effect of motorcycle helmet. A finite element modeling. *JSME International Journal Series A*, *44*(1), 185–192. https://doi.org/10.1299/jsmea.44.185

Choi, W. J., Kaur, H., & Robinovitch, S. N. (2014). Measurement of the effect of playground surface materials on hand impact forces during upper limb fall arrests. *Journal of Applied Biomechanics*, *30*(2), 276–281. https://doi.org/10.1123/jab.2013-0081

Cobb, B. R., MacAlister, A., Young, T. J., Kemper, A. R., Rowson, S., & Duma, S. M. (2014). Quantitative comparison of Hybrid III and National Operating Committee on Standards for Athletic Equipment headform shape characteristics and implications on football helmet fit. *Proceedings of the Institution of Mechanical Engineers, Part P: Journal of*

Sports Engineering and Technology, *229*(1), 39–46. https://doi.org/10.1177/1754337114548245

Cobb, B. R., Urban, J. E., Davenport, E. M., Rowson, S., Duma, S. M., Maldjian, J. A., Whitlow, C. T., Powers, A. K., & Stitzel, J. D. (2013). Head impact exposure in youth football: elementary school ages 9-12 years and the effect of practice structure. *Annals of Biomedical Engineering*, *41*(12), 2463–2473. https://doi.org/10.1007/s10439-013-0867-6

Cobb C, Moorehead A, Pan, C. S., Wimer BM, & Wu, J. Z. (2021). Effects of proper helmet wearing on the protection performance for industrial helmets. In *Cdc.gov*. International Society for Occupational Ergonomics and Safety (ISOES). https://stacks.cdc.gov/view/cdc/222969

Cooke, H. M. (2024). *The Development of a Head and Neck Support Device for Children with Cerebral Palsy.* (Master's thesis). Queen's University. https://queensu.scholaris.ca/bitstreams/dcbe0264-d09e-48a5-bff4-9ab55659c44f/download

Cronbach, L. J., & Meehl, P. E. (1955). Construct validity in psychological tests. *Psychological Bulletin, 52* (4), 281–302. https:// https://doi.org/10.1037/h0040957

Crowe, L. M., Catroppa, C., Babikian & Asarnow, V., & Babl, F. E. (2012). Head injuries in children under 3 years. *Injury*, *43*(12), 2141–2145. https://doi.org/10.1016/j.injury.2012.07.195

Daniel, I. M., Gdoutos, E. E., Wang, K. A., & Abot, J. L. (2002). Failure modes of composite sandwich beams. *International Journal of Damage Mechanics*, *11*(4), 309–334. https://doi.org/10.1106/105678902027247

Deekollu, D., Besag, F. M. C., & Aylett, S. E. (2005). Seizure-related injuries in a group of young people with epilepsy wearing protective helmets: Incidence, types and circumstances. *Seizure*, *14*(5), 347–353. https://doi.org/10.1016/j.seizure.2005.04.008

De Santis, A., Siciliano, B., De Luca, A., & Bicchi, A. (2008). An atlas of physical human–robot interaction. *Mechanism and Machine Theory*, *43*(3), 253–270. https://doi.org/10.1016/j.mechmachtheory.2007.03.003

Diamond, A. (2013). Executive functions. *Annual Review of Psychology*, *64*(1), 135–168. https://doi.org/10.1146/annurev-psych-113011-143750

Dibb, A. T., Cutcliffe, H. C., Luck, J. F., Cox, C. A., Myers, B. S., Bass, C. R., Arbogast, K. B., Seacrist, T., & Nightingale, R. W. (2014). Pediatric head and neck dynamics in frontal impact: Analysis of important mechanical factors and proposed neck performance corridors for 6- and 10-year-old ATDs. *Traffic Injury Prevention*, *15*(4), 386–394. https://doi.org/10.1080/15389588.2013.824568

DiGiacomo, G., Tsai, S., & Bottlang, M. (2021). Impact performance comparison of advanced snow sport helmets with dedicated rotation-damping systems. *Annals of Biomedical Engineering*, *49*(10), 2805–2813. https://doi.org/10.1007/s10439-021-02723-0

Donald, K. A., Samia, P., Kakooza-Mwesige, A., & Bearden, D. (2014). Pediatric cerebral palsy in Africa: a systematic review. *Seminars in Pediatric Neurology*, *21*(1), 30–35. https://doi.org/10.1016/j.spen.2014.01.001

Dubucs, X., Lecuyer, L., Balen, F., Henri, C., Emond, M., Lepage, B., Hélène Colineaux, & Charpentier, S. (2023). Validation of the cutaneous impact location to predict intracranial lesion among elderly admitted to the Emergency Department after a ground-level fall. *Injury*, *54*(5), 1306–1313. https://doi.org/10.1016/j.injury.2023.02.023

Dubucs, X., Mercier, É., Boucher, V., Lauzon, S., Balen, F., Charpentier, S., & Emond, M. (2024). Association between frailty and head impact location after ground-level fall in older adults. *The Journal of Emergency Medicine*. https://doi.org/10.1016/j.jemermed.2024.01.005

Dupuis, O., Silveira, R., Dupont, C., Mottolese, C., Kahn, P., Dittmar, A., & René-Charles Rudigoz. (2005). Comparison of "instrument-associated" and "spontaneous" obstetric depressed skull fractures in a cohort of 68 neonates. *American Journal of Obstetrics & Gynecology, 192*(1), 165–170. https://doi.org/10.1016/j.ajog.2004.06.035

Dymek, M., Ptak, M., Ratajczak, M., Fernandes, F. A. O., Kwiatkowski, A., & Wilhelm, J. (2021). Analysis of HIC and hydrostatic pressure in the human head during NOCSAE tests of American football helmets. *Brain Sciences*, *11*(3), 287. https://doi.org/10.3390/brainsci11030287

Emmerik, R. E. A., Ducharme, S. W., Amado, A. C., & Hamill, J. (2016). Comparing dynamical systems concepts and techniques for biomechanical analysis. *Journal of Sport and Health Science*, *5*(1), 3–13. https://doi.org/10.1016/j.jshs.2016.01.013

Esterley, M. T., Krach, L. E., Pederson, K., Wandersee, N. G., Tierney, S. C., & Boyer, E. R. (2024). Physical and psychosocial consequences of falls in ambulatory individuals with cerebral palsy by age and gross motor function. *Archives of Physical Medicine and Rehabilitation*, *106*(5). https://doi.org/10.1016/j.apmr.2024.12.010

Esterley, M., Krach, L. E., Pederson, K., Tierney, S. C., Wandersee, N. G., & Boyer, E. R. (2025). Fall experiences of ambulatory children and adults with cerebral palsy: A qualitative study using thematic content analysis. *Developmental Medicine & Child Neurology*, *28*(1), 7–13. https://doi.org/10.1111/dmcn.16474

Ewing, C. L., & Irving, A. M. (1969). Evaluation of head protection in aircraft. *Aerospace Medicine, 40*, 596–599.

Fahlstedt, M., Kleiven, S., & Li, X. (2019). Current playground surface test standards underestimate brain injury risk for children. *Journal of Biomechanics*, *89*, 1–10. https://doi.org/10.1016/j.jbiomech.2019.03.038

Feist, F., Wagner, M., Baumann, G., Spirk, S., Biegler, V., Jiang, Q., & Tiina Nypelö. (2024). A cellulosic fibre foam as a bicycle helmet impact liner for brain injury mitigation in oblique impacts. *Heliyon*, *11*(1), e40790–e40790. https://doi.org/10.1016/j.heliyon.2024.e40790

Friedman, D. E., Chiang, S., & Tobias, R. S. (2012). Do recurrent seizure-related head injuries affect seizures in people with epilepsy? *Epilepsy & Behavior*, *23*(2), 159–161. https://doi.org/10.1016/j.yebeh.2011.11.003

Fung, Y. C. (2013). *Biomechanics*. Springer Science & Business Media.

Gabler, L. F., Crandall, J. R., & Panzer, M. B. (2018). Development of a metric for predicting brain strain responses using head kinematics. *Annals of Biomedical Engineering*, *46*(7), 972–985. https://doi.org/10.1007/s10439-018-2015-9

Gandhi, S., R. Kumaravelan, Ramesh, S., Venkatesan, M., & Ponraj, M. R. (2014). Performance analysis of motorcycle helmet under static and dynamic loading. *Mechanics and Mechanical Engineering*, *18*.

Gennarelli, T. A., Thibault, L. E., Adams, J. H., Graham, D. I., Thompson, C. J., & Marcincin, R. P. (1982). Diffuse axonal injury and traumatic coma in the primate. *Annals of Neurology*, *12*(6), 564–574. https://doi.org/10.1002/ana.410120611

Gibson, L. J., & Ashby, M. F. (1999). *Cellular solids*. Cambridge University Press.

Gilardi, G., & Sharf, I. (2002). Literature survey of contact dynamics modelling. *Mechanism and Machine Theory*, *37*(10), 1213–1239. https://doi.org/10.1016/s0094-114x(02)00045-9

Gillett, J. G., Lichtwark, G. A., Boyd, R. N., & Barber, L. A. (2018). Functional anaerobic and strength training in young adults with cerebral palsy. *Medicine & Science in Sports & Exercise*, *50*(8), 1549–1557. https://doi.org/10.1249/mss.0000000000001614

Goldsmith, W., & Plunkett, J. (2004). A biomechanical analysis of the causes of traumatic brain injury in infants and children. *The American Journal of Forensic Medicine and Pathology*, *25*(2), 89–100. https://doi.org/10.1097/01.paf.0000127407.28071.63

Greenwald, R. M., Gwin, J. T., Chu, J. J., & Crisco, J. J. (2008). Head impact severity measures for evaluating mild traumatic brain injury risk exposure. *Neurosurgery*, *62*(4), 789–798. https://doi.org/10.1227/01.neu.0000318162.67472.ad

GuardianHelmets. (2020). *Cerebral palsy helmet for kids and adults*. Guardian Helmets. https://guardianhelmets.com/cerebral-palsy-helmet/

Hassan Vand, M., Tippner, J., & Brabec, M. (2023). Effects of species and moisture content on the behaviour of solid wood under impact. *Holz Als Roh- Und Werkstoff*, *82*(1), 23–34. https://doi.org/10.1007/s00107-023-01986-9

Hägglund, G., Andersson, S., Düppe, H., Lauge-Pedersen, H., Nordmark, E., & Westbom, L. (2005). Prevention of severe contractures might replace multilevel surgery in cerebral palsy: results of a population-based health care programme and new techniques to reduce spasticity. *Journal of pediatric orthopedics. Part B*, *14*(4), 269–273. https://doi.org/10.1097/01202412-200507000-00007

Higgins, M., Halstead, P. D., Snyder-Mackler, L., & Barlow, D. (2007). Measurement of impact acceleration: mouthpiece accelerometer versus helmet accelerometer. *PubMed*, *42*(1), 5–10.

Hodgkinson, I., C Bérard, F Chotel, & J Bérard. (2002). Bassin oblique et scoliose chez le patient infirme moteur cérébral non-marchant: étude descriptive de 234 patients de plus de 15 ans [Pelvic obliquity and scoliosis in non-ambulatory patients with cerebral palsy: a descriptive study of 234 patients over 15 years of age]. *PubMed*, *88*(4), 337–341. https://doi.org/10.1016/s0168-6054(01)00177-5

Hoshizaki, T., Post, A. M., Zerpa, C. E., Legace, E., Hoshizaki, T. B., & Gilchrist, M. D. (2022). Evaluation of two rotational helmet technologies to decrease peak rotational acceleration in cycling helmets. *Scientific Reports*, *12*(1). https://doi.org/10.1038/s41598-022-11559-0

Huang, X., Zheng, Q., Chang, L., & Cai, Z. (2022). Study on protective performance and gradient optimization of helmet foam liner under bullet impact. *Scientific Reports*, *12*(1). https://doi.org/10.1038/s41598-022-20533-9

Hughes, J., Maguire, S., Jones, M. P., Theobald, P., & Alison Mary Kemp. (2016). *Biomechanical characteristics of head injuries from falls in children younger than 48 months*. *101*(4), 310–315. https://doi.org/10.1136/archdischild-2014-306803

Johnson, K. L. (2004). *Contact mechanics*. Cambridge University Press.

Jory, C., Oak, K., Organ, C., Mclean, B., & Shankar, R. (2019). Head first – Review of epilepsy head injury risk and protection. *Seizure*, *71*, 66–79. https://doi.org/10.1016/j.seizure.2019.06.013

Kajtaz, M., Karren, J., & Subic, A. (2016). Experimental investigation into suitability of smart polymers as an impact-absorbing material for an improved rugby headgear. *Proceedings* *of the Institution of Mechanical Engineers, Part P: Journal of Sports Engineering and Technology, 230*(2), 107–117. https://doi.org/10.1177/1754337115595157

Kazl, C., & Torres, A. (2019). Definition, classification, and epidemiology of concussion. *Seminars in Pediatric Neurology*, *30*, 9–13. https://doi.org/10.1016/j.spen.2019.03.003

Kelley, M. E., Kane, J. M., Espeland, M. A., Miller, L. E., Powers, A. K., Stitzel, J. D., & Urban, J. E. (2017). Head impact exposure measured in a single youth football team during practice drills. *Journal of Neurosurgery. Pediatrics*, *20*(5), 489–497. https://doi.org/10.3171/2017.5.PEDS16627

King, A. I., Yang, K. H., Zhang, L., Hardy, W., & Viano, D. C. (2003). Is head injury caused by linear or angular acceleration. *Proceedings of the IRCOBI Conference. Lisbon, Portugal.*, 1–12.

Kis, M., Saunders, F. W., Kis, M., Irrcher, I., Tator, C. H., Bishop, P. J., & ten Hove, M. W. (2013). A method of evaluating helmet rotational acceleration protection using the Kingston Impact Simulator (KIS Unit). *Clinical Journal of Sport Medicine*, *23*(6), 470–477. https://doi.org/10.1097/jsm.0b013e318295a80f

Kleiven, S. (2006). Evaluation of head injury criteria using a finite element model validated against experiments on localized brain motion, intracerebral acceleration, and intracranial pressure. *International Journal of Crashworthiness*, *11*(1), 65–79. https://doi.org/10.1533/ijcr.2005.0384

Kleiven, S. (2013). Why Most Traumatic brain injuries are not caused by linear acceleration but skull fractures are. *Frontiers in Bioengineering and Biotechnology*, *1*. https://doi.org/10.3389/fbioe.2013.00015

Knowles, B. M., & Dennison, C. R. (2017). Predicting cumulative and maximum brain strain measures from HybridIII head kinematics: A combined laboratory study and post-Hoc regression analysis. *Annals of Biomedical Engineering*, *45*(9), 2146–2158. https://doi.org/10.1007/s10439-017-1848-y

Kong, C. K., Tse, P. W. T., & Lee, W. Y. (1999). Bone age and linear skeletal growth of children with cerebral palsy. *Developmental Medicine & Child Neurology*, *41*(11), 758–765. https://doi.org/10.1111/j.1469-8749.1999.tb00536.x

Kuppermann, N., Holmes, J. F., Dayan, P. S., Hoyle, J. D., Atabaki, S. M., Holubkov, R., Nadel, F. M., Monroe, D., Stanley, R. M., Borgialli, D. A., Badawy, M. K., Schunk, J. E., Quayle, K. S., Mahajan, P., Lichenstein, R., Lillis, K. A., Tunik, M. G., Jacobs, E. S., Callahan, J. M., & Gorelick, M. H. (2009). Identification of children at very low risk of clinically-important brain injuries after head trauma: a prospective cohort study. *The Lancet*, *374*(9696), 1160–1170. https://doi.org/10.1016/s0140-6736(09)61558-0

Jones, E., & Smith, L. (2026). Performance and durability of Taekwondo headgear. *Sports Engineering*, *29*(1). https://doi.org/10.1007/s12283-026-00550-x

Islam, M. A., Kader, M. A., Hazell, P. J., Escobedo, J. P., Brown, A. D., & M. Saadatfar. (2020). Effects of impactor shape on the deformation and energy absorption of closed cell aluminium foams under low velocity impact. *Materials & Design*, *191*, 108599–108599. https://doi.org/10.1016/j.matdes.2020.108599

Lachance, C. C., Feldman, F., Laing, A. C., Leung, P. M., Robinovitch, S. N., & Mackey, D. C. (2016). Study protocol for the flooring for injury prevention (FLIP) study: a randomised controlled trial in long-term care. *Injury Prevention*, *22*(6), 453–460. https://doi.org/10.1136/injuryprev-2016-042008

Lachance, C. C., Jurkowski, M. P., Dymarz, A. C., Robinovitch, S. N., Feldman, F., Laing, A. C., & Mackey, D. C. (2017). Compliant flooring to prevent fall-related injuries in older adults: A scoping review of biomechanical efficacy, clinical effectiveness, cost-effectiveness, and workplace safety. *PloS one*, *12*(2), e0171652. https://doi.org/10.1371/journal.pone.0171652

Laing, A. C., & Robinovitch, S. N. (2009). Low stiffness floors can attenuate fall-related femoral impact forces by up to 50% without substantially impairing balance in older women. *Accident Analysis & Prevention*, *41*(3), 642–650. https://doi.org/10.1016/j.aap.2009.03.001

Li, S., Li, Q. M., Tse, K. M., & Pang, T. (2024). Functionally graded foam materials for head impact protection. *Thin-Walled Structures*, *203*, 112193. https://doi.org/10.1016/j.tws.2024.112193

Li, Z., Chen, W., & Hao, H. (2019). Mechanical properties of carbon foams under quasi-static and dynamic loading. *International Journal of Mechanical Sciences*, *161-162*, 105039. https://doi.org/10.1016/j.ijmecsci.2019.105039

Lin, C. Y., Chang, L.-T., Huang, T. J., Tsai, K. H., Li, C. S., & Chang, G. L. (2008). Finite element analysis of honeycomb-core foam on shock-absorbing capability against childhood head injury. *IFMBE Proceedings*, 135–138. https://doi.org/10.1007/978-3-540-69367-3_36

Loyd, A. M., Nightingale, R. W., Luck, J. F., Bass, C. 'Dale', Cutcliffe, H. C., & Myers, B. S. (2019). The response of the pediatric head to impacts onto a rigid surface. *Journal of Biomechanics*, *93*, 167–176. https://doi.org/10.1016/j.jbiomech.2019.06.027

Maâlej, A. J., Krichen, M., & Jmaïel, M. (2015). A comparative evaluation of state-of-the-art load and stress testing approaches. *International Journal of Computer Applications in Technology*, *51*(4), 283. https://doi.org/10.1504/ijcat.2015.070491

Macarthur, C., Hu, X., Wesson, D. E., & Parkin, P. C. (2000). Risk factors for severe injuries associated with falls from playground equipment. *Accident Analysis & Prevention*, *32*(3), 377–382. https://doi.org/10.1016/s0001-4575(99)00079-2

Macchitella, L., Accogli, G., Barraco, G., Nicolardi, V., Pirani, G., Ferrante, C., Oliva, M. C., Fanizza, I., Gallo, I., De Rinaldis, M., & Trabacca, A. (2024). A two-step neurorehabilitation program utilizing extended reality and telerehabilitation for children with cerebral palsy: A pilot study on effectiveness, adherence, and technical feasibility. *Applied Sciences*, *14*(24), 11961. https://doi.org/10.3390/app142411961

Maiti, S. K., Gibson, L. J., & Ashby, M. F. (1984). Deformation and energy absorption diagrams for cellular solids. *Acta Metallurgica*, *32*(11), 1963–1975. https://doi.org/10.1016/0001-6160(84)90177-9

Margulies, S. S., & Thibault, L. E. (1992). A proposed tolerance criterion for diffuse axonal injury in man. *Journal of Biomechanics*, *25*(8), 917–923. https://doi.org/10.1016/0021-9290(92)90231-o

Marjoux, D., Baumgartner, D., Deck, C., & Willinger, R. (2008). Head injury prediction capability of the HIC, HIP, SIMon and ULP criteria. *Accident Analysis & Prevention*, *40*(3), 1135–1148. https://doi.org/10.1016/j.aap.2007.12.006

Martini, D. N., Sabin, M. J., DePesa, S. A., Leal, E. W., Negrete, T. N., Sosnoff, J. J., & Broglio, S. P. (2011). The chronic effects of concussion on gait. *Archives of Physical Medicine and Rehabilitation*, *92*(4), 585–589. https://doi.org/10.1016/j.apmr.2010.11.029

Marur, P. R., Simha, K. R. Y., & Nair, P. S. (1994). Dynamic analysis of three points bends specimens under impact. *International Journal of Fracture*, *68*(3), 261–273. https://doi.org/10.1007/bf00013071

Massaad, F., Dierick, F., van den Hecke, A., & Detrembleur, C. (2004). Influence of gait pattern on the body's centre of mass displacement in children with cerebral palsy. *Developmental Medicine and Child Neurology*, *46*(10), 674–680. https://doi.org/10.1017/s0012162204001136

McDonald, M. W., Black, S. E., Copland, D. A., Corbett, D., Dijkhuizen, R. M., Farr, T. D., Jeffers, M. S., Kalaria, R. N., Karayanidis, F., Leff, A. P., Nithianantharajah, J., Pendlebury, S., Quinn, T. J., Clarkson, A. N., & O'Sullivan, M. J. (2019). Cognition in stroke rehabilitation and recovery research: Consensus-based core recommendations from the second Stroke Recovery and Rehabilitation Roundtable. *International Journal of Stroke*, *14*(8), 774–782. https://doi.org/10.1177/1747493019873600

McIntosh, A. S., & Lai, A. (2013). Motorcycle helmets: head and neck dynamics in helmeted and unhelmeted oblique impacts. *Traffic Injury Prevention*, *14*(8), 835–844. https://doi.org/10.1080/15389588.2013.774083

Mckee, A. C., & Daneshvar, D. H. (2015). The neuropathology of traumatic brain injury. *Handbook of Clinical Neurology*, *127*(1), 45–66. https://doi.org/10.1016/b978-0-444-52892-6.00004-0

McNamara, E. H., Grillakis, A. A., Tucker, L. B., & McCabe, J. T. (2020). The closed-head impact model of engineered rotational acceleration (CHIMERA) as an application for traumatic brain injury pre-clinical research: A status report. *Experimental Neurology*, *333*, 113409. https://doi.org/10.1016/j.expneurol.2020.113409

Meaney, D. F., & Smith, D. H. (2011). Biomechanics of concussion. *Clinics in Sports Medicine*, *30*(1), 19–31. https://doi.org/10.1016/j.csm.2010.08.009

Meaney, D. F., Morrison, B., & Dale Bass, C. (2014). The mechanics of traumatic brain injury: A review of what we know and what we need to know for reducing its societal burden. *Journal of Biomechanical Engineering*, *136*(2), 0210081–02100814. https://doi.org/10.1115/1.4026364

Meriam, J. L., & Kraige, L. G. (2007). *Engineering mechanics*. Wiley.

Michael-Asalu, A., Taylor, G., Campbell, H., Lelea, L. L., & Kirby, R. S. (2019). Cerebral palsy: Diagnosis, epidemiology, eenetics, and clinical update. *Advances in Pediatrics*, *66*, 189–208. https://doi.org/10.1016/j.yapd.2019.04.002

Miller, L. E., Urban, J. E., Kelley, M. E., Powers, A. K., Whitlow, C. T., Maldjian, J. A., Rowson, S., & Stitzel, J. D. (2018). Evaluation of brain response during head impact in youth athletes using an anatomically accurate finite element model. *Journal of Neurotrauma*, *36*(10), 1561–1570. https://doi.org/10.1089/neu.2018.6037

Mills, N. J. (2006). Finite element models for the viscoelasticity of open-cell polyurethane foam. *Cellular Polymers*, *25*(5), 293–316. https://doi.org/10.1177/026248930602500502

Moody, J. N., Hayes, J. P., Buckley, T. A., Schmidt, J. D., Broglio, S. P., McAllister, T. W., McCrea, M., Pasquina, P. F., & Caccese, J. B. (2022). Age of first concussion and cognitive, psychological, and physical outcomes in NCAA collegiate student athletes. *Sports Medicine*, *52*(11), 2759–2773. https://doi.org/10.1007/s40279-022-01719-7

Moore, R. B., Pindus, D. M., Drolette, E. S., Scudder, M. R., Raine, L. B., & Hillman, C. H. (2015). *The persistent influence of pediatric concussion on attention and cognitive* *control during flanker performance*. *109*, 93–102. https://doi.org/10.1016/j.biopsycho.2015.04.008

Morgan, L. C. (2003). *Pediatric head trauma: Cerebral perfusion pressure as an indicator of outcome* (Order No. 3095105). Available from Nursing & Allied Health Collection. (305324946). https://www.proquest.com/dissertations-theses/pediatric-head-trauma-cerebral-perfusion-pressure/docview/305324946/se-2

Mosleh, Y., Vander Sloten, J., Depreitere, B., & Ivens, J. (2017). Novel composite foam concept for head protection in oblique impacts. *Advanced Engineering Materials*, *19*(10), 1700059. https://doi.org/10.1002/adem.201700059

Mosleh, Y., Cajka, M., Depreitere, B., Jos Vander Sloten, & Ivens, J. (2018). Designing safer composite helmets to reduce rotational accelerations during oblique impacts. *Proceedings of the Institution of Mechanical Engineers, Part H: Journal of Engineering in Medicine*, *232*(5), 479–491. https://doi.org/10.1177/0954411918762622

Nakken, K. O., & Lossius, R. (1993). Skader ved epileptiske anfall [Injuries in epileptic seizures]. *Tidsskrift for den Norske Laegeforening : Tidsskrift for Praktisk Medicin, ny Raekke*, *113*(21), 2690–2692.

Nashner, L. M., Shumway-Cook, A., & Marin, O. (1983). Stance posture control in select groups of children with cerebral palsy: Deficits in sensory organization and muscular coordination. *Experimental Brain Research*, *49*(3). https://doi.org/10.1007/bf00238781

Neguyen, R., & Tellez-Zenteno, J. (2009). Injuries in epilepsy: A review of its prevalence, risk factors, type of injuries and prevention. *Neurology International*, *1*(1), 20. https://doi.org/10.4081/ni.2009.e20

Nelson, K. B., & Blair, E. (2015). Prenatal factors in singletons with cerebral palsy born at or near Term. *New England Journal of Medicine*, *373*(10), 946–953. https://doi.org/10.1056/nejmra1505261

Neufeld, M. Y., Chistik, V., Kogan, E., & Korczyn, A. D. (2002). Physically traumatic events in patients with epilepsy compared with non-epileptic subjects. *Seizure*, *9*(8), 595–597. https://doi.org/10.1053/seiz.2000.0469

Newman, J. A., Beusenberg, M. C., Shewchenko, N., Withnall, C., & Fournier, E. (2005). Verification of biomechanical methods employed in a comprehensive study of mild traumatic brain injury and the effectiveness of American football helmets. *Journal of Biomechanics*, *38*(7), 1469–1481. https://doi.org/10.1016/j.jbiomech.2004.06.025

NOCSAE. (2017). *NOCSAE overview*. Https://Nocsae.org/. https://nocsae.org/wp-content/uploads/2018/04/NOCSAE-Overview-5-17.pdf

NOCSAE. (2025). *Standard test method and equipment used in evaluating the performance characteristics of headgear/equipment | NOCSAE*. Nocsae.org. https://nocsae.org/standard-test-method-and-equipment-used-in-evaluating-the-performance-characteristics-of-headgear-equipment/

Nokes, L. D. M., Roberts, A. M., & Knight, B. H. (1995). Use of the gadd severity index in forensic medicine: A case study. *Forensic Science International*, *76*(2), 85–90. https://doi.org/10.1016/0379-0738(95)01801-8

Obembe, A. O., Johnson, O. E., & Ola, M. C. (2013). Gross motor function in cerebral palsy: The association with age, motor type and topographical distribution. *Nigerian Journal of Medical Rehabilitation*, *16*(2). https://doi.org/10.34058/njmr.v16i2.79

Orr, T. J., Emal Lesha, Kramer, A. H., Arba Cecia, Dugan, J. E., Schwartz, B., & Einhaus, S. L. (2024). Traumatic brain injury: A comprehensive review of biomechanics and molecular pathophysiology. *World Neurosurgery (Print)*, *185*. https://doi.org/10.1016/j.wneu.2024.01.084

Oskoui, M., Ng, P., Dorais, M., Pigeon, N., Koclas, L., Lamarre, C., Malouin, F., Richards, C. L., Shevell, M., & Joseph, L. (2017). Accuracy of administrative claims data for cerebral palsy diagnosis: a retrospective cohort study. *CMAJ Open*, *5*(3), E570–E575. https://doi.org/10.9778/cmajo.20170013

Ouellet, S., Cronin, D., & Worswick, M. (2006). Compressive response of polymeric foams under quasi-static, medium and high strain rate conditions. *Polymer Testing*, *25*(6), 731–743. https://doi.org/10.1016/j.polymertesting.2006.05.005

Ouyang, J., Zhu, Q., Zhao, W., Xu, Y., Chen, W., & Zhong, S. (2005). Biomechanical Assessment of the Pediatric Cervical Spine Under Bending and Tensile Loading. *Spine*, *30*(24), E716–E723. https://doi.org/10.1097/01.brs.0000192280.53831.70

Palisano, R., Rosenbaum, P., Walter, S., Russell, D., Wood, E., & Galuppi, B. (1997). Development and reliability of a system to classify gross motor function in children with cerebral palsy. *Developmental Medicine and Child Neurology*, *39*(4), 214–223. https://doi.org/10.1111/j.1469-8749.1997.tb07414

Parslow, R. C., Morris, K. P., Tasker, R. C., Forsyth, R. J., Hawley, C. A., UK Paediatric Traumatic brain injury study steering group, & paediatric intensive care society study group (2005). Epidemiology of traumatic brain injury in children receiving intensive care in the UK. *Archives of Disease in Childhood*, *90*(11), 1182–1187. https://doi.org/10.1136/adc.2005.072405

Patel, D. R., Neelakantan, M., Pandher, K., & Merrick, J. (2020). Cerebral palsy in children: A clinical overview. *Translational Pediatrics*, *9*(S1), S125–S135. https://doi.org/10.21037/tp.2020.01.01

Patrick, L. M. (1966). Head impact protection. In W. F. Caveness & A. E. Walker (Eds.), *Head injury conference* (pp. 41–48). Lippincott.

Pennock, B., Kivi, D., & Zerpa, C. (2021). Effect of neck strength on simulated head impacts during falls in female ice hockey players. *International Journal of Exercise Science*, *14*(1), 446–461. https://doi-org.ezproxy.lakeheadu.ca/10.70252/OXUE1359

Petel, O. E., Ouellet, S., Higgins, A. J., & Frost, D. L. (2012). The elastic–plastic behaviour of foam under shock loading. *Shock Waves*, *23*(1), 55–67. https://doi.org/10.1007/s00193-012-0414-7

Pintar, F. A., Philippens, M. M. G. M., Zhang, J., & Yoganandan, N. (2013). Methodology to determine skull bone and brain responses from ballistic helmet-to-head contact loading using experiments and finite element analysis. *Medical Engineering & Physics*, *35*(11), 1682–1687. https://doi.org/10.1016/j.medengphy.2013.04.015

Piwowarczyk, S., Obłój, P., Janicki, Ł., Kowalik, K., Łukaszuk, A., & Siemiński, M. (2024). Seizure-related head injuries: A narrative review. *Brain Sciences*, *14*(5), 473. https://doi.org/10.3390/brainsci14050473

Post, A., Hoshizaki, B., & Gilchrist, M. D. (2012). Finite element analysis of the effect of loading curve shape on brain injury predictors. *Journal of Biomechanics*, *45*(4), 679–683. https://doi.org/10.1016/j.jbiomech.2011.12.005

Puderbaugh, M., & Emmady, P. D. (2023). Neuroplasticity. In *StatPearls*. StatPearls Publishing.

Rahimidehgolan, F., & Altenhof, W. (2023). Compressive behavior and deformation mechanisms of rigid polymeric foams: A review. *Composites Part B: Engineering*, *253*, 110513–110513. https://doi.org/10.1016/j.compositesb.2023.110513

Ramirez, B. J., Misra, U., & Gupta, V. (2018). Viscoelastic foam-filled lattice for high energy absorption. *Mechanics of Materials*, *127*, 39–47. https://doi.org/10.1016/j.mechmat.2018.08.011

Rao, S., Stino, A., Seraji-Bozorgzad, N., Shah, A. K., & Basha, M. M. (2020). Seizure-related injury and postictal aggression in refractory epilepsy patients. *Epilepsy Research*, *160*, 106281. https://doi.org/10.1016/j.eplepsyres.2020.106281

Rayne, J. M., & Maslen, K. R. (1969). Factors in the design of protective helmets. *Aerospace Medicine, 40*, 631–637.

Regis School. (2022). Soft helmet sizing guide. https://www.theregisschool.org/uploaded/athletics/ls/Soft_Helmet_Sizing_Guide.pdf

Robertson, C. M. T., Ricci, M. F., O'Grady, K., Oskoui, M., Goez, H., Yager, J. Y., & Andersen, J. C. (2017). Prevalence estimate of cerebral palsy in Northern Alberta: births, 2008-2010. *Canadian Journal of Neurological Sciences / Journal Canadien Des Sciences Neurologiques*, *44*(4), 366–374. https://doi.org/10.1017/cjn.2017.33

Romero, P., Zheng, S., & Cuitiño, A. M. (2008). *Modeling the dynamic response of visco-elastic open-cell foams*. *56*(5), 1916–1943. https://doi.org/10.1016/j.jmps.2007.11.007

Rosenbaum, P., Paneth, N., Leviton, A., Goldstein, M., Bax, M., Damiano, D., Dan, B., & Jacobsson, B. (2007). A report: The definition and classification of cerebral palsy April 2006. *Developmental Medicine & Child Neurology*, *49*(6), 8–14. https://doi.org/10.1111/j.1469-8749.2007.tb12610.x

Rowson, S., & Duma, S. M. (2011). Development of the STAR evaluation system for football helmets: Integrating player head impact exposure and risk of concussion. *Annals of Biomedical Engineering*, *39*(8), 2130–2140. https://doi.org/10.1007/s10439-011-0322-5

Rowson, S., Duma, S. M., Beckwith, J. G., Chu, J. J., Greenwald, R. M., Crisco, J. J., Brolinson, P. G., Duhaime, A.-C., McAllister, T. W., & Maerlender, A. C. (2011). Rotational head kinematics in football impacts: An injury risk function for concussion. *Annals of Biomedical Engineering*, *40*(1), 1–13. https://doi.org/10.1007/s10439-011-0392-4

Russell-Jones, D. L., & Shorvon, S. D. (1989). The frequency and consequences of head injury in epileptic seizures. *Journal of Neurology, Neurosurgery & Psychiatry*, *52*(5), 659–662. https://doi.org/10.1136/jnnp.52.5.659

Rybak, T. (2021). *Towards examining the effectiveness of boxing headguards with thermoplastic polyurethane in mitigating acceleration and risk of head injury using a dynamic head model.* [Master Thesis, Lakehead university]. http://knowledgecommons.lakeheadu.ca/handle/2453/4745

Santhosh, S., Saravanan, C., Rajaguru, K., Suresh Kumar, B., & Sathish, T. (2021). Fabrication and analysis of aluminium foam with glass fiber based on PMC for helmet applications. *Materials Today: Proceedings*, *37*, 1286–1288. https://doi.org/10.1016/j.matpr.2020.06.461

Sărăndan, S., Negru, R., Marşavina, L., Mihuţa, M. S., & Şerban, D.-A. (2022). Numerical analysis of a Rugby union protective headgear under impact loading. *Materials Today: Proceedings*. https://doi.org/10.1016/j.matpr.2022.11.500

Sedlák, M., Wazir, A., Dima, A., Gazda, J., & Radoslav Morochovič. (2023). Cutaneous impact location predicts intracranial injury among the elderly population with traumatic brain injury. *Open Access Emergency Medicine*, *Volume 15*, 265–275. https://doi.org/10.2147/oaem.s422785

Senthilkumar, M., Anbumani, N., & Hayavadana, J. (2011). Elastane fabrics – A tool for stretch applications in sports. *Indian Journal of Fibre & Textile Research*, *36*(3), 300–307. https://www.researchgate.net/publication/269338309_Elastane_fabrics-A_tool_for_stretch_applications_in_sports

Sewport. (2019). *What is Lycra fabric: properties, how its made and where*. Sewport. https://sewport.com/fabrics-directory/lycra-fabric?utm_source

Shahabpoor, E., & Pavic, A. (2016). Human-structure dynamic interaction during short-distance free falls. *Shock and Vibration*, *2016*, 1–12. https://doi.org/10.1155/2016/2108676

Shankar, S., Nithyaprakash, R., Praveen, S., Sathish Kumar, S., & Sriram, A. M. (2020). Analysis of motor cycle helmet under static and dynamic conditions considering different materials. *Materials Today: Proceedings*. https://doi.org/10.1016/j.matpr.2020.08.327

Shargawi, A. A., Jorgensen, M. J., Hakansson, N. A., Amick, R. Z., & Ramazan Asmatulu. (2023). Energy absorbency and impact resistance of D3O® materials under dynamic impact loadings. *American Journal of Aerospace Engineering*. https://doi.org/10.11648/j.ajae.20231001.11

Shumway-Cook, A., Hutchinson, S., Kartin, D., Price, R., & Woollacott, M. (2003). Effect of balance training on recovery of stability in children with cerebral palsy. *Developmental Medicine & Child Neurology*, *45*(09). https://doi.org/10.1017/s0012162203001099

Singh, A., Kumar, D., & Ganpule, S. (2024). Biomechanical response of head surrogate with and without the helmet. *Journal of Biomechanical Engineering*, *146*(3). https://doi.org/10.1115/1.4062968

Skulski, J. (2011). *A longitudinal study of playground surfaces to evaluate accessibility: year one findings*. Bloomington, IN: National Center on Accessibility. https://scholarworks.iu.edu/dspace/items/e286641a-54ea-4021-aab6-663bcfdcd99c?utm=

Smith, D. H., Nonaka, M., Miller, R., Leoni, M., Chen, X.-H., Alsop, D., & Meaney, D. F. (2000). Immediate coma following inertial brain injury dependent on axonal damage in the brainstem. *Journal of Neurosurgery*, *93*(2), 315–322. https://doi.org/10.3171/jns.2000.93.2.0315

Smith, L., Kelly, K. D., Prkachin, G., & Voaklander, D. C. (2008). The prevalence of cerebral palsy in British Columbia, 1991-1995. *Canadian Journal of Neurological Sciences/Journal Canadien Des Sciences Neurologiques*, *35*(3), 342–347. https://doi.org/10.1017/s0317167100008933

Sneed, J. R., Keilp, J. G., Brickman, A. M., & Roose, S. P. (2008). The specificity of neuropsychological impairment in predicting antidepressant non-response in the very old depressed. *International Journal of Geriatric Psychiatry*, *23*(3), 319–323. https://doi.org/10.1002/gps.1889

Sushinsky, G. (2005). *Surfacing materials for indoor play areas impact attenuation test report*. https://www.cpsc.gov/s3fs-public/surfacing.pdf

Tang, M., Huang, G., Zhang, H., Liu, Y., Chang, H., Song, H., Xu, D., & Wang, Z. (2017). Dependences of rheological and compression mechanical properties on cellular structures for impact-protective materials. *ACS Omega*, *2*(5), 2214–2223. https://doi.org/10.1021/acsomega.7b00242

Thill, M., Krach, L. E., Pederson, K., Wandersee, N. G., Sandy Callen Tierney, & Boyer, E. R. (2023). Physical and psychosocial consequences of falls in individuals with cerebral palsy. *MedRxiv (Cold Spring Harbor Laboratory)*. https://doi.org/10.1101/2023.08.16.23294077

Thompson-Bagshaw, D. W., Quarrington, R. D., & Jones, C. F. (2022). A Review of the compressive stiffness of the human head. *Annals of Biomedical Engineering*, *50*(12), 1750–1761. https://doi.org/10.1007/s10439-022-03099-5

Tierney, G. (2021). Concussion biomechanics, head acceleration exposure and brain injury criteria in sport: a review. *Sports Biomechanics*, *23*(11), 1–29. https://doi.org/10.1080/14763141.2021.2016929

Tse, K. M., Tan, L. B., Yang, B., Tan, V. B. C., & Lee, H. P. (2016). Effect of helmet liner systems and impact directions on severity of head injuries sustained in ballistic impacts: A finite element (FE) study. *Medical & Biological Engineering & Computing*, *55*(4), 641–662. https://doi.org/10.1007/s11517-016-1536-3

Unterharnscheidt, F. J. (1972). Die traumatischen hirnschäden. mechanogenese, pathomorphologie und klinik [Traumatic brain injuries. Mechanogenesis, pathomorphology, and clinical aspects]. *Zeitschrift Für Rechtsmedizin*, *71*(3), 153–220. https://doi.org/10.1007/bf02076624

US Access Board. (2019). *United States access board*. Access-Board.gov. https://www.access-board.gov

Veliz, P., McCabe, S. E., Eckner, J. T., & Schulenberg, J. E. (2021). Trends in the prevalence of concussion reported by US adolescents, 2016-2020. *JAMA*, *325*(17), 1789–1791. https://doi-org.ezproxy.lakeheadu.ca/10.1001/jama.2021.1538

Vanden Bosche, K., Mosleh, Y., Depreitere, B., Vander Sloten, J., Verpoest, I., & Ivens, J. (2017). Anisotropic polyethersulfone foam for bicycle helmet liners to reduce rotational acceleration during oblique impact. *Proceedings of the Institution of Mechanical Engineers, Part H: Journal of Engineering in Medicine*, *231*(9), 851–861. https://doi.org/10.1177/0954411917711201

Versace, J. (1971). A Review of the severity index*, 15th Stapp Car Crash Conference San Diego, California, United States*, https://doi.org/10.4271/710881

Vincer, M. J., Allen, A. C., Allen, V. M., Baskett, T. F., & O'Connell, C. M. (2014). Trends in the prevalence of cerebral palsy among very preterm infants (<31 weeks' gestational age). *Paediatrics & Child Health*, *19*(4), 185–189. https://doi.org/10.1093/pch/19.4.185

Ward, S. (1995). Head injuries in the accident and emergency department. *Emergency Medicine Journal*, *12*(1), 73–74. https://doi.org/10.1136/emj.12.1.73-c

Warrington, S. A., Wright, C. M., & ALSPAC Study Team (2001). Accidents and resulting injuries in premobile infants: data from the ALSPAC study. *Archives of Disease in Childhood*, *85*(2), 104–107. https://doi.org/10.1136/adc.85.2.104

Weaver, A. A., Danelson, K. A., & Stitzel, J. D. (2012). Modeling brain injury response for rotational velocities of varying directions and magnitudes. *Annals of Biomedical Engineering*, *40*(9), 2005–2018. https://doi.org/10.1007/s10439-012-0553-0

Willsallen, H., Heller, J., Kark, L., & Hilbert, B. J. (2014). Mechanical testing of braided polyurethane elastic fiber and braided polyester for equine laryngoplasty. *Veterinary Surgery*, *44*(2), 223–230. https://doi.org/10.1111/j.1532-950x.2014.12184.x

Woollacott, M. H., & Shumway-Cook, A. (2005). Postural dysfunction during standing and walking in children with cerebral palsy: What are the underlying problems and what new therapies might improve balance? *Neural Plasticity*, *12*(2-3), 211–219. https://doi.org/10.1155/np.2005.211

Wu, J. Z., Pan, C. S., Cobb, C., Moorehead, A., Kau, T.-Y., & Wimer, B. M. (2022). Evaluation of the fall protection of type I industrial helmets. *Annals of Biomedical Engineering*, *50*(11), 1565–1578. https://doi.org/10.1007/s10439-022-02922-3

Yang, B., Zuo, Y., & Chang, Z. (2021). Evaluation of energy absorption capabilities of polyethylene foam under impact deformation. *Materials*, *14*(13), 3613–3613. https://doi.org/10.3390/ma14133613

Yoganandan, N., Gennarelli, T. A., Zhang, J., Pintar, F. A., Takhounts, E., & Ridella, S. A. (2009). Association of contact loading in diffuse axonal injuries from motor vehicle crashes. *The Journal of Trauma: Injury, Infection, and Critical Care*, *66*(2), 309–315. https://doi.org/10.1097/ta.0b013e3181692104

Youssef, G., Reed, N., Huynh, N. U., Rosenow, B., & Manlulu, K. (2020). Experimentally validated predictions of impact response of polyurea foams using viscoelasticity based on bulk properties. *Mechanics of Materials*, *148*, 103432. https://doi.org/10.1016/j.mechmat.2020.103432

Yu, H. Y., & Dennison, C. R. (2018). A Laboratory study on effects of cycling helmet fit on biomechanical measures associated with head and neck injury and dynamic helmet retention. *Journal of Biomechanical Engineering*, *141*(1). https://doi.org/10.1115/1.4040944

Yu, X., Baker, C. E., & Mazdak Ghajari. (2023). Head impact location, speed and angle from falls and trips in the workplace. *Annals of Biomedical Engineering*. https://doi.org/10.1007/s10439-023-03146-9

Yu, X., Halldin, P., & Mazdak Ghajari. (2022). Oblique impact responses of Hybrid III and a new headform with more biofidelic coefficient of friction and moments of inertia. *Frontiers in Bioengineering and Biotechnology*, *10*. https://doi.org/10.3389/fbioe.2022.860435

Zaman, R., Hossain, M. I., Raiyan, A. Z., Chowdhury, S., Jackson, A., Koster, A. T., & Adnan, A. (2025). A biomechanical study of neck strength and impact dynamics on head and neck injury parameters. *Frontiers in Bioengineering and Biotechnology*, *13*. https://doi.org/10.3389/fbioe.2025.1597267

Zhang, J., Yoganandan, N., & Pintar, F. A. (2009). Dynamic biomechanics of the human head in lateral impacts. *Annals of advances in automotive medicine. Association for the Advancement of Automotive Medicine. Annual Scientific Conference*, *53*, 249–256.

Zhang, K., Chen, Y., Feng, C., Xiang, X., Zhang, X., Dai, Y., & Niu, W. (2025). Machine learning based finite element analysis for personalized prediction of pressure injury risk in patients with spinal cord injury. *Computer Methods and Programs in Biomedicine*, *261*, 108648. https://doi.org/10.1016/j.cmpb.2025.108648

Zhang, L., Yang, K. H., & King, A. I. (2001). Comparison of brain responses between frontal and lateral impacts by finite element modeling. *Journal of Neurotrauma*, *18*(1), 21–30. https://doi.org/10.1089/089771501750055749

Zhang, X., Yang, B., Wu, J., Li, X., & Zhou, R. (2024). Research progress on helmet liner materials and structural applications. *Materials*, *17*(11), 2649–2649. https://doi.org/10.3390/ma17112649

Appendixes

Appendix A

Table 1

Means, SD, and SE for Measures of Linear Acceleration and HIC

Ground Surfaces	Impact Location	LA			HIC			N
		Means	SD	SE	Means	SD	SE	
Linoleum	Front	242.75	60.57	14.24	595.84	223.08	64.03	13
	Side	186.68	51.21	14.24	608.85	246.25	64.03	13
	Back	216.25	40.29	14.24	751.51	222.50	64.03	13
Carpet	Front	223.27	51.62	12.70	577.77	224.28	62.31	13
	Side	178.41	47.25	12.70	583.68	233.69	62.31	13
	Back	210.69	37.35	12.70	714.49	215.67	62.31	13
Wood	Front	210.23	52.91	12.88	620.32	234.74	64.39	13
	Side	184.29	44.51	12.88	620.66	234.74	64.39	13
	Back	218.22	41.13	12.88	769.06	226.95	64.39	13
Foam	Front	176.50	54.37	12.41	554.58	302.49	71.40	13
	Side	129.78	39.73	12.41	432.82	228.38	71.40	13
	Back	178.37	38.44	12.41	634.96	234.89	71.40	13

Appendix B

Table 2

Means, SD, and SE for Measures of Rotational Acceleration and AGSI

Ground Surfaces	Impact Location	RA			AGSI			N
		Means	SD	SE	Means	SD	SE	
Linoleum	Front	10186.363	2668.338	678.092	3625.9605	1705.107	533.630	13
	Side	13986.294	2824.704	678.092	6356.8338	2431.514	533.630	13
	Back	13505.048	1683.321	678.092	6773.7006	1511.966	533.630	13
Carpet	Front	12359.665	2276.547	564.727	5012.8293	1596.864	462.926	13
	Side	14379.621	2367.148	564.727	6647.5972	2203.118	462.926	13
	Back	12025.563	1285.185	564.727	4836.1341	976.744	462.926	13
Wood	Front	10723.456	1174.223	440.595	4322.4375	1014.254	372.650	13
	Side	12770.854	1732.626	440.595	5159.0396	1252.886	372.650	13
	Back	13499.527	1786.065	440.595	6976.7761	1678.519	372.650	13
Foam	Front	13362.539	1550.438	392.405	6233.3839	1609.676	360.122	13
	Side	13592.111	1576.411	392.405	5996.9301	1342.592	360.122	13
	Back	117793.167	1597.596	392.405	5137.2509	814.995	360.122	13